Design Issues in Multirate Digital Filter Banks, Including Transmultiplexers

Thesis by

Ravinder David Koilpillai

In Partial Fulfillment of the Requirements
for the Degree of
Doctor of Philosophy

California Institute of Technology
Pasadena, California
1991
(Submitted December 3, 1990)

to my parents and Kohila

Acknowledgements

It gives me great pleasure to acknowledge all those who have helped me in my studies and research work at Caltech, and thereby enriching my stay here. First and foremost, I am deeply grateful to my advisor Professor P. P. Vaidyanathan for guiding me in my research work. I admire his sharp intuition and tremendous creativity. The weekly meetings that we had, his availability and willingness to spend a lot of his time to help me in my work were always invaluable. In his person, I see a truly dedicated researcher and teacher, and this has made the greatest impact in my educational experience at Caltech. I also thank him for the generous financial support (research and teaching assistantships) that I received throughout my stay at Caltech.

I would like to thank my fellow-students in the DSP group - Truong Nguyen, Zinnur Doganata, Quan Hoang, Vincent Liu, Vinay Sathe and Tsu-Han Chen. Our regular group meetings were very valuable - in terms of helpful discussions, generating new ideas and learning new things. I would like to add a special note of thanks to Truong for his friendship and for all his encouragement.

I would like to thank all the members of my candidacy and thesis defense committees: Professors Abu-Mostafa, Franklin, Goodman, McEliece and Posner. Each of them is a uniquely gifted teacher and researcher. I consider myself fortunate for having studied under their teaching.

My parents, by their own example taught me the valuable disciplines of hard work and perseverance. They have been my pillars of love, strength and guidance. I thank my parents and my sister Manju, for always encouraging me to do 'better than my best'. The one person who has always been at my side (through the long hours of arduous work), providing constant encouragement, love and support has been my wife Kohila. She is truly my greatest blessing. Together, we thank our family members and friends for their love and prayers.

Above all, my deepest gratitude and earnest praise are to God. Through all my experiences at Caltech, my faith in God has been strengthened. This is my prayer

Take my life and let it be,

Consecrated Lord to Thee,

Take my intellect and use,

Every power as thou shalt choose.

Abstract

Several aspects of the theory and design of FIR digital filter banks for analysis/synthesis systems are studied in this thesis. In particular, we focus on filter banks satisfying the perfect reconstruction (PR) property. We present a new approach to design PR filter banks wherein the filter bank is obtained by cosine-modulation of a linear-phase prototype filter of length $N = 2mM$, $m \geq 1$ (where M is the number of channels). The PR property is satisfied because the polyphase component matrix of the modulated filter bank is lossless. This is achieved by satisfying the necessary and sufficient condition – a pairwise power complementary property between the $2M$ polyphase components of the prototype. In this approach, regardless of the number of channels, we still design only the prototype. The design procedure involves the two-channel lossless lattice. This approach compares favorably (in terms of the number of parameters to be optimized and the ease of design) with other design techniques. Design examples and detailed comparisons are presented.

The existing approaches for designing PR filter banks include the lattice based methods, which structurally force the polyphase component matrix to be lossless. New initialization procedures, which can be used to initialize the values of all the lattice parameters (prior to optimization), are presented. The main advantage is that we can get 'good' initializations by using conventional Quadrature Mirror Filter (QMF) banks and pseudo-QMF banks (which can be readily designed, but do not satisfy PR). It is shown that these filter banks have polyphase component matrices that are 'approximately' lossless. The initialization also enables the design of a family of PR filter banks.

In conventional approaches to pseudo-QMF design, the prototype filter is obtained by optimization, wherein lies the main computational effort. We present a new approach in which the prototype of a M-channel filter bank is obtained by spectral

factorization (of a $2M^{th}$ band filter), thereby eliminating the need for optimization. The overall transfer function $T(z)$ has linear-phase and an approximate 'flat' magnitude response in the region $\epsilon \leq \omega \leq (\pi - \epsilon)$ where ϵ depends on the transition bandwidth of the prototype $0 \leq \epsilon \leq \frac{\pi}{2M}$. A new spectral factorization algorithm (non-iterative) which is based on the Inverse Linear Predictive Coding (LPC) technique is presented. Design examples for the above method are obtained by using this algorithm.

Finally, we consider a dual of the QMF circuit – the transmultiplexer (TMUX). Traditional TMUX designs suppress the undesirable crosstalk. The crosstalk-free transmultiplexer (CF-TMUX) focuses on crosstalk cancellation, rather that suppression. It is shown that the filters of a CF-TMUX are the same as the filters of a 1-skewed AF-QMF bank. In addition, if the QMF bank satisfies PR, then the TMUX also achieves PR.

Contents

1 Introduction **1**

2 Review of Results in Digital Filter Banks **9**

2.1 Decimator and Interpolator 9

2.2 Polyphase Decomposition 11

2.3 Results from PR-QMF Theory 14

2.3.1 Parametrization of Unitary Matrices 16

2.3.2 Lattice Structure for PR-QMF Banks with Pairwise Symmetry 19

2.4 Pseudo-QMF Theory - A Brief Review 21

3 Initialization Techniques for PR-QMF Design **24**

3.1 Initialization for Two-Channel PR-QMF Design 25

3.2 Initialization for M-Channel PR-QMF design 31

3.2.1 PR-QMF Design based on the Lossless Lattice 32

3.2.2 PR-QMF Design based on the Pairwise Symmetric Lattice . . 41

3.3 Summary 44

4 Modulated FIR Filter Banks Satisfying Perfect Reconstruction **46**

4.1 Modulated Filter Banks – An Overview 49

4.1.1 A Key Observation about Pseudo-QMF Banks 49

4.1.2 Polyphase Implementation of Modulated Filter Banks 53

4.2 Modulated PR Filter Banks with $N = 2mM, \quad m \geq 1$ 55

4.3 Design of Prototype ($N = 2mM$) 58
4.3.1 Two-Channel Lossless Lattice 59
4.3.2 Satisfying the Pairwise Power Complementary Constraint . . . 61
4.3.3 Design Steps 64
4.3.4 **Increasing the Length of the Prototype** 66
4.3.5 Two-Stage Design for Long Length Prototypes 66
4.3.6 Implementation and Complexity of Modulated PR Banks . . . 67
4.4 Examples of Modulated PR Filter Banks 68
4.5 Summary 77

5 A Spectral Factorization Approach to Pseudo-QMF Design 83
5.1 Spectral Factorization Approach 86
5.2 Design of the Prototype Filter 97
5.3 Summary 101

6 New Results on Crosstalk-free Transmultiplexers 103
6.1 Transmultiplexer Analysis 107
6.1.1 Simplified Equivalent of the Transmultiplexer 107
6.1.2 Necessary and Sufficient Condition for CC 110
6.1.3 Relation between CF-TMUX filters and AF-QMF banks . . . 112
6.1.4 Alternate Derivation of the CC Condition (Vetterli) 116
6.1.5 Relation between Vetterli's result and Lemma 6.3 118
6.2 Approximate Crosstalk Cancellation 119
6.3 Design Comparison 121
6.4 Summary 125

A Spectral Factorization using the Inverse LPC Technique 126
A.1 Introduction 126

A.2 Linear Predictive Coding (LPC) 128
A.3 The Spectral Factorization Algorithm 129
A.3.1 Computational Complexity 130
A.4 Comparison 130
A.5 Applications of Spectral Factorization 133
A.6 Summary 133

B A Pseudo-QMF Design Example **135**
B.1 Design Considerations 136

List of Figures

1.1 The M-channel maximally decimated circuit 2

2.1 (a) The M-fold decimator 10

2.1 (b) The L-fold interpolator 10

2.2 The noble identities for multirate systems 11

2.3 The representation of the QMF circuit of Fig. 1.1 in terms of the polyphase component matrices $\mathbf{E}(z^M)$ and $\mathbf{R}(z^M)$. 13

2.4 An equivalent representation of the QMF circuit of Fig. 1.1 in terms of the polyphase component matrices $\mathbf{E}(z)$ and $\mathbf{R}(z)$. 13

2.5 (a) Characterization of a FIR lossless matrix $\mathbf{U}_{L-1}(z)$ 15

2.5 (b) Structure of the degree-one factor $\mathbf{V}_k(z)$ 15

2.6 Factorization of the matrix $\mathbf{U}_0$ in term of Givens rotations 17

(a) $\mathbf{U}_0$ represented in terms of $\mathbf{T}_m$ 17

(b) The typical structure for the matrix $\mathbf{T}_m$ (for $m = 3$) 17

(c) Details of each 'criss-cross' used in $\mathbf{T}_m$ 17

2.7 Householder factorization of a unitary matrix $\mathbf{U}_0$ 18

2.8 Implementation of the analysis filters of a pairwise symmetric PR-QMF bank. 21

3.1 Denormalized implementation of the QMF lattice 26

3.2 Design example 3.1. 30

(a) Magnitude response of the conventional QMF filter. 30

(b) Magnitude response of the PR-QMF filter. 30

3.3 Design example 3.2. 36

(a) Responses of the filters of the pseudo-QMF bank, ... 36

(b) Plot of the reconstruction error of the overall analysis/synthesis system, ... 36

(c) Plot of the total aliasing error. 36

3.4 Design example 3.2. Magnitude responses of the PR-QMF banks for different values of ϵ (as multiples of π)

(a) 0.0834 (b) 0.1270 (c) 0.1470 39

3.5 Design example 3.3. Magnitude responses of three of the filters of the 5-channel PR-QMF bank (filter length = 54). 44

4.1 Polyphase implementation of the cosine-modulated analysis filter bank. 54

4.2 (a) The two-channel lossless lattice with four-multiplier lattice sections. $c_j = \cos\theta_j$ and $s_j = \sin\theta_j$. 60

4.2 (b) The two-channel lossless lattice with two-multiplier lattice sections. α is the scaling multiplier 60

4.2 (c) Typical four-multiplier implementation of the p^{th} lattice section of the k^{th} lattice. 60

4.2 (d)A block diagram of the lattices used in the design of an M-channel prototype $H(z)$. The total number of lattices $= r + 1 = \lfloor \frac{M}{2} \rfloor$. 62

4.3 (a) Implementation of a cosine-modulated filter bank derived from a linear phase prototype filter of length $N = 2mM$ (including pseudo-QMF banks). **C** is the Type IV Discrete Cosine Transform (DCT) matrix. 69

4.3 (b)Implementation of cosine-modulated PR analysis filter bank. Each polyphase component pair $\left\{G_k(-z^{2M}), G_{M+k}(-z^{2M})\right\}$ is implemented by a two-channel lossless lattice. (A total of M lattices are used). The cosine-modulation block is given in Fig. 4.3(a). 70

4.4 Design example 4.1. Magnitude responses of 17-channel prototype after Step 1 (Min. energy) and Step 2 (Minimax) (a) $N = 68$ (b) $N = 102$ (c) $N = 136$ 73

4.5 Design example 4.1. 74

(a) Response of the 17-channel prototype ($N = 102$), ... 74

(b) 17-channel cosine-modulated PR filter bank. 74

5.1 (a) The M-channel maximally decimated QMF circuit. 88

5.1 (b) The desired responses of the prototype $H(z)$ of an M-channel pseudo-QMF bank. 88

5.2 A typical four-channel pseudo-QMF bank 90

(a) The analysis filters $H_k(z)$, ... 90

(b) The synthesis filters $F_k(z)$. 90

5.3 The four-channel pseudo-QMF bank ($W = W_4$) 91

(a) $U_2(z)$ and its shifted versions, ... 91

(b) $V_2(z)$ and its shifted versions, ... 91

(c) The synthesis filter $F_2(z)$, ... 91

(d) The six significant terms in $Y_2(z)$. 91

5.4 Design example 5.1. 100

(a) Response of the prototype filter $H(z)$, ... 100

(b) Response of the 8-channel filter bank, ... 10

(c) Magnitude response of $T(z)$, ... 100

(d) Expanded view of (c), ... 100

(e) Plot of aliasing error. 100

5.5 Design example 5.2 102

(a) Reponse of the prototype filter $H(z)$, ... 102

(b) Response of the 8-channel filter bank, ... 102

(c) Magnitude response of $T(z)$, ... 102

(d) Expanded view of (c), ... 102

(e) Plot of aliasing error. 102

6.1 The transmultiplexer system. 105

6.2 (a) Spectrum of input signal $x_i(n)$ 105

6.2 (b) Spectrum of the FDM signal $y(n)$ 105

6.3 The polyphase representation of the transmultiplexer system in Fig. 6.1.110

6.4 Equivalent structure for the transmultiplexer system in Fig. 6.3. . . . 110

6.5 A circuit with an interpolator, a delay and a decimator. 111

6.6 The simplified equivalent representation of the transmultiplexer system in Fig. 6.1. 111

6.7 Conventional 60-channel FDM signal with voice and signaling information. (refer to Bonnerot et al. [Bon78]). 126

B.1. Pseudo-QMF design 138

(a) The desired response of the prototype $H(z)$, ... 138

(b) The response of the prototype shifted by $\frac{\pi}{M}$, ... 138

(c) The "flatness constraint." 138

B.2. Design example B.1. 8-channel pseudo-QMF bank 141

(a) The magnitude response of the prototype (length = 40), ... 141

(b) The responses of the analysis/synthesis filters. 141

B.3. Design example B.1. 142

(a) Magnitude response of $T(z)$ - case 1, ... 142

(b) Magnitude response of $T(z)$ - case 2, ... 142

(c) Plot of the total aliasing error. 142

List of Tables

3.1 Design example 3.1. The values of the parameters of the QMF lattice – initial and optimized 31

3.2 Design example 3.2. Initial estimates of the lattice parameters, obtained from a pseudo-QMF design 38

3.3 Design example 3.2. Final values of the lattice parameters 38

3.4 Design example 3.2. The impulse response coefficients of the analysis filters of the PR-QMF bank (after optimization) 40

3.5 Design example 3.2. Comparison between Modulated PR-Banks and Pseudo-QMF Banks - 3 Channel (filter length = 24) 40

3.6 Design example 3.3. Initial values of the lattice parameters obtained from a pseudo-QMF design ($\mathbf{v}_k$ - degree-one factors and $\mathbf{u}_k$ - Householder vectors 45

3.7 Design example 3.3. Final values of the lattice parameters 45

4.1 Example in Section 4.1.1. The first row of $\tilde{\mathbf{E}}(z)\mathbf{E}(z)$ of a 3-channel pseudo-QMF design. 52

4.2 Comparison of the number of parameters optimized in the design of Modulated PR banks, Pseudo-QMF banks and lattice-based PR-QMF banks. 64

4.3 Design example 4.1. Design of a 17-channel Modulated PR bank prototype 72

4.4 Design example 4.1. Comparison of the 17-channel Modulated PR bank prototype after Step 1 and Step 2 of the optimization 72

4.5 Design example 4.1. Impulse response coefficients of prototype ($N = 102$) of a 17-channel modulated PR filter bank. 75

4.6 (a) Design example 4.2. Comparison between Modulated PR-banks and Pseudo-QMF Banks - 7 Channel (N = 42) 77

4.6 (b) Design example 4.2. Comparison between Modulated PR-banks and Pseudo-QMF Banks - 17 Channel (N = 102) 77

4.7 Comparison of implementation complexity of Modulated PR banks and Pseudo-QMF Banks MPU (APU) - Multiplications (Additions) per unit time 69

4.8 Appendix 4.A. Relation between the matrices $\{\mathbf{A}_0', \mathbf{A}_1'\}$ and $\{\mathbf{A}_0, \mathbf{A}_1\}$ 81

6.1 Comparison of performance of transmultiplexers designed by the CC method and the traditional method (each design with different N, A_s) . 126

6.2 Comparison of performance of transmultiplexers designed by the CC method and the traditional method (each design with different $A_s, \Delta f$) 126

B.1 Design example B.1. Impulse response coefficients of the linear phase prototype $H(z)$ (length=40). Hence $h(n) = h(39 - n)$. 143

B.2 Design example B.1. Impulse response coefficients of $T'(z)$ (only the non-zero coefficients are shown) 143

Chapter 1

Introduction

There has been a tremendous growth in digital technology in recent years and the current trend is towards increasing use of digital techniques. With the improvements in VLSI technology (the ability to build high speed circuits) and with the advent of digital signal processor chips, the scope and applications of digital signal processing (DSP) have been tremendously broadened. The key areas of DSP applications are in telecommunications, speech and image processing, and a host of related fields. Even with the increasing speeds of operation, the search for faster, more efficient algorithms is always present, particularly in view of real-time applications.

A multirate system [Cro83] is a discrete-time system in which the sampling rate (and hence the spacing between samples) can vary from point to point. This results in more efficient processing of signals because the sampling rate at the various nodes can be chosen to be as small as possible. In recent years, there has been tremendous progress and research in this field of multirate systems. An excellent tutorial article on the applications of multirate systems appeared in [Vai90]. Many current applications like digital audio systems, sub-band coding techniques (for speech and image compression),and analog voice privacy systems are mentioned. Further applications include new techniques for adaptive filtering in sub-bands, derivation of new sampling theorems for efficient compression of signals and design of filters with adjustable multilevel responses.

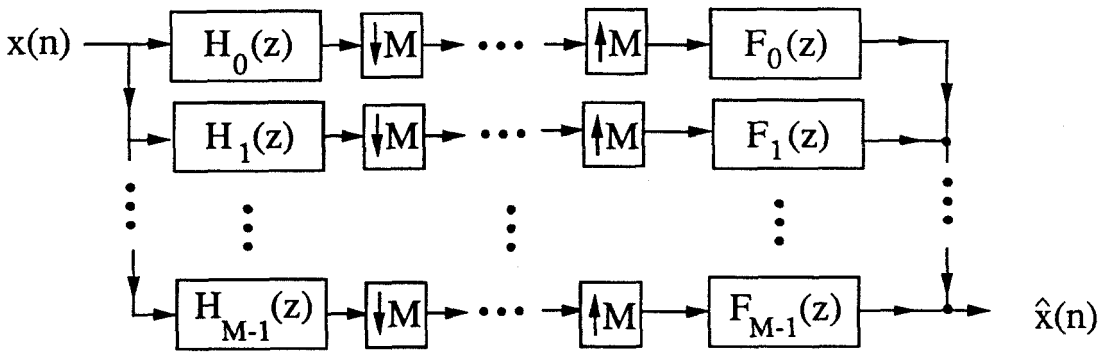

Fig. 1.1. The M-channel, maximally decimated QMF circuit (also known as the sub-band coding circuit.)

One of the topics in multirate DSP that has been extensively studied is that of digital filter banks, primarily because it finds application in a wide spectrum of areas viz., speech compression, voice privacy, radar and sonar signal processing and spectral estimation. In these applications the input signal $x(n)$ is split into frequency sub-bands and then the sub-band signals are processed separately. Finally, the sub-band signals are then re-combined to obtain $\hat{x}(n)$ which is called the *reconstructed signal.* Fig 1.1 shows the schematic of the circuit for this application. The signal is split into M-channels, where M is arbitrary. The filters $[H_0(z),\ H_1(z)\ \cdots\ H_{M-1}(z)]$ are called the *analysis filters* and the filters $[F_0(z),\ F_1(z)\ \cdots\ F_{M-1}(z)]$ are called the *synthesis filters.* Together, they are referred to as the analysis and synthesis filter banks. In Fig 1.1, the other two types of building blocks are the decimator (down-sampler) and the interpolator (up-sampler). These are a part of every multirate system and their description/operation is discussed in Chapter 2.

The M-channel analysis filter bank splits the input signal $x(n)$ into the sub-band signals each of which is down-sampled by a factor of M. Hence it is called maximally decimated. After the decimated sub-band signals are processed (which could typically involve transmitting from one end and receiving at the other end or storage retrieval),

they are up-sampled and combined using the synthesis filter bank. The decimation (down-sampling) introduces aliasing. So, the analysis and synthesis filter bank must be designed such that the effect of aliasing is canceled or minimized.

It was first shown in [Croi76] that for two-channel sub-band coding circuit, the analysis filters $H_0(z)$, $H_1(z)$ and synthesis filters $F_0(z)$, $F_1(z)$ can be chosen such that the aliasing is completely canceled. This is referred to as the Quadrature Mirror Filter (QMF) solution, because of the symmetry of the filters with respect to the quadrature frequency $\frac{\pi}{2}$. Since then, the two-channel sub-band coding circuit has also been called the 'QMF circuit.' In the case of M-channel case, it is called 'M-channel QMF circuit' (though the term QMF circuit is clearly a misnomer in this case!).

The extension of the QMF technique for aliasing cancellation (AC) to the M-channel has been done by several researchers. This is commonly referred to as Pseudo-QMF theory [Nus81,Roth83,Nus84,Mas85,Chu85,Cox86]. In the above-mentioned approaches, the aliasing is either canceled or minimized, so we can write a transfer function between the input $X(z)$ and the output $\widehat{X}(z)$. Depending on the nature of the transfer function, $\widehat{X}(z)$ could have magnitude and/or phase distortion. So, in general, in the QMF circuit, the three errors are :

1. Aliasing
2. Magnitude distortion
3. Phase distortion

(Note that we are assuming that processing (channel transmission, etc.) of the decimated sub-band signals does not introduce any errors). If aliasing is completely canceled, it is called an *alias-free* QMF circuit (AF-QMF). If all three errors are removed, then it is called a *perfect reconstruction* QMF bank (PR-QMF) circuit. The condition for perfect reconstruction (PR) is that the output must be just a delayed

version of the input, i.e. $\hat{x}(n) = x(n - n_0)$, where n_0 is a positive integer.

In [Vai87a,Vet87] it was shown that PR can be achieved in the M-channel case also - thus throwing open an interesting field of study. Researchers have published extensively on the topic of PR-QMF banks [Prin86,Vai88a,Ngu88b,Vai89,Vet89,Nay90, Koi90,Mal90b].

The work in this thesis deals with the diverse issues in the design of multirate digital filter banks, and in particular M-channel QMF banks where $M \geq 2$. Before giving a detailed outline of the research work presented in this thesis, a list of commonly used abbreviations is given.

Abbreviations :

DSP – Digital Signal Processing

QMF – Quadrature Mirror Filter (used synonymously with sub-band coding)

AC – Aliasing Cancellation

PR – Perfect Reconstruction

PR-QMF bank – Filter bank that satisfies the PR property

AF-QMF bank – Filter bank that achieves AC

FIR – Finite Impulse Response

IIR – Infinite Impulse Response

Outline of Thesis

In Chapter 2, we review a number of results from earlier work in QMF theory and multirate digital filter banks. These results serve as a foundation for the research work presented in the subsequent chapters of this thesis. The reviewed results include the input/output relations of the decimator and the interpolator (which are the basic building blocks of multirate systems), the noble identities in multirate DSP, and the

two types of polyphase decomposition. Using these results, we obtain an equivalent representation to the QMF circuit (Fig. 1.1) in terms of the polyphase component matrices of the analysis and synthesis filter banks. Following that, we summarize the results pertaining to FIR filter banks that satisfy the PR property and that have lossless polyphase component matrices. The characterization of FIR lossless transfer matrices and real unitary matrices are given in detail. These results yield lattice structures for the design of PR-QMF banks.

The lattice structure, which in addition to the PR property also forces the pairwise symmetry between the filters, is also discussed. Finally, the main results from pseudo-QMF theory are summarized. This widely used technique deals with the design and implementation of cosine-modulated filter banks (derived from a single prototype filter). In pseudo-QMF banks the phase distortion is eliminated whereas the aliasing and magnitude distortions can be made very small (but are present, nevertheless).

Chapter 3 deals with new initialization techniques for the design of PR-QMF banks, based on the optimization of the parameters of the lattice structures mentioned above. In all cases, we use other designs (like pseudo-QMF designs, which do not satisfy PR but yet have 'good' filters) to obtain an initialization of all the lattice parameters. This enables quicker convergence of the optimization routines. These lattice based approaches for the design of M-channel PR-QMF banks are attractive when the number of channels is small, i.e., for $M \leq 7$. For a higher number of channels, the design becomes increasingly difficult owing to the large number of parameters being optimized. This is due to the fact that optimizing the polyphase component matrix is equivalent to optimizing all the individual filters of the PR-QMF bank.

This leads us to the question - "Is it possible to design PR-QMF banks in which the filters are obtained by the modulation of a single prototype (as in pseudo-QMF

designs)" ? The motivation is the fact that designing only the prototype filter will involve much fewer parameters than designing the entire filter bank. The answer to this question is in the affirmative and the details are discussed in Chapter 4. Here, we assume the prototype filter to be a linear phase filter of length $N = 2mM$ where M is the number of channels and m is any positive integer. First we derive the necessary and sufficient condition on the polyphase component matrix of a cosine-modulated filter bank to satisfy the lossless property. Based on this, we obtain a design procedure (also based on a lattice structure). The many advantages of modulated PR filter banks over pseudo-QMF and existing PR-QMF designs are mentioned. Design examples and comparisons are included to highlight these advantages. Efficient implementation of modulated PR banks and their computational complexity are discussed.

The conventional approach to design pseudo-QMF banks is based on the optimization of the impulse response coefficients of the prototype filter. The optimization involves the minimization of a non-linear, multivariable objective function, and this constitutes the main computational effort in the design process. In Chapter 5, we present a new approach to the design of pseudo-QMF banks, which does not involve any optimization. In this approach, the prototype filter of an M-channel filter bank is obtained as a spectral factor of a $2M^{th}$ band filter. The aliasing cancellation (AC) constraint is derived such that all the significant aliasing terms are canceled. The overall transfer function $T(z)$ of the analysis/synthesis system has linear-phase and an approximately 'flat' magnitude response in the frequency region $\epsilon \leq \omega \leq (\pi - \epsilon)$, where ϵ depends on the transition bandwidth of the prototype filter and $0 < \epsilon < \frac{\pi}{2M}$. Design examples based on this spectral factorization approach are included.

In Chapter 6, the transmultiplexer (TMUX) circuit is studied as a dual of the QMF circuit. The problem of crosstalk poses severe constraints in conventional TMUX designs, since they focus on crosstalk suppression. In QMF theory, conditions for

aliasing cancellation can be obtained. In the same manner, the conditions under which crosstalk in transmultiplexers can be completely canceled are obtained. This is done by using the results from QMF theory (owing to the duality between the two). This study of TMUX, based on polyphase component matrices, brings out the close relation between the TMUX and QMF circuits and also gives a design procedure for crosstalk-free transmultiplexers. The improved performance of crosstalk cancellation over crosstalk suppression is shown by design examples.

The design techniques, discussed in Chapter 3 (for two-channel PR-QMF design) and in Chapter 5 (for the design of the prototype filter of an M-channel pseudo-QMF bank), are based on Spectral Factorization. In Appendix A, we present a new algorithm for spectral factorization. This efficient, non-iterative algorithm uses the well-known Inverse Linear Predictive Coding technique, based on the 'inverse autocorrelations.' This algorithm can be used to compute the minimum phase spectral factor of any moving average (MA) autocorrelation sequence. Comparisons of this method with other spectral factorization techniques are included.

Notations used in the Thesis

The variable ω is used to denote frequency. The frequency response of a discrete-time transfer function (a digital filter) $H(z)$ is expressed as $H(e^{j\omega}) = |H(e^{j\omega})|e^{j\phi(\omega)}$, where $|H(e^{j\omega})|$ is the magnitude response and $\phi(\omega)$ is the phase response. In all the plots, we use the 'normalized frequency' which is $f = \frac{\omega}{2\pi}$. Unless mentioned otherwise, the impulse response coefficients of the filter $H(z)$ can be assumed to be real. If $H(z)$ has real coefficients, then $|H(e^{j\omega})|$ is always plotted for $0 \leq f \leq 0.5$ (because the magnitude response is symmetric with respect to $\omega = 0$).

In this thesis, our primary focus is on FIR filter banks. An FIR transfer function (with real coefficients) $H(z) = \sum_{n=0}^{N-1} h(n)z^{-n}$ is said to have *linear phase* if its phase response $\phi(\omega)$ has the form $k_0 - k_1\omega$. In the time domain, this property is reflected

as a symmetry in the impulse response coefficients of $H(z)$, i.e., they satisfy $h(k) = ch(N-1-k)$, $c = \pm 1$ [Rab75]. Bold-faced letters $\mathbf{v}$, $\mathbf{R}$, $\mathbf{h}(z)$, etc. denote vectors and matrices. $\mathbf{I}_M$ stands for the $M \times M$ identity matrix and $\mathbf{J}_M$ is the $M \times M$ "reverse operator." For example, $\mathbf{J}_3 = \begin{bmatrix} 0 & 0 & 1 \\ 0 & 1 & 0 \\ 1 & 0 & 0 \end{bmatrix}$.

The quantities $\mathbf{R}^T$, $\mathbf{R}^\dagger$, $\mathbf{R}^*$ denote the transpose, the transpose-conjugate and the complex conjugate respectively of the matrix $\mathbf{R}$. The *tilde* accent on the function $\widetilde{\mathbf{U}}(z)$ is defined such that $\widetilde{\mathbf{U}}(z) = \mathbf{U}_*^T(z^{-1})$, $\forall z$, where the subscript asterisk $(*)$ denotes conjugation of the coefficients. For example, if $H(z) = h_0 + h_1 z^{-1}$, then $H_*(z) = h_0^* + h_1^* z^{-1}$.

An $M \times M$ constant matrix $\mathbf{R}$ is said to be unitary (orthogonal if $\mathbf{R}$ is real) if $\mathbf{R}^\dagger \mathbf{R} = c\mathbf{I}_M$, $c \neq 0$. The McMillan degree of $\mathbf{U}(z)$, a $M \times M$ matrix of transfer function is defined as the minimum number of scalar delays (i.e., z^{-1} blocks) required to implement it. We define the complex constant $W_k \triangleq e^{-j\frac{2\pi}{k}}$, where k is an integer. This constant is used in a number of places in the thesis. The subscript k is omitted only if it is obvious from the context. The Discrete Fourier Transform (DFT) [Opp75, Rab75] of an M-point sequence $[x(0), x(1), \cdots x(M-1)]$ is defined as

$$X(k) = \sum_{n=0}^{M-1} x(n) W_M^{nk}, \quad 0 \leq k \leq M-1. \tag{1.1}$$

The inverse DFT (IDFT) is defined as

$$x(n) = \frac{1}{M} \sum_{k=0}^{M-1} X(k) W_M^{-nk}, \quad 0 \leq n \leq M-1. \tag{1.2}$$

An important property of W_M that is often used is

$$\sum_{k=0}^{M-1} W_M^{nk} = \begin{cases} M, & \text{if } n \text{ is a multiple of } M, \\ 0, & \text{otherwise.} \end{cases} \tag{1.3}$$

Chapter 2

Review of Results in Digital Filter Banks

In this chapter, we review a number of results that will be used in the subsequent chapters. First, the basic building blocks in multirate DSP – the decimator and the interpolator, are mentioned along with the two noble identities of multirate DSP. Next, we introduce polyphase decomposition [Bel76], which is widely used in studying digital filter banks. Using this tool, we can obtain an equivalent representation of the QMF circuit (Fig. 1.1) in terms of the polyphase component matrices of the analysis and synthesis filters, then the results from earlier work in PR-QMF theory are reviewed. Our focus is on the class of perfect reconstruction (PR) filter banks whose polyphase component matrices are lossless. Hence, the characterization of FIR transfer matrices that satisfy the losslessness property is also mentioned. Finally, the results from pseudo-QMF theory, which deal with the design of QMF banks in which the aliasing error and the amplitude distortion can be made very small (but are present, nevertheless) are summarized. The results reviewed in this chapter serve as a foundation for the research work presented in this thesis.

2.1 Decimator and Interpolator

These are the basic building blocks of any multirate digital system. The representation of an M-fold decimator (or down-sampler) and an L-fold interpolator (or up-sampler) are shown in Fig. 2.1(a),(b) respectively. The input-output relations of these two

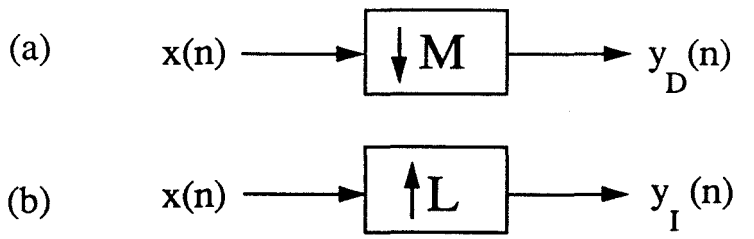

Fig. 2.1 (a) The M-fold decimator
(b) The L-fold interpolator

building blocks are :

$$\textbf{Decimator} \qquad \begin{cases} y_D(n) &= x(Mn), \\ Y_D(z) &= \frac{1}{M}\sum_{\ell=0}^{M-1} X(z^{\frac{1}{M}} W_M^{\ell}), \end{cases} \tag{2.1}$$

where W_M is the complex constant defined in Chapter 1,

$$\textbf{Interpolator} \qquad \begin{cases} y_I(n) &= \begin{cases} x(\frac{n}{L}), & \text{if } n \text{ is a multiple of L} \\ 0, & \text{otherwise,} \end{cases} \\ Y_I(z) &= X(z^L). \end{cases} \tag{2.2}$$

In the time domain, decimation by a factor of M corresponds to retaining one out of every M samples (i.e., by discarding $(M-1)$ samples) as given by (2.1). This compression in the time-domain results in a 'stretching' in the frequency domain and also produces shifted versions (in frequency) of the input. So if the input is not suitably band-limited, then decimation causes an overlap of the stretched, shifted versions which is called *aliasing*. On the other hand, interpolation by a factor of L corresponds to inserting $(L-1)$ zero-valued samples between every two samples of the input, thereby increasing the sample rate by a factor of L. This results in a 'compression' in the frequency domain, as given by (2.2) along with the creation of $(L-1)$ *images*. The basic difference between aliasing (due to decimation) and imaging (due to interpolation) is that the former can result in the loss of information while in the latter, there is no loss of information. Decimators and interpolators are both linear systems but are *time-varying*.

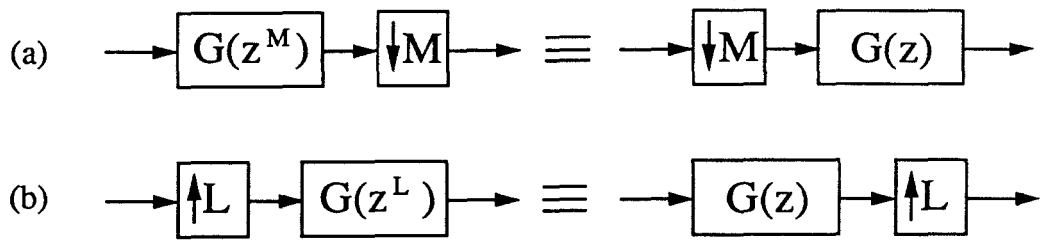

Fig. 2.2. Noble identities for multirate systems.

Two Noble Identities : In multirate systems, we often encounter interconnections of decimators and interpolators with filters and other transfer function blocks. The two identities (called the noble identities) given in Fig. 2.2(a),(b) play an important role in the efficient implementation of these interconnections. The two identities hold if $G(z)$ is a rational transfer function, i.e., a ratio of two polynomials in z^{-1}. They can be readily verified by using (2.1) and (2.2) respectively.

2.2 Polyphase Decomposition

This fundamental tool, which is widely used in multirate DSP, was originally introduced in [Bel76]. There are two types of polyphase decomposition – Type 1 and Type 2, as defined in [Vai90]. Let $H(z) = \sum_{n=-\infty}^{\infty} h(n)z^{-n}$ be a digital transfer function. Then $H(z)$ can always be expressed as

$$H(z) = \sum_{\ell=0}^{M-1} z^{-\ell} E_\ell(z^M), \qquad \text{(Type 1)} \tag{2.3}$$

and

$$H(z) = \sum_{\ell=0}^{M-1} z^{-(M-1-\ell)} R_\ell(z^M), \qquad \text{(Type 2)} \tag{2.4}$$

where $E_\ell(z)$ and $R_\ell(z)$ are the Type 1 and Type 2 polyphase components respectively of the transfer function $H(z)$, and M is an integer. The value of M is chosen depending on the decimation/interpolation factor involved in the circuit.

In our application, we are dealing solely with FIR filters. So in all cases, the polyphase components can be obtained by inspection. Consider $\{H_k(z),\ F_k(z)\}$, the M-channel QMF bank (FIR) shown in Fig. 1.1. Using polyphase decomposition of Type 1 for the analysis filters and of Type 2 for the synthesis filters, we can write

$$H_k(z) = \sum_{\ell=0}^{M-1} z^{-\ell} E_{k,\ell}(z^M), \quad 0 \le k \le M-1, \tag{2.5}$$

$$F_k(z) = \sum_{\ell=0}^{M-1} z^{-(M-1-\ell)} R_{\ell,k}(z^M), \quad 0 \le k \le M-1. \tag{2.6}$$

Hence, the analysis and synthesis filter banks can be expressed as

$$\begin{bmatrix} H_0(z) \\ \vdots \\ H_{M-1}(z) \end{bmatrix} = \begin{bmatrix} E_{0,0}(z^M) & \cdots & E_{0,M-1}(z^M) \\ \vdots & \vdots & \vdots \\ E_{M-1,0}(z^M) & \cdots & E_{M-1,M-1}(z^M) \end{bmatrix} \begin{bmatrix} 1 \\ \vdots \\ z^{-(M-1)} \end{bmatrix}, \tag{2.7}$$

$$[F_0(z) \ \cdots \ F_{M-1}(z)] = \begin{bmatrix} z^{-(M-1)} & \cdots & 1 \end{bmatrix} \begin{bmatrix} R_{0,0}(z^M) & \cdots & R_{0,M-1}(z^M) \\ \vdots & \vdots & \vdots \\ R_{M-1,0}(z^M) & \cdots & R_{M-1,M-1}(z^M) \end{bmatrix}. \tag{2.8}$$

Equations (2.7) and (2.8) can also be expressed as

$$\mathbf{h}(z) = [H_0(z) \ \cdots \ H_{M-1}(z)] = \mathbf{E}(z^M)\mathbf{e}_M(z), \tag{2.9}$$

$$\mathbf{f}^T(z) = [F_0(z) \ \cdots \ F_{M-1}(z)] = z^{-(M-1)}\tilde{\mathbf{e}}_M(z)\mathbf{R}(z^M), \tag{2.10}$$

where $\mathbf{e}_M^T(z) = \begin{bmatrix} 1 & z^{-1} & \cdots & z^{-(M-1)} \end{bmatrix}$. The $M \times M$ matrices $\mathbf{E}(z)$ and $\mathbf{R}(z)$ are called the *polyphase component matrices* of the analysis and synthesis filter banks respectively and are defined as

$$[\mathbf{E}(z)]_{k,\ell} \triangleq E_{k,\ell}(z) \quad \text{and} \quad [\mathbf{R}(z)]_{k,\ell} \triangleq R_{k,\ell}(z), \quad 0 \le k, \ell \le M-1. \tag{2.11}$$

Since all the analysis and synthesis filters are FIR, all the elements of $\mathbf{E}(z)$ and $\mathbf{R}(z)$ are also FIR transfer functions.

We now obtain an equivalent representation of the QMF circuit in Fig. 1.1 in terms of the polyphase component matrices $\mathbf{E}(z)$ and $\mathbf{R}(z)$. Using the results in (2.9) and (2.10) in Fig. 1.1, we get Fig. 2.3. Further, using the noble identities, the decimators

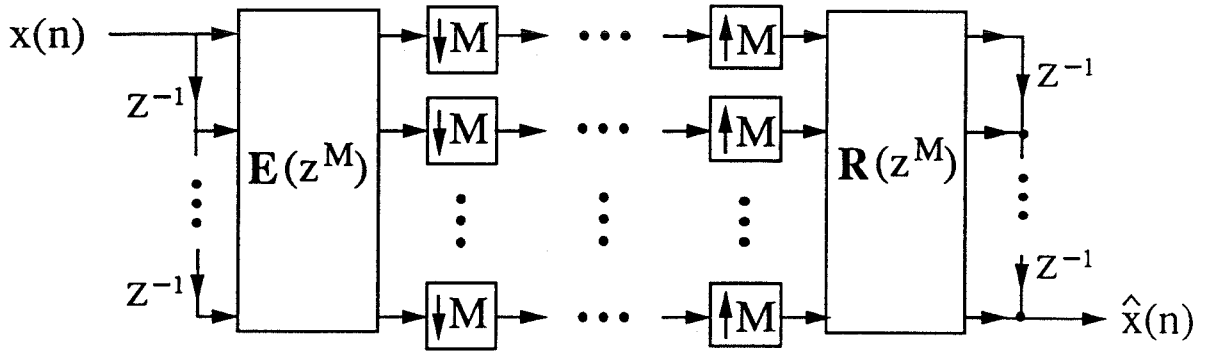

Fig. 2.3. The representation of the QMF circuit of Fig.1 in terms of the polyphase component matrices $E(z^M)$ and $R(z^M)$.

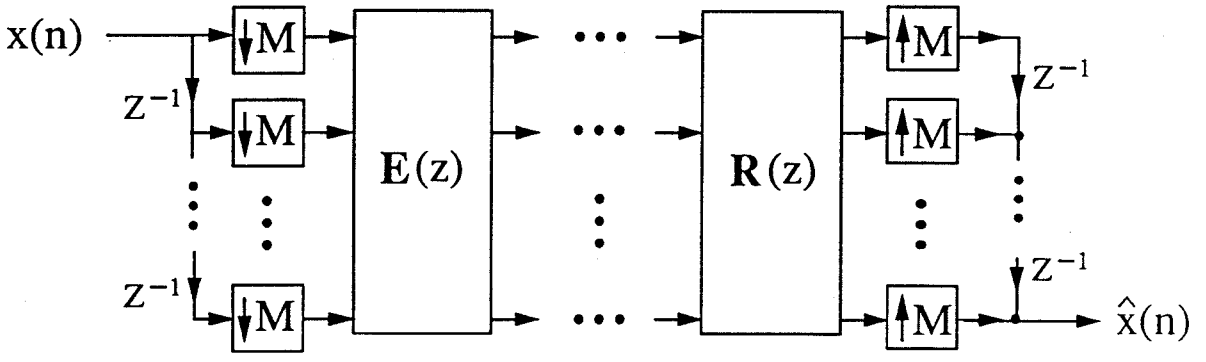

Fig. 2.4. An equivalent representation of the QMF circuit of Fig.1 in terms of the polyphase component matrices E(z) and R(z).

and interpolators in Fig. 2.3 can be appropriately moved in order to give Fig. 2.4. In the subsequent chapters, we will repeatedly refer to this representation of the QMF circuit (Fig. 2.4).

2.3 Results from PR-QMF Theory

The results in Lemma 3.1 and Property 3.4 [Vai87a] can be summarized as follows

Lemma 2.1 : Consider the maximally decimated QMF bank with FIR analysis filters. Let $\mathbf{E}(z)$ be the polyphase component matrix of the analysis filters. Then any two of the following three statements imply the remaining statement :

1. $\mathbf{E}(z)$ is lossless,
2. The analysis and synthesis filters are related as

$$F_k(z) = c\widetilde{H}_k(z), \quad 0 \leq k \leq M-1, \tag{2.12}$$

   where c is a constant,

3. The analysis/synthesis system satisfies the PR property. $\Diamond$

Definition : A $p \times r$ matrix of transfer functions, $\mathbf{U}(z)$, is said to be *lossless* if it is stable and it satisfies the property

$$\widetilde{\mathbf{U}}(z)\mathbf{U}(z) = d\mathbf{I}_r, \tag{2.13}$$

where $\mathbf{I}_M$ is the identity matrix and d is a real, positive constant. $\Diamond$

From the above Lemma, we see that if $\mathbf{E}(z)$ is lossless, then we can always obtain a PR-QMF system by choosing the synthesis filters as in (2.12). In other words, the losslessness of $\mathbf{E}(z)$ is a sufficient condition for obtaining a PR-QMF system. So we focus on the class of FIR filter banks whose polyphase component matrices are lossless. Next, we present the results pertaining to the characterization of lossless transfer matrices, which structurally ensures that the lossless property is satisfied. From [Vai89], we have the following result.

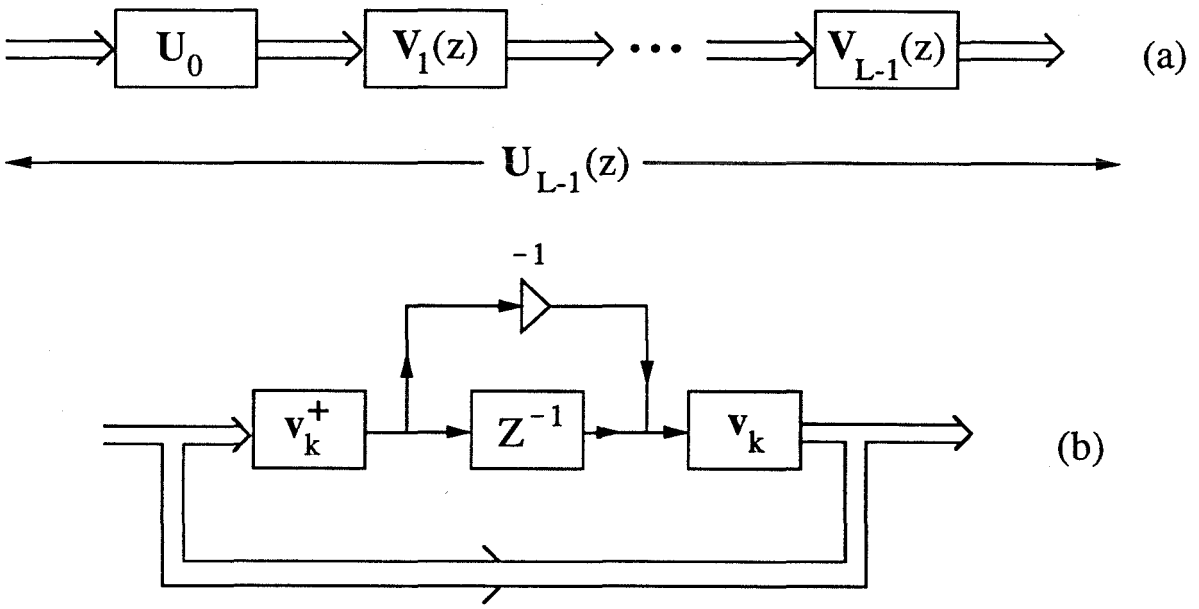

Fig. 2. 5. (a). Characterization of a FIR lossless matrix $\mathbf{U}_{L-1}(z)$
(b). Structure of the degree-one factor $\mathbf{V}_k(z)$

Lemma 2.2 : Let $\mathbf{U}_{L-1}(z)$ be any $M\times M$ causal, FIR transfer matrix. Then, $\mathbf{U}_{L-1}(z)$ is lossless of McMillan degree $(L-1)$ if and only if it can be written in the form

$$\mathbf{U}_{L-1}(z) = \mathbf{V}_{L-1}(z)\mathbf{V}_{L-2}(z)\cdots\mathbf{V}_1(z)\mathbf{U}_0, \tag{2.14}$$

where $\mathbf{U}_0$ is constant $M\times M$ unitary matrix and $\mathbf{V}_k(z)$ is a degree-one FIR lossless matrix of the form

$$\mathbf{V}_k(z) = \left[\mathbf{I}_M - \mathbf{v}_k\mathbf{v}_k^\dagger + z^{-1}\mathbf{v}_k\mathbf{v}_k^\dagger\right], \tag{2.15}$$

where $\mathbf{v}_k$ is a $M\times 1$ column vector with unit norm. $\diamondsuit$.

This result is shown pictorially in Fig. 2.5(a),(b). The implementation in Fig. 2.5(a) is referred to as the *lossless lattice* since any $M\times M$ FIR transfer matrix that is lossless can be realized in this form and conversely, every transfer matrix realized in this form is necessarily lossless. In particular, any polyphase component matrix $\mathbf{E}(z)$ obtained

by using the lossless lattice is guaranteed to satisfy the lossless property.

2.3.1 Parametrization of Unitary Matrices

The implementation of (2.14) involves the $M \times M$ unitary matrix $\mathbf{U}_0$. We now consider two parametrizations of the unitary matrix $\mathbf{U}_0$, satisfying $\mathbf{U}_0^\dagger \mathbf{U}_0 = \mathbf{I}_M$.

1. Using Givens rotations [Mur62,Doga88] : This is the well known parametrization of a real, $M \times M$ unitary matrix by using $\frac{M(M-1)}{2}$ Givens rotations. An $M \times M$ Givens rotation that operates in the ij^{th} plane has the form

$$\mathbf{\Theta}_{i,j} = \begin{array}{c} \\ 0 \\ 1 \\ \vdots \\ \mathrm{i} \\ \vdots \\ \mathrm{j} \\ \vdots \\ (\mathrm{M\text{-}1}) \end{array} \begin{array}{c} \begin{array}{ccccccccc} 0 & 1 & \cdots & \mathrm{i} & \cdots & \mathrm{j} & \cdots & (\mathrm{M\text{-}1}) \end{array} \\ \begin{bmatrix} 1 & & & & & & & \\ & 1 & & & & & & \\ & & \ddots & & & & & \\ & & & c_{ij} & & -s_{ij} & & \\ & & & & \ddots & & & \\ & & & s_{ij} & & c_{ij} & & \\ & & & & & & \ddots & \\ & & & & & & & 1 \end{bmatrix} \end{array}, \qquad 0 \le i,j \le M-1, \tag{2.16}$$

where $c_{ij} = \cos\theta_{i,j}$ and $s_{ij} = \sin\theta_{i,j}$. Clearly $\mathbf{\Theta}_{i,j}$ is a unitary matrix. By proper choice of the rotation angles $\theta_{i,j}$, we can express the unitary matrix $\mathbf{U}_0$ as

$$\mathbf{U}_0 = \mathbf{\Lambda} \underbrace{[\mathbf{\Theta}_{M-2,M-1}]}_{\mathbf{T}_{M-1}} \underbrace{[\mathbf{\Theta}_{M-3,M-1}\mathbf{\Theta}_{M-3,M-2}]}_{\mathbf{T}_{M-2}} \cdots \underbrace{[\mathbf{\Theta}_{0,M-1}\mathbf{\Theta}_{0,M-2}\cdots\mathbf{\Theta}_{0,1}]}_{\mathbf{T}_1}, \tag{2.17}$$

where $\mathbf{\Lambda}$ is an $M \times M$ diagonal matrix whose entries are $[\mathbf{\Lambda}]_{i,i} = \pm 1$. This implementation of $\mathbf{U}_0$ is shown in Fig. 2.6.

2. Using the Householder Factorization : This is another parametrization of unitary matrices, which is very convenient.

Definition : An $M \times M$ Householder matrix $\mathbf{G}$ has the form

$$\mathbf{G} = \left[\mathbf{I}_M - 2\mathbf{u}\mathbf{u}^\dagger\right], \tag{2.18}$$

where $\mathbf{u}$ is an $M \times 1$ vector with unit norm. $\diamondsuit$

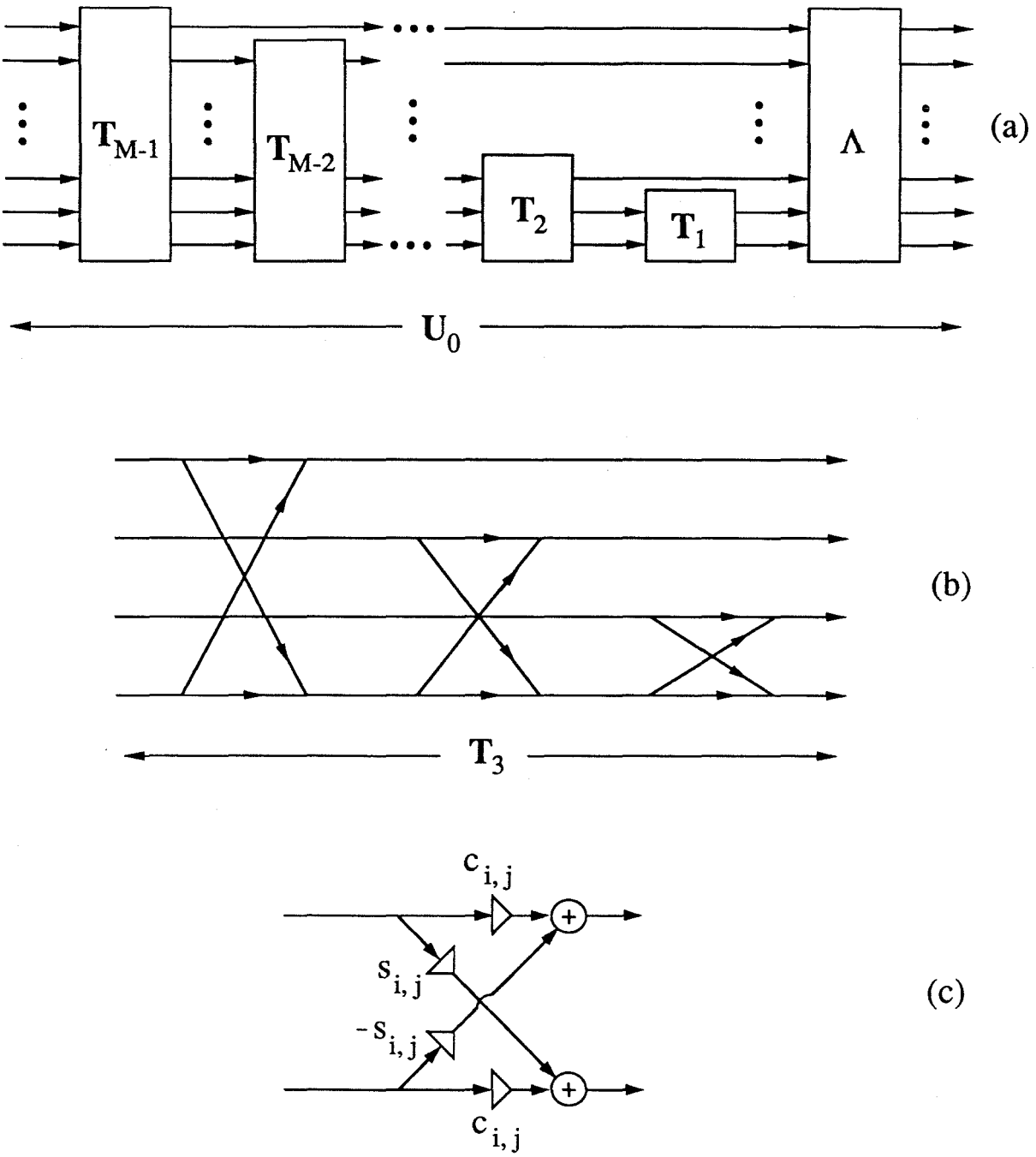

Fig. 2.6. Factorization of the matrix $\mathbf{U}_0$ in terms of Givens rotations
(a) $\mathbf{U}_0$ represented in terms of $\mathbf{T}_m$
(b) The typical structure for the matrix $\mathbf{T}_m$ (for m=3)
(c) Details of each 'criss-cross' used in $\mathbf{T}_m$
$c_{i,j} = \cos\theta_{i,j}$ and $s_{i,j} = \sin\theta_{i,j}$

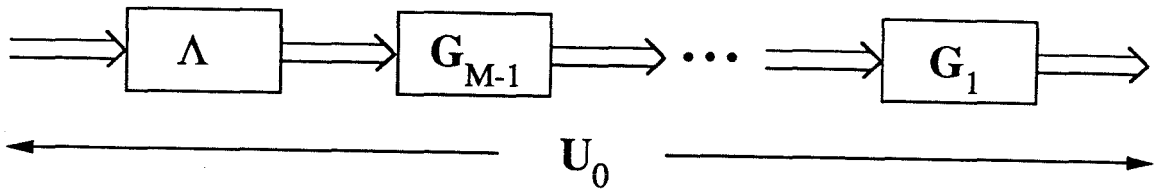

Fig. 2.7. Householder factorization of a unitary matrix $\mathbf{U}_0$

Fact 2.1 : Let $\mathbf{v} = [v_0\ v_1\ \cdots\ v_{M-1}]^T$ be some $M\times 1$ non-zero vector with real entries. Define the vector $\mathbf{w}$ as $\mathbf{w} \triangleq \mathbf{v} + s\|\mathbf{v}\|\mathbf{e}_1$, where $\mathbf{e}_1^T = [1\ 0\ \cdots\ 0]$ and $s = \pm 1$. Then

$$\left[\mathbf{I}_M - 2\mathbf{u}\mathbf{u}^\dagger\right]\mathbf{v} = -s\|\mathbf{v}\|\mathbf{e}_1, \tag{2.19}$$

where $\mathbf{u} = \frac{\mathbf{w}}{\|\mathbf{w}\|}$. $\Diamond$

By successively using Fact 2.1, we get

Fact 2.2 : Any $M\times M$ real unitary matrix $\mathbf{U}_0$ can be represented in the form

$$\mathbf{U}_0 = \mathbf{G}_1\mathbf{G}_2\cdots\mathbf{G}_{M-1}\mathbf{\Lambda}, \tag{2.20}$$

where $\mathbf{\Lambda}$ is an $M\times M$ diagonal matrix whose entries are $[\mathbf{\Lambda}]_{i,i} = \pm 1$, and the matrices $\mathbf{G}_i$ are Householder matrices. $\Diamond$

This implementation of $\mathbf{U}_0$ is shown in Fig. 2.7. Let $\mathbf{u}_i$ be the unit norm vectors associated with the corresponding Householder matrix $\mathbf{G}_i$. The vectors $\mathbf{u}_i$ have the structure shown below.

$$[\mathbf{u}_1\ \mathbf{u}_2\ \cdots\ \mathbf{u}_{M-1}] = \begin{bmatrix} \mathrm{x} & 0 & 0 & \cdots & 0 \\ \mathrm{x} & \mathrm{x} & 0 & \cdots & 0 \\ \mathrm{x} & \mathrm{x} & \mathrm{x} & \cdots & 0 \\ \vdots & \vdots & \vdots & \vdots & \vdots \\ \mathrm{x} & \mathrm{x} & \mathrm{x} & \cdots & 0 \\ \mathrm{x} & \mathrm{x} & \mathrm{x} & \cdots & \mathrm{x} \\ \mathrm{x} & \mathrm{x} & \mathrm{x} & \cdots & \mathrm{x} \end{bmatrix}, \tag{2.21}$$

where 'x' represents a non-zero entry. Each $\mathbf{u}_i$ has $(M+1-i)$ non-zero entries, but owing to the unit norm constraint, it has only $(M-i)$ degrees of freedom. Hence the

Householder factorization (2.20) of unitary matrices involves a total of $\frac{M(M-1)}{2}$ degrees of freedom, which is the same as in the case of the Givens rotation parametrization.

However, since the Householder factorization preserves the unitariness of $\mathbf{U}_0$ even under coefficient quantization and since it has a simple structure, it is more convenient to use this factorization for M-channel PR-QMF designs (particularly for large M).

2.3.2 Lattice Structure for PR-QMF Banks with Pairwise Symmetry

In [Ngu88b], lattice structures have been derived for M-channel filter banks which in addition to satisfying the PR property, also satisfy a pairwise symmetry property between the filters. The main advantage in forcing the pairwise symmetry is that the number of parameters involved in the design of the PR-QMF bank is reduced by nearly a factor of two. Our focus will be on the design of PR-QMF banks where M is prime, because for other values of M, we can obtain the PR-QMF bank by a tree-structured implementation. For example, for $M = 6$, the PR-QMF bank can be obtained by cascading a 2-channel and a 3-channel PR-QMF bank. Hence, we consider the pairwise symmetric lattice derived in [Ngu88b] for odd values of M.

Let $[H_0(z)\ H_1(z)\ \cdots\ H_{M-1}(z)]$ be an M-channel analysis filter bank. (M is assumed to be odd). The pairwise symmetry constraint forces the following relation between pairs of filters

$$H_{M-1-k}(z) = H_k(-z), \quad 0 \leq k \leq M-1. \tag{2.22}$$

This also gives $H_{\frac{M-1}{2}}(z) = H_{\frac{M-1}{2}}(-z)$, which forces the filter $H_{\frac{M-1}{2}}(z)$ to be a function of z^2. We will obtain the pairwise symmetric PR-QMF lattice structure for the special case $M = 3$, and then generalize the result for arbitrary M (which is odd). For 3-channel designs, the pairwise symmetry constraint is

$$H_2(z) = H_0(-z), \tag{2.23}$$

$$H_1(z) = \text{a function of } z^2. \tag{2.24}$$

Hence the analysis filters can be expressed as

$$\mathbf{h}(z) = \begin{bmatrix} H_0(z) \\ H_1(z) \\ H_2(z) \end{bmatrix} = \frac{1}{\sqrt{2}} \underbrace{\begin{bmatrix} 1 & 0 & 1 \\ 0 & \sqrt{2} & 0 \\ 1 & 0 & 1 \end{bmatrix}}_{\mathbf{R}_3} \underbrace{\begin{bmatrix} 1 & & \\ & 1 & \\ & & z^{-3} \end{bmatrix}}_{\mathbf{\Gamma}(z^3)} \begin{bmatrix} \alpha_0(z^2) \\ \alpha_1(z^2) \\ \alpha_2(z^2) \end{bmatrix} \tag{2.25}$$

Expressing the $\alpha_i(z)$ in terms of their Type 1 polyphase components $A_{i,j}$,

$$\begin{bmatrix} \alpha_0(z) \\ \alpha_1(z) \\ \alpha_2(z) \end{bmatrix} = \mathbf{A}(z^3) \underbrace{\begin{bmatrix} 1 \\ z^{-1} \\ z^{-2} \end{bmatrix}}_{\mathbf{e}_3(z)}. \tag{2.26}$$

Substituting (2.26) in (2.25), we get

$$\mathbf{h}(z) = \frac{1}{\sqrt{2}} \mathbf{R}_3 \mathbf{\Gamma}(z^3) \mathbf{A}(z^6) \mathbf{e}_3(z^2). \tag{2.27}$$

For general M (where M is odd), we get

$$\mathbf{h}(z) = \frac{1}{\sqrt{2}} \mathbf{R}_M \mathbf{\Gamma}(z^M) \mathbf{A}(z^{2M}) \mathbf{e}_M(z^2). \tag{2.28}$$

In (2.28), if $\mathbf{A}(z)$ is lossless, then we can always find a synthesis filter bank, as shown below, such that the overall system satisfies PR. The synthesis filter bank can be expressed as

$$\mathbf{f}^T(z) = [F_0(z) \ \cdots \ F_{M-1}(z)] = \frac{z^{-s}}{\sqrt{2}} \tilde{\mathbf{e}}_M(z^2) \widetilde{\mathbf{A}}(z^{2M}) \tilde{\mathbf{\Gamma}}(z^M) \mathbf{R}_M^{\dagger}, \tag{2.29}$$

where s is a positive integer which is chosen such that the synthesis filters $F_k(z)$ are causal. The implementation of the analysis filters of a pairwise symmetric PR-QMF bank (2.28), is shown in Fig. 2.8. This figure is referred to as the pairwise symmetric PR-QMF lattice structure.

The main advantage of using the pairwise symmetric lattice is that there is a savings in the number of parameters being optimized. In this approach, we design the lossless matrix $\mathbf{A}(z)$ (given in (2.28)) whereas in the approach presented in [Vai87a], the lossless matrix $\mathbf{E}(z)$ (defined in (2.9)) is optimized. Both $\mathbf{A}(z)$ and $\mathbf{E}(z)$ are FIR transfer matrices but the order of the former is approximately half of the order of

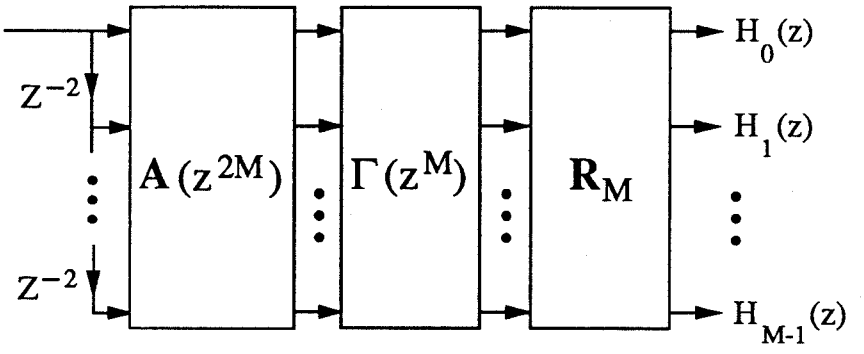

Fig. 2.8. Implementation of the analysis filters of a pairwise symmetric PR-QMF bank.

the latter. This directly results in the savings in terms of the number of parameters [Doga88]. Another advantage of imposing the pairwise symmetry is that the objective function to be minimized is simpler, i.e., for a 3-channel PR-QMF design with analysis filters $\{H_0(z),\ H_1(z),\ H_2(z)\}$, the approach in [Vai87a] uses the objective function

$$\phi = \int_{\frac{\pi}{3}+\epsilon}^{\pi} |H_0(e^{j\omega})|^2 d\omega + \int_0^{\frac{\pi}{3}-\epsilon} |H_1(e^{j\omega})|^2 d\omega + \int_{\frac{2\pi}{3}+\epsilon}^{\pi} |H_1(e^{j\omega})|^2 d\omega + \int_0^{\frac{2\pi}{3}-\epsilon} |H_2(e^{j\omega})|^2 d\omega, \tag{2.30}$$

whereas with the pairwise symmetric lattice, the objective function used is

$$\phi = \int_{\frac{\pi}{3}+\epsilon}^{\pi} |H_0(e^{j\omega})|^2 d\omega + \int_0^{\frac{\pi}{3}-\epsilon} |H_1(e^{j\omega})|^2 d\omega. \tag{2.31}$$

The other two terms are not required because of the symmetry forced on the magnitude responses of the filters. This advantage becomes significant when designing PR-QMF banks for large M (the number of channels).

2.4 Pseudo-QMF Theory - A Brief Review

Pseudo-QMF theory is well known [Roth83,Mas85,Nus81,Nus84,Chu85,Cox86] and is widely used. It deals with the extension of the two-channel QMF solution [Croi76] to M channels, where M is arbitrary. Two primary assumptions, upon which pseudo-

QMF designs are based, are listed below.

1. The desired analysis and synthesis filters are "good" filters, i.e., they have narrow transition bands and high stopband attenuation – which implies that the overlap between non-adjacent filters is negligible.

2. With the previous assumption being satisfied, the significant aliasing terms are those due to the overlap of filters in adjacent channels. These terms will be canceled by the aliasing cancellation (AC) constraint imposed on the analysis and synthesis filters.

The main results are summarized below (refer to [Roth83,Mas85,Cox86] for details) :

1. The first step is the design of the prototype filter $H(z) = \sum_{n=0}^{N-1} h(n)z^{-n}$, which is a linear-phase lowpass filter. The typical response of an M-channel prototype is shown in Fig. 5.1. In the design of $H(z)$, the following two constraints are imposed: (a) the minimization of the stopband energy of $H(z)$ and (b) the flatness constraint, to minimize the magnitude distortion (the reconstruction error) between the output and the input.

2. $H_k(z)$ and $F_k(z)$, the analysis and synthesis filters respectively of the pseudo-QMF bank are obtained by modulation of the prototype $H(z)$ as shown below.

$$H_k(z) = \left[a_k c_k H(ze^{-j(2k+1)\frac{\pi}{2M}}) + a_k^* c_k^* H(ze^{j(2k+1)\frac{\pi}{2M}})\right], \quad 0 \le k \le M-1, \quad (2.32)$$

$$F_k(z) = \left[a_k^* c_k H(ze^{-j(2k+1)\frac{\pi}{2M}}) + a_k c_k^* H(ze^{j(2k+1)\frac{\pi}{2M}})\right], \quad 0 \le k \le M-1, \quad (2.33)$$

where a_k and c_k are complex constants given by $a_k = e^{j\theta_k}$, $c_k = e^{-j(2k+1)\frac{\pi}{2M}(\frac{N-1}{2})}$ and N is the length of the prototype. $h_k(n)$ and $f_k(n)$, the impulse responses of $H_k(z)$ and $F_k(z)$ respectively are given by

$$h_k(n) = 2h(n)\cos\left((2k+1)\frac{\pi}{2M}(n - \frac{N-1}{2}) + \theta_k\right), \quad 0 \le n \le N-1, \quad (2.34)$$

$$f_k(n) = 2h(n)\cos\left((2k+1)\frac{\pi}{2M}(n - \frac{N-1}{2}) - \theta_k\right), \quad 0 \le n \le N-1. \quad (2.35)$$

From (2.34) and (2.35), we can verify that the analysis and synthesis filters are related as

$$f_k(n) = h_k(N-1-n) \quad \text{and} \quad F_k(z) = z^{-(N-1)}H_k(z^{-1}), \tag{2.36}$$

for $0 \leq k \leq M-1$.

3. The θ_k are chosen to satisfy the AC constraint which ensures that all the significant aliasing terms are canceled. Hence, the overall system is 'approximately' alias-free. The condition on θ_k is

$$\theta_{k+1} = \theta_k \pm \frac{\pi}{2}, \qquad 0 \leq k < M-1. \tag{2.37}$$

Further, in order to ensure a 'flat' response at all frequencies (including $\omega = 0$ and $\omega = \pi$), we require

$$\theta_0 = \pm(\frac{\pi}{4} + \ell\frac{\pi}{2}) \quad \text{and} \quad \theta_{M-1} = \pm(\frac{\pi}{4} + m\frac{\pi}{2}), \tag{2.38}$$

where ℓ, m are integers. Each choice of sign in (2.37), (2.38) and the values of ℓ, m can be made entirely independent of other choices. In this thesis, we will use the choice

$$\theta_k = (-1)^k\frac{\pi}{4}, \quad 0 \leq k \leq M-1, \tag{2.39}$$

which satisfies both (2.37) and (2.38). It must be noted that several other choices are possible [Roth83,Vet89].

4. $T(z)$, the overall transfer function of the analysis/synthesis system is given by

$$T(z) = \frac{1}{M}\sum_{k=0}^{M-1} H_k(z)F_k(z) = \frac{z^{-(N-1)}}{M}\sum_{k=0}^{M-1} H_k(z)H_k(z^{-1}). \tag{2.40}$$

Hence, $T(z)$ has linear-phase and the analysis/synthesis system is free from phase distortion.

A complete pseudo-QMF design example is given in Appendix B.

Chapter 3

Initialization Techniques for PR-QMF Design

In this chapter, initialization procedures for the lattice-based PR-QMF design techniques are presented. These design approaches can be used for the design of M-channel PR-QMF banks, where $M \geq 2$. The theory of PR-QMF banks has been widely studied [Smi84,Vai87a,Vet87]. In [Smi84], it was first established that for the two-channel QMF circuit, the analysis and synthesis filters can be designed such that perfect reconstruction (PR) of the input can be achieved, i.e, $\hat{x}(n) = x(n - n_0)$, where n_0 is a positive integer. It was then shown in [Vai87a,Vet87] that PR can be achieved for the M-channel QMF circuits (Fig. 1.1). In particular, in [Vai87a], the relation between PR-QMF banks and the lossless property of their polyphase component matrices was established. This also showed that it is possible to obtain PR-QMF banks in which both the analysis and synthesis filters are FIR filters. Our focus is on this class of FIR PR-QMF designs, i.e, the design techniques based on forcing the polyphase component matrix of the filter bank to be lossless.

The design procedures, both in the two-channel case [Vai88a] as well as the M-channel case [Vai87a,Ngu88b,Vai89], are based on lattice structures which structurally ensure the PR property. These lattice structures are characterized by lattice parameters. The above methods involve optimization, i.e., the minimization of a non-linear objective function of the lattice parameters. As with all design methods involving optimization, obtaining 'good' initializing values (for the variables being optimized)

plays an important role in getting good results and in reducing the time required for the optimization to converge. The main objective of this chapter is to present procedures for obtaining suitable initialization of the lattice parameters for the different design approaches. For the two-channel PR-QMF design, the initialization is obtained from conventional QMF designs [Jon80,Cro83]. The details are given in Section 3.1. For the case of M-channel PR-QMF designs ($M \geq 3$), the initialization is obtained from Pseudo-QMF designs [Roth83,Nus81,Mas85] and the details are presented in Section 3.2.

Notation : In order to improve the clarity of the presentation, we introduce the following notation (just for this chapter) : the filters, polyphase components etc., belonging to QMF banks that do not satisfy the PR property, will have a *prime* notation (as in $H_0'(z)$) in order to distinguish them from their counterparts in the PR-QMF case, which will be denoted as usual.

3.1 Initialization for Two-Channel PR-QMF Design

We now consider the two-channel PR-QMF design procedure presented in [Vai88a]. Two filters $H_0(z) = \sum_{n=0}^{N-1} h_0(n)z^{-n}$ and $H_1(z) = \sum_{n=0}^{N-1} h_1(n)z^{-n}$ are said to be a Power Complementary Image (PCI) pair if

$$|H_0(e^{j\omega})|^2 + |H_1(e^{j\omega})|^2 = d, \quad \forall\omega, \tag{3.1}$$

where d is a non-zero constant, and

$$H_1(z) = z^{-(N-1)}H_0(-z^{-1}). \tag{3.2}$$

It is shown in [Vai88a] that every PCI pair of transfer functions (FIR) can be implemented by the lattice in Fig. 3.1. This lattice structure, which is referred to as the QMF lattice, is a cascade of lattice sections (normalized or denormalized). In Fig. 3.1, we have the representation in terms of the denormalized lattice sections,

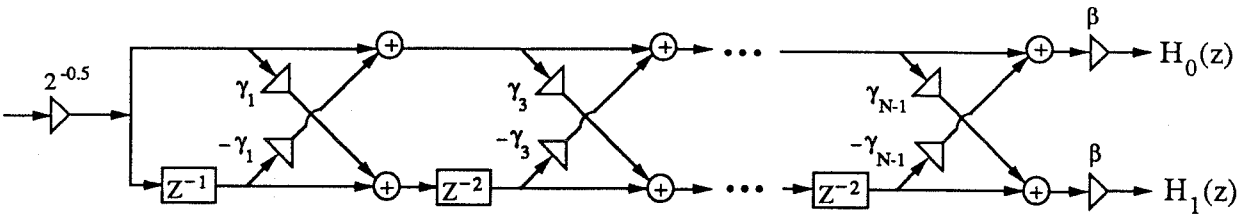

Fig. 3.1. Denormalized implementation of the QMF lattice

which requires the scaling multiplier β which is given by $\beta = \prod_m \frac{1}{\sqrt{1+\gamma_{2m+1}^2}}$.

It is shown in Section III [Vai88a] that any filter bank $\{H_0(z),\ H_1(z)\}$ obtained by optimizing the parameters of the QMF lattice has the property that its polyphase component matrix $\mathbf{E}(z)$ is lossless. From Lemma 2.1, we know that the losslessness of $\mathbf{E}(z)$ is sufficient to ensure PR. Using Type 1 polyphase decomposition [Vai90], we can express the analysis filter bank as

$$\mathbf{h}(z) = \begin{bmatrix} H_0(z) \\ H_1(z) \end{bmatrix} = \underbrace{\begin{bmatrix} E_{00}(z^2) & E_{01}(z^2) \\ E_{10}(z^2) & E_{11}(z^2) \end{bmatrix}}_{\mathbf{E}(z)} \begin{bmatrix} 1 \\ z^{-1} \end{bmatrix}. \tag{3.3}$$

$(N-1)$, the order of $H_0(z)$ (and hence that of $H_1(z)$) is odd [Vai87a]. Owing to (3.2), the polyphase components of $H_0(z)$ and $H_1(z)$ are related as

$$E_{10}(z^2) = -z^{-(N-2)}\tilde{E}_{01}(z^2), \quad E_{11}(z^2) = z^{-(N-2)}\tilde{E}_{00}(z^2). \tag{3.4}$$

Substituting (3.4) in (3.3) and using the fact that the polyphase component matrix $\mathbf{E}(z)$ (for the lattice implementation) is lossless, we get the condition

$$2[\tilde{E}_{00}(z^2)E_{00}(z^2) + \tilde{E}_{01}(z^2)E_{01}(z^2)] = 1. \tag{3.5}$$

Our aim is to initialize the parameters (γ_ks) of the QMF lattice such that we can design 2-channel PR-QMF banks.

Initialization : In [Jon80,Cro83], the conventional two-channel QMF bank design is given. These QMF banks $\{H_0'(z),\ H_1'(z)\}$ do not satisfy the PR property since

there is reconstruction error in the signal $\hat{x}(n)$. The conditions that are imposed on the design are

(a) QMF constraint :

$$H_1'(z) = H_0'(-z). \tag{3.6}$$

(b) Flatness constraint :

$$|H_0'(e^{j\omega})|^2 + |H_1'(e^{j\omega})|^2 \simeq 1, \quad \forall\omega. \tag{3.7}$$

Since both $H_0'(z)$ and $H_1'(z)$ are designed to have linear phase, we know from [Vai85] that the flatness constraint (3.7) cannot be satisfied with strict equality (but is satisfied to within a certain deviation, which is minimized during optimization). This is the reason for the reconstruction error. Writing the Type 1 polyphase decomposition for $\{H_0'(z), H_1'(z)\}$ and using the QMF constraint (3.6), we get

$$\mathbf{h}'(z) = \begin{bmatrix} H_0'(z) \\ H_1'(z) \end{bmatrix} = \begin{bmatrix} E_0'(z^2) & E_1'(z^2) \\ E_0'(z^2) & -E_1'(z^2) \end{bmatrix} \begin{bmatrix} 1 \\ z^{-1} \end{bmatrix}. \tag{3.8}$$

Since both filters are linear phase, (3.8) can be expressed as

$$\mathbf{h}'(z) = \begin{bmatrix} E_0'(z^2) & z^{-(N-2)}\tilde{E}_0'(z^2) \\ E_0'(z^2) & -z^{-(N-2)}\tilde{E}_0'(z^2) \end{bmatrix} \begin{bmatrix} 1 \\ z^{-1} \end{bmatrix}. \tag{3.9}$$

Using (3.7) and (3.9), it can be shown that 4 $\tilde{E}_0'(z^2)E_0'(z^2) \simeq 1$. This is true for all conventional QMF designs.

Since conventional QMF banks can be readily designed, $E_0'(z)$ (the polyphase component of $H_0'(z)$) is easily obtained. We now use $E_0'(z)$ to initialize the parameters of the QMF lattice (to design PR-QMF banks). The proposed initialization procedure is given below :

(a) Choose $E_{00}(z) = E_0'(z)$.

(b) Using the spectral factorization method given in [Mia82], compute $E_{01}(z)$ such that it satisfies (3.5). The spectral factorization algorithm given in Appendix A

works equally well. Since both methods yield the the minimum phase spectral factor, $E_{01}(z)$ will be denoted as $E_{1,min}(z)$.

(c) Using the same method, compute $E_{0,min}(z)$ as the minimum phase spectral factor of $\tilde{E}_{00}(z)E_{00}(z)$. It can be verified that

$$2[\tilde{E}_{0,min}(z)E_{0,min}(z) + \tilde{E}_{1,min}(z)E_{1,min}(z)] = 1. \tag{3.10}$$

Let $H_0^{(0)}(z)$ be the initialized filter, which is obtained as

$$H_0^{(0)}(z) = E_{0,min}(z^2) + z^{-1}E_{1,min}(z^2), \tag{3.11}$$

where both $E_{0,min}(z)$ and $E_{1,min}(z)$ have been obtained by spectral factorization, as explained above. Using $H_0^{(0)}(z)$, we can synthesize the QMF lattice, thus obtaining an initialization of the lattice parameters (γ_ks).

Spectral Factorization : The method presented in [Mia82] computes the minimum phase spectral factor by Cepstral techniques, whereas the algorithm in Appendix A uses the inverse Linear Predictive Coding (LPC) technique. $E_{0,min}(z)$ and $E_{1,min}(z)$ are obtained by two separate spectral factor computations. Each of these computations involves spectral factorization of a sequence of length $(N-1)$, where N is the length of the filter $H_0(z)$. In comparison, the PR-QMF design method in [Smi84] involves the spectral factorization of a half-band filter of length $(2N-1)$ to obtain $H_0(z)$. Further, the zeros of the half-band filter, which lie on the unit circle, pose a serious difficulty in spectral factorization. On the other hand, neither $E_{0,min}(z)$ nor $E_{1,min}(z)$ have zeros on the unit circle (or close to it). Hence, there is no difficulty in the spectral factor computation.

Optimization : The objective function that is minimized is the stopband energy $\phi_s = \frac{1}{\pi}\int_{\omega_s}^{\pi} |H_0(e^{j\omega})|^2 d\omega$. The optimization of the lattice parameters is done by using *e04jaf* [NAG], which is a quasi-Newton algorithm. Several design examples were done, one of which is documented below as design example 3.1. In all the examples,

it was observed that the above initialization scheme worked well and led to quicker convergence than if the lattice parameters were initialized by arbitrary choice.

Design Steps : We can summarize the above method for the design of 2-channel PR-QMF banks as follows :

1. Design a conventional QMF bank $\{H_0'(z), H_1'(z)\}$.
2. Obtain $E_{0,min}$ and $E_{1,min}$ by spectral factor computations.
3. Synthesize the lattice using $H_0^{(0)}(z)$ and hence obtain an initial estimate of the lattice parameters (γ_ks).
4. Use optimization to obtain the desired PR-QMF bank $\{H_0(z), H_1(z)\}$.

Design Example 3.1 : Consider a conventional QMF bank $\{H_0'(z), H_1'(z)\}$ designed by the method in [Jon80,Cro83]. $H_0'(z)$ is a linear phase filter of length 32 with stopband edge $\omega_s = 0.622\pi$ radians and stopband attenuation $A_s = 53.4$ dB. Its magnitude response is shown in Fig. 3.2(a). In this two-channel QMF bank, the aliasing is completely canceled but the peak-to-peak reconstruction error E_{p-p} (the deviation in satisfying the flatness constraint) is $E_{p-p} = 2.97$ E-03. $E_{0,min}(z)$ and $E_{1,min}(z)$ are computed individually by the spectral factorization algorithm in [Mia82]. Then using (3.11), we get $H_0^{(0)}(z)$, from which we obtain an initialization of the parameters of the QMF lattice, γ_{2m+1}, $0 \leq m \leq 15$. These initial values are shown in Table 3.1. The same table also includes the values of the same parameters after optimization. The optimization required 2244 objective function evaluations.† The optimized filter $H_0(z)$ has $A_s = 53.44$ dB and $\omega_s = 0.616\pi$ radians. Its magnitude response is shown in Fig. 3.2(b). Since $\{H_0(z), H_1(z)\}$ is a PR-QMF bank, there is no reconstruction error and so it performs better than the filter bank $\{H_0'(z), H_1'(z)\}$.

†In each iteration step of the optimization, several objective function evaluations are required – to estimate the gradient, to bracket the minimum, to compute the optimum step size etc. In all the design examples presented in this chapter, the number of objective function evaluations required for the optimization to converge is also given. This number gives a rough idea of the typical amount of computation involved in these designs (and hence, the amount of time taken to do them).

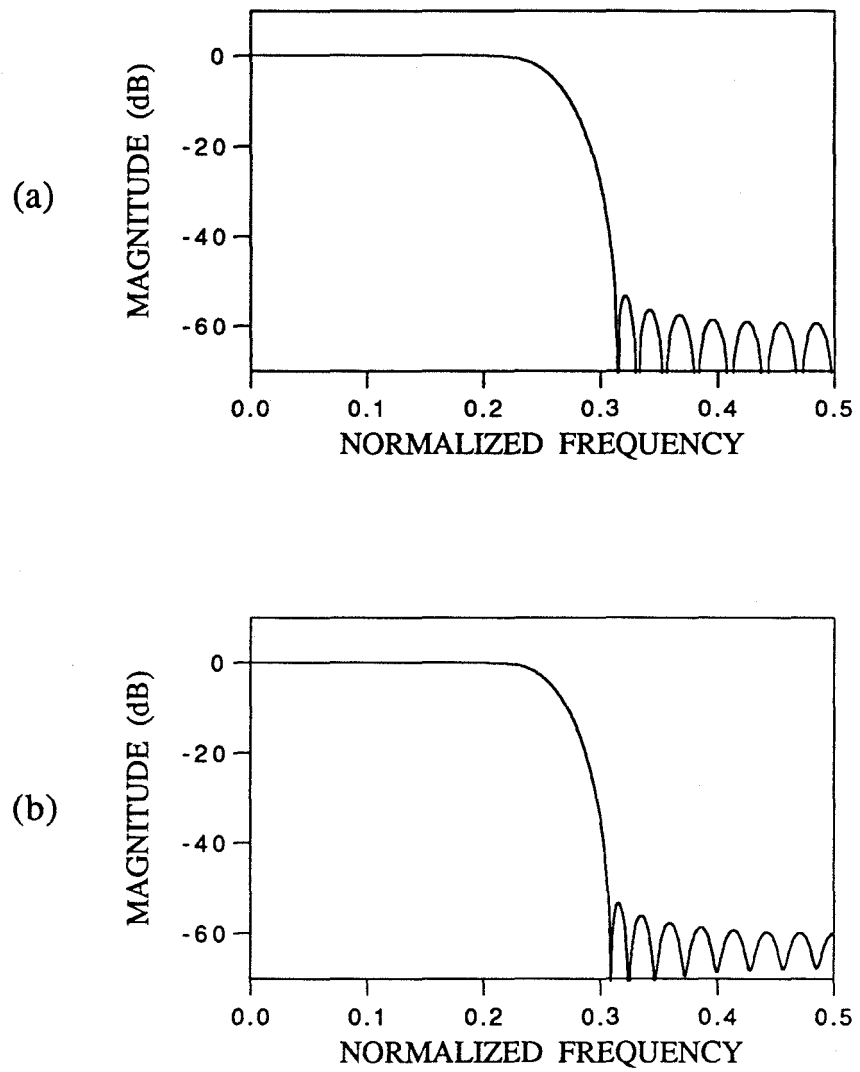

Fig. 3.2. Design example 3.1.
(a) Magnitude response of the conventional QMF filter,
(b) Magnitude response of the PR-QMF filter.

Table 3.1 : Design example 3.1. The values of the parameters of the QMF lattice – initial and optimized

m	γ_{2m+1} (initial)	γ_{2m+1} (optimized)
0	-1.0003428707521840 E 00	-4.3917013718020950 E 00
1	-1.5757869444709961 E-04	1.4390985796019320 E 00
2	5.8764055933039594 E-05	-0.8346483944576103 E 00
3	-1.0152571826719751 E-04	0.5663583875653382 E 00
4	2.9285603444370026 E-05	-0.4106025790146088 E 00
5	4.1862550465248009 E-05	0.3064482892951790 E 00
6	-1.1982619264486099 E-04	-0.2306183763629460 E 00
7	1.4291838513335176 E-05	0.1724706358377301 E 00
8	-7.0048131733623905 E-05	-0.1266158573353771 E 00
9	-1.0516281571665291 E-04	9.0159165781343906 E-02
10	2.6237145302113543 E-04	-6.1461835143995266 E-02
11	-2.1470812917944522 E-04	3.9487419177623329 E-02
12	1.2675853637729456 E-04	-2.3414945636680114 E-02
13	-5.8559563855515047 E-05	1.2414851571670356 E-02
14	2.0400702073522024 E-05	-5.5553078133802171 E-03
15	-4.4435566156077461 E-06	1.8178975775898513 E-03

A further advantage is that the QMF lattice ensures the PR property even in the presence of coefficient quantization.

3.2 Initialization for M-Channel PR-QMF design

In this section, we deal with the design of PR-QMF banks for $M \geq 3$ (in particular, for M prime). Two well-known design approaches are presented in [Vai87a,Ngu88b]. Both these approaches to PR-QMF design are based on forcing the polyphase component matrix $\mathbf{E}(z)$ to satisfy the lossless property (by using lattice structures). It is shown in Section 4.2 that in pseudo-QMF designs [Roth83,Nus81,Mas85], it is possible to obtain designs such that the polyphase component matrix $\mathbf{E}'(z)$ is *approximately* lossless, i.e., satisfying $\widetilde{\mathbf{E}}'(z)\mathbf{E}'(z) \simeq \mathbf{I}_M$. The objective of this section is to present a

procedure for extracting an initial estimate of the lattice parameters involved in the PR-QMF design from the matrix $\mathbf{E}'(z)$. The details are presented as follows :

1. The design of PR-QMF banks, using the lattice structure (2.14) to obtain lossless $\mathbf{E}(z)$, is given in [Vai87a]. An initialization procedure for this design approach is discussed in Section 3.2.1.

2. The design of PR-QMF banks, using the pairwise symmetric lattice structure (2.28), is given in [Ngu88b,Vai89]. An initialization procedure for this design approach is discussed in Section 3.2.2.

The main results in [Vai87a,Ngu88b,Vai89] pertaining to these design approaches have been summarized in Section 2.3. Design examples, obtained by using the proposed initialization scheme, are given for both approaches.

3.2.1 PR-QMF Design based on the Lossless Lattice

As outlined in Lemma 2.1, if $\mathbf{E}(z)$, the polyphase component matrix of the analysis filter bank, is lossless, then we can always find the matrix $\mathbf{R}(z)$ (and hence, all the synthesis filters) such that the analysis/synthesis system achieves perfect reconstruction (PR). Specifically, if $\mathbf{E}(z)$ is lossless, we choose

$$\mathbf{R}(z) = z^{-n_1}\widetilde{\mathbf{E}}(z), \tag{3.12}$$

and this gives the following relation between the analysis and synthesis filters

$$F_k(z) = z^{-n_2}\widetilde{H}_k(z), \quad 0 \leq k \leq M-1, \tag{3.13}$$

where n_1 and n_2 are positive constants that ensure causality. This result is presented in [Vai87a] and is used therein to obtain a design procedure for FIR PR-QMF banks based on the design of lossless $\mathbf{E}(z)$. Since we are dealing solely with FIR filter banks, all the entries of the $M \times M$ matrix $\mathbf{E}(z)$ are FIR transfer functions.

Using Lemma 2.2, the lossless matrix $\mathbf{E}(z)$ can be represented as

$$\mathbf{E}(z) = \mathbf{V}_j(z)\ \mathbf{V}_{j-1}(z)\ \cdots\ \mathbf{V}_1(z)\ \mathbf{E}_0, \tag{3.14}$$

where $\mathbf{E}_0$ is a constant $M \times M$ unitary matrix, j is the McMillan degree of $\mathbf{E}(z)$, and $\mathbf{V}_k(z)$ is a degree-one FIR lossless matrix of the form

$$\mathbf{V}_k(z) = \left[\mathbf{I}_M - \mathbf{v}_k\mathbf{v}_k^\dagger + z^{-1}\mathbf{v}_k\mathbf{v}_k^\dagger\right], \quad 1 \le k \le j, \tag{3.15}$$

where $\mathbf{v}_k$ is a $M \times 1$ column vector with unit norm.

The characterization of $\mathbf{E}(z)$ given in (3.14) is such that the lossless property of $\mathbf{E}(z)$ is preserved as long as each of the vectors $(\mathbf{v}_k)$ has unit norm and $\mathbf{E}_0$ is a unitary matrix. The vectors are forced to have unit norm by using a normalizing constraint, while the unitariness of $\mathbf{E}_0$ is ensured by using one of the parametrizations given in Chapter 2.

Suppose $\mathbf{E}_0$ is parametrized using Givens rotations as in (2.17). Then in the design process, the degrees of freedom are the components of the $\mathbf{v}_k$ vectors and the $\frac{M(M-1)}{2}$ rotation (θs) from $\mathbf{E}_0$. Together these variables are referred to as the lattice parameters, since they characterize the lossless lattice (Fig.2.5(a)) which is used to obtain $\mathbf{E}(z)$. The total number of degrees of freedom in the design is $j(M-1) + \frac{M(M-1)}{2}$.

The task before us is to design the matrix $\mathbf{E}(z)$ such that it yields 'good' filters. In general, $H_0(z)$ is a lowpass filter, $H_1(z)\ \cdots\ H_{M-2}(z)$ are bandpass filters and $H_{M-1}(z)$ is a highpass filter. Since $\mathbf{E}(z)$ is lossless, perfect reconstruction of the input is guaranteed even if the analysis/synthesis filters are not good filters, but such designs are not of much practical value. In order to obtain good filters, we optimize the lattice parameters to minimize the following objective function

$$\phi \triangleq \sum_{k=0}^{M-1} \int_{\text{stopband}} |H_k(e^{j\omega})|^2 d\omega. \tag{3.16}$$

Several optimization routines such as *e04jaf* [NAG] and *zxmin* [IMSL] are readily

available and can be used for the design. All the examples presented in this section were obtained by using *e04jaf*, which is a quasi-Newton algorithm.

Initialization : We will now obtain a procedure to initialize all the lattice parameters, by using a suitable pseudo-QMF design. Any pseudo-QMF bank can be expressed in the form given in (2.9), i.e,

$$\mathbf{h}'(z) = \mathbf{E}'(z^M)\mathbf{e}_M(z), \tag{3.17}$$

where $\mathbf{E}'(z)$ is the polyphase component matrix. We will use the order reduction method given in [Doga88,Vai89], which consists of successively obtaining the degree-one factors of the form in (3.15) in order to express $\mathbf{E}'(z)$ as in (3.14). The number of degree-one factors is equal to the McMillan degree of $\mathbf{E}'(z)$. However, there are two issues that must be mentioned. The first is that, given any matrix $\mathbf{E}'(z)$, it is not possible to know by inspection its McMillan degree (which is typically greater than the order $\mathbf{E}'(z)$). So we do not know *a priori* the number of degree-one factors. Secondly, since $\mathbf{E}'(z)$ is only *approximately* lossless, there is some error/approximation involved in the order reduction process (which is discussed next).

Order reduction : Let p be the McMillan degree of $\mathbf{E}'(z)$. Expressing $\mathbf{E}'(z)$ in terms of its matrix impulse response coefficients, we have

$$\mathbf{E}'(z) = \sum_{k=0}^{q} \mathbf{e}'(k)z^{-n}, \quad q \leq p, \tag{3.18}$$

where q is the order of $\mathbf{E}'(z)$. Then, we can write

$$\mathbf{E}'(z) \simeq \mathbf{V}(z)\ \mathbf{E}'_1(z), \tag{3.19}$$

where $\mathbf{V}(z)$ is a degree-one factor of the form (3.15) and $\mathbf{E}'_1(z)$ has McMillan degree $(p-1)$. Since $\mathbf{V}(z)$ is lossless, (3.19) can be written as

$$\mathbf{E}'_1(z) \simeq \widetilde{\mathbf{V}}(z)\mathbf{E}'(z), \tag{3.20}$$

$$\simeq \left[\mathbf{I}_M - \mathbf{v}\mathbf{v}^\dagger + z\mathbf{v}\mathbf{v}^\dagger\right]\left[\mathbf{e}'(0) + \mathbf{e}'(1)z^{-1} + \cdots + \mathbf{e}'(q)z^{-q}\right]. \tag{3.21}$$

If the following two conditions

$$\mathbf{v}\mathbf{v}^\dagger \mathbf{e}'(0) = \mathbf{0} \quad \text{and} \quad \left[\mathbf{I} - \mathbf{v}\mathbf{v}^\dagger\right] \mathbf{e}'(q) = \mathbf{0}, \tag{3.22}$$

are satisfied, then $\mathbf{E}'_1(z)$ is causal, with order $(q-1)$. As mentioned earlier, since $\mathbf{E}(z)$ is approximately lossless, the conditions in (3.22) are only approximately satisfied. A reduction in order will not always happen at every step, although the McMillan degree will decrease at every step (3.20). The order reduction process is repeated to get all the degree-one factors. Then, $\mathbf{E}'(z)$ can be expressed as

$$\mathbf{E}'(z) \simeq \mathbf{V}_p(z)\mathbf{V}_{p-1}(z)\cdots\mathbf{V}_1(z)\mathbf{E}'_0, \tag{3.23}$$

where $\mathbf{E}'_0$ is an approximately orthogonal matrix, satisfying $\mathbf{E}'^\dagger_0\ \mathbf{E}'_0 \simeq \mathbf{I}_M$. This is due to the approximations involved in the order reduction process. Using these vectors $\mathbf{v}_k$ (obtained from $\mathbf{V}_k(z)$) and the Givens rotations $\theta_{i,j}$ (obtained from the parametrization of $\mathbf{E}'_0$), all the lattice parameters can be initialized. Then the design of $\mathbf{E}(z)$, the polyphase component matrix of the PR-QMF bank, is done by minimizing the objective function in (3.16).

Design example 3.2 : This example demonstrates the design of a 3-channel PR-QMF bank using the initialization scheme described above. First, we design the prototype filter of a 3-channel pseudo-QMF bank as outlined in Appendix B. The length of the prototype is 18. Its stopband edge $\omega_s = 0.321\pi$ radians and its stopband attenuation $A_s = 40.91$ dB. The magnitude responses of the analysis filters are shown in Fig 3.3(a). The overall transfer function of the analysis/synthesis system and its total aliasing error are plotted in Fig. 3.3(b),(c) respectively. The values of the aliasing error E_a and the peak-to-peak reconstruction error E_{p-p} (both of which are defined in Section 4.5) are $E_a = 1.962$ E-03 and $E_{p-p} = 2.137$ E-02. It was verified that $\mathbf{E}'(z)$, the polyphase component matrix of this pseudo-QMF bank is approximately lossless.

Using the order reduction procedure, the degree-one factors $\mathbf{V}_k(z)$ (of the form in

(a)

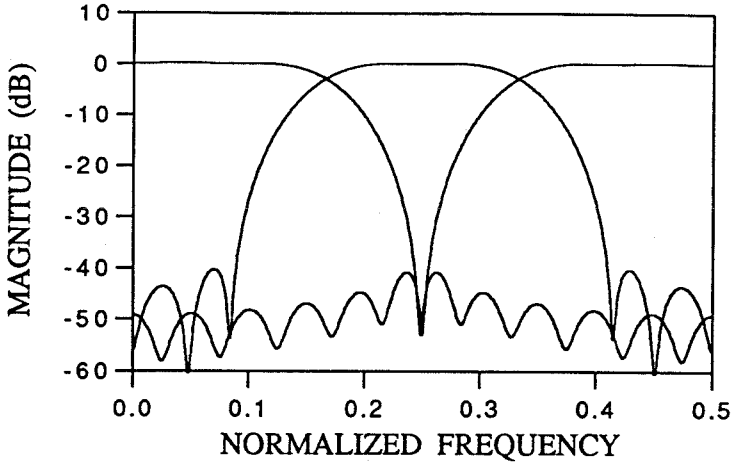

(b)

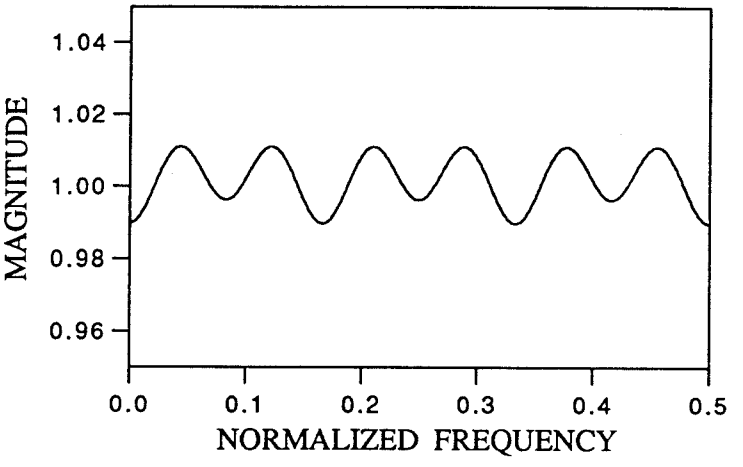

(c)

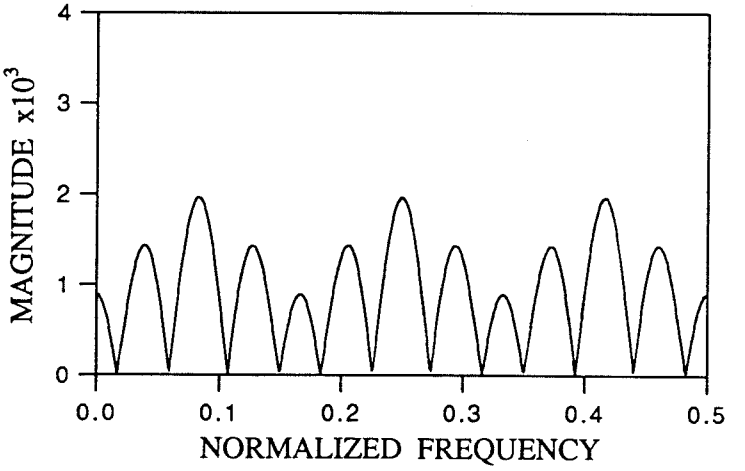

Fig.3.3. Design example 3.2.
(a) Responses of the filters of the pseudo-QMF bank,
(b) Plot of the reconstruction error of the overall analysis/synthesis system,
(c) Plot of the total aliasing error.

(3.15)) are successively obtained. Each vector $\mathbf{v}_k$ is a 3×1 column vector with unit norm. For this example, the number of degree-one factors required is 7. So we have a factorization of the form in (3.14), as given below :

$$\mathbf{E}'(z) \simeq \mathbf{V}_7(z)\mathbf{V}_6(z)\cdots\mathbf{V}_1(z)\mathbf{E}'_0. \tag{3.24}$$

The 3×3 matrix $\mathbf{E}'_0$ is parametrized by 3 Givens rotations (θ_1, θ_2, θ_3). The values of the components of the vectors ($\mathbf{v}_k$) and the Givens rotations are shown in Table 3.2. These are the initial values of the 24 lattice parameters. We now optimize the lattice parameters using the objective function given in (2.30) (which is the same as the one in (3.16)), with $\epsilon = 0.0834\pi$ radians. The optimization took $\simeq$ 33,000 objective function evaluations to reach convergence. The values of the lattice parameters, on completion of the optimization, are given in Table 3.3. The magnitude responses of the filters of the optimized PR-QMF bank are plotted in Fig. 3.4(a) and their impulse response coefficients are shown in Table 3.4.

An important advantage of this initialization scheme is that by varying the parameter ϵ in the objective function (2.30), a family of PR-QMF banks can be designed (all using the same initialization). To illustrate this, the PR-QMF design was repeated for two other values of ϵ. The magnitude responses of the filter banks obtained in these designs are plotted in Fig. 3.4(b),(c) and the characteristics of the filter $H_0(z)$ in the three designs are compared below.

ϵ	$H_0(z)$	
(radians)	A_s dB	ω_s (rads.)
0.0834π	30.39	0.4306π
0.1270π	40.85	0.4698π
0.1470π	42.89	0.4902π

There is however one drawback in this approach. The length of the filters of the pseudo-QMF bank (used to obtain the initialization) is 18, but the length of the filters of the PR-QMF bank is higher, i.e., it is 24. This is typically the case, with the

Table 3.2 : Design example 3.2. Initial estimates of the lattice parameters, obtained from a pseudo-QMF design

m	$v_{m,1}$	$v_{m,2}$	$v_{m,3}$
1	0.5773502691896260	-0.5773502691896262	-0.5773502691896251
2	0.4324535288279615	0.8160083572068758	-0.3835548283789152
3	0.5773502691896253	-0.5773502691896261	-0.5773502691896257
4	0.4324535288279615	0.8160083572068758	-0.3835548283789151
5	-0.5505320312517256	0.2469273029108523	-0.7974593341625775
6	-0.5505320312517251	0.2469273029108518	-0.7974593341625779
7	0.4082482904638632	0.8164965809277258	-0.4082482904638632

θ_0	θ_1	θ_2
-0.8236602888260015	-0.6009059143758730	-0.2090635984302468

Table 3.3 : Design example 3.2. Final values of the lattice parameters

m	$v_{m,1}$	$v_{m,2}$	$v_{m,3}$
1	0.3368076614231423	0.9216509182457436	-0.1926659910400688
2	-0.3006410452846464	-0.9421456864549457	0.1482446200861748
3	-0.5545157817682095	0.4997508089535401	-0.6654031685529260
4	0.3845065939607754	-0.1240761338655100	-0.9147457527672219
5	0.3413774834607199	-0.1832664857042431	-0.9218865488787883
6	-0.4826676305021870	0.4231124742712617	-0.7668166616483078
7	0.3033122476669819	0.9033274637661588	-0.3033169524128225

θ_0	θ_1	θ_2
-0.7832580899461068	-0.5943706750376255	-0.5953809812513522

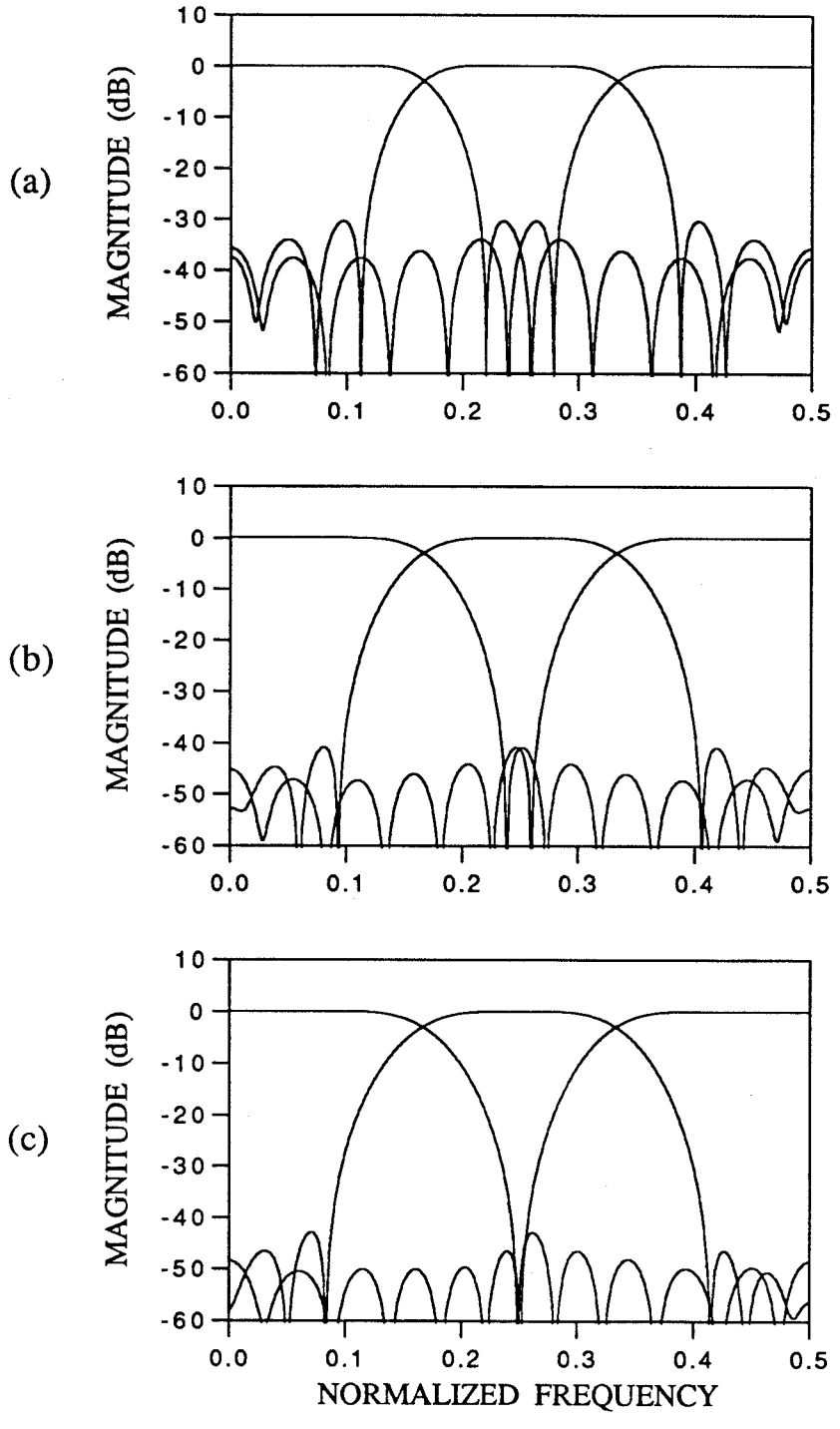

Fig. 3.4. Design example 3.2.
Magnitude responses of the PR-QMF banks for different values of ε (as multiples of π)
(a) 0.0834 (b) 0.1270 (c) 0.1470

Table 3.4 : Design example 3.2. The impulse response coefficients of the analysis filters of the PR-QMF bank (after optimization)

n	$h_0(n)$	$h_1(n)$	$h_2(n)$
0	4.9462993915470467 E-02	3.8814637115525130 E-08	4.9462342291861514 E-02
1	9.8774250330729021 E-02	-6.6331630579525680 E-02	-9.8773720034830675 E-02
2	0.1235028832746365 E 00	6.3494367358307713 E-07	0.1235028585888483 E 00
3	0.1345876166028245 E 00	5.5682886637826140 E-02	-0.1345877809427378 E 00
4	0.1886651893199945 E 00	-3.2188220193407613 E-07	0.1886645460056310 E 00
5	0.3198660916296569 E 00	0.1499034730891619 E 00	-0.3198643357761491 E 00
6	0.4697712625341564 E 00	-1.4403888064506987 E-06	0.4697696725304774 E 00
7	0.5017862605914835 E 00	-0.4764125826730772 E 00	-0.5017866263418652 E 00
8	0.3273539918370653 E 00	3.4414793318449100 E-06	0.3273568328563814 E 00
9	8.3402994192643999 E-03	0.6587300231592239 E 00	-8.3439947397166842E-03
10	-0.2610123836864501 E 00	-3.5737571111027489 E-06	-0.2610105097035103 E 00
11	-0.3143303364195794 E 00	-0.5131226199532311 E 00	0.3143313504330736 E 00
12	-0.1560727810294523 E 00	1.7864947939733034 E-06	-0.1560754184628922 E 00
13	5.4544296922768007 E-02	0.1792545961240279 E 00	-5.4542368186644805 E-02
14	0.1576788797132729 E 00	3.2304209215960888 E-07	0.1576789774518040 E 00
15	0.1088331375349715 E 00	6.7917873597733103 E-02	-0.1088345802685564 E 00
16	2.3635725633640819 E-03	-8.2749318000368242 E-07	2.3647175342638911 E-03
17	-6.5230536614374016 E-02	-9.1657654266537589 E-02	6.5230829395399717 E-02
18	-3.6023487094694551 E-02	7.8603267322091552 E-08	-3.6024002146398088E-02
19	-5.3750818218272205 E-04	-1.6011605750543437 E-03	5.3775056856027615 E-04
20	1.4427409577514129 E-02	1.7872224989182173 E-07	1.4427474693207895 E-02
21	8.1920832756822298 E-03	2.4397741486878843 E-02	-8.1922103449648329 E-03
22	-2.6612082682038321 E-08	-7.9256361520537074 E-08	2.6612495468156476 E-08
23	-3.2809139826357097 E-03	-9.7712496925717492 E-03	3.2809648736449957 E-03

Table 3.5 : Design example 3.2. Comparison between Modulated PR-Banks and Pseudo-QMF Banks – 3 Channel (filter length = 24)

	Prototype		Reconstruction	Aliasing
	A_s (dB)	ω_s (rads.)	Error (E_{p-p})	Error (E_a)
Pseudo-QMF bank	29.02	0.2146π	1.194 E-03	1.550 E-02
	29.91	0.2152π	1.157 E-03	3.605 E-02
	30.51	0.2152π	9.038 E-04	5.901 E-02
	34.02	0.2146π	4.348 E-04	2.141 E-01
PR-QMF bank	30.39	0.2153π	6.865 E-16	1.998 E-15

increase in the length being controlled by the number of degree-one factors obtained in (3.23). However, once the initialization is obtained, the PR-QMF banks can be designed quite easily, as demonstrated in this example.

In order to make this design example complete, we compare the PR-QMF bank (filter length = 24) with pseudo-QMF banks with the same filter length and transition bandwidths. The designs are compared in terms of their performance as measured by the aliasing error (E_a) and the peak-to-peak reconstruction error (E_{p-p}). The results are compiled in Table 3.5. From this comparison, it can be seen that in pseudo-QMF designs, we can tradeoff between the errors E_a and E_{p-p}, but cannot achieve the performance of the PR-QMF banks.

3.2.2 PR-QMF Design based on the Pairwise Symmetric Lattice

The details of the pairwise symmetric lattice are given in Section 2.3.2. Along with that, the advantages of using this structure are also discussed. In this section, we focus on obtaining an initialization procedure for the parameters of the pairwise symmetric lattice (2.28) from a suitable pseudo-QMF design.

In Section 2.3.2, it is shown that for the pairwise symmetric lattice, the analysis filter bank of an M-channel PR-QMF bank is expressed as

$$\mathbf{h}(z) = \frac{1}{\sqrt{2}}\mathbf{R}_M\mathbf{\Gamma}(z^M)\mathbf{A}(z^{2M})\mathbf{e}_M(z^2). \tag{3.25}$$

A sufficient condition for ensuring PR is that the matrix $\mathbf{A}(z)$ is lossless. In order to ensure its losslessness, $\mathbf{A}(z)$ is characterized in a manner identical to the characterization of $\mathbf{E}(z)$ in the previous section, as given by (3.14). So we will avoid repeating the same details and will directly use a design example to outline the initialization scheme.

Initialization : Consider the design of a 5-channel PR-QMF bank $\{H_0(z), \cdots H_4(z)\}$ (satisfying pairwise symmetry) with the initialization being obtained from a 5-channel

pseudo-QMF bank $\{H'_0(z), \cdots H'_4(z)\}$. Using (2.34) and (2.39), we have

$$h'_k(n) = 2h'(n)\cos\left((2k+1)\frac{\pi}{10}(n-\frac{N-1}{2}) + (-1)^k\frac{\pi}{4}\right), \quad 0 \le k \le 4. \tag{3.26}$$

Assume that the length of the prototype filter, N, is even. Then the following symmetry relations can be verified :

$$H'_4(z) = \begin{cases} H'_0(-z), & \text{if } \frac{N}{2} \text{ is odd,} \\ -H'_0(-z), & \text{if } \frac{N}{2} \text{ is even.} \end{cases} \tag{3.27}$$

A similar relation holds between $H'_1(z)$ and $H'_3(z)$. The filter $H'_2(z)$ satisfies

$$H'_2(z) = \begin{cases} \alpha'_2(z^2), & \text{if } \frac{N}{2} \text{ is odd,} \\ z^{-1}\alpha'_2(z^2), & \text{if } \frac{N}{2} \text{ is even.} \end{cases} \tag{3.28}$$

From (3.27) and (3.28), it can be seen that this pseudo-QMF bank indeed satisfies the pairwise symmetry condition (2.22) (to within a scale factor, ± 1).

Design example 3.3 : Consider a pseudo-QMF bank with a prototype filter of length 46, designed as in Appendix B. The prototype filter has stopband attenuation $A_s = 53.52$ dB and stopband edge $\omega_s = 0.1838\pi$ radians. The aliasing and reconstruction errors for the overall analysis/synthesis system using this pseudo-QMF bank are $E_a = 1.977$ E-04 and $E_{p-p} = 7.828$ E-02 respectively. The pseudo-QMF bank can be expressed as follows :

$$\mathbf{h}'(z) = \begin{bmatrix} H'_0(z) \\ H'_1(z) \\ H'_2(z) \\ H'_3(z) \\ H'_4(z) \end{bmatrix} = \frac{1}{\sqrt{2}} \begin{bmatrix} 1 & 0 & 0 & 0 & 1 \\ 0 & 1 & 0 & 1 & 0 \\ 0 & 0 & \sqrt{2} & 0 & 0 \\ 0 & 1 & 0 & -1 & 0 \\ 1 & 0 & 0 & 0 & -1 \end{bmatrix} \begin{bmatrix} 1 & & & & \\ & 1 & & & \\ & & 1 & & \\ & & & z^{-1} & \\ & & & & z^{-1} \end{bmatrix} \begin{bmatrix} \alpha'_0(z^2) \\ \alpha'_1(z^2) \\ \alpha'_2(z^2) \\ \alpha'_3(z^2) \\ \alpha'_4(z^2) \end{bmatrix}. \tag{3.29}$$

Using (3.29), $z^{-4}\mathbf{h}'(z)$ can be expressed in the form of (2.28), with $M = 5$, where $\mathbf{A}'(z)$ is the polyphase component matrix of $[z^{-2}\alpha'_0(z),\ z^{-2}\alpha'_1(z),\ z^{-2}\alpha'_2(z),\ \alpha'_3(z),\ \alpha'_4(z)]^T$.

Since the length of the filters of the pseudo-QMF bank is 46, it can be verified that $z^{-2}\alpha'_0(z)$ is a polynomial of length 25. So each of the elements of $\mathbf{A}'(z)$ is a polynomial of length ≤ 5. Next, we do the order reduction (as explained in the previous section) to get the degree-one factors of $\mathbf{A}'(z)$. In this example, the number of degree-one

factors required is 4. So we can express $\mathbf{A}'(z)$ (as in (3.23))

$$\mathbf{A}'(z) \simeq \mathbf{V}_4(z)\mathbf{V}_3(z)\mathbf{V}_2(z)\mathbf{V}_1(z)\mathbf{A}'_0, \tag{3.30}$$

where $\mathbf{A}'_0$ is a 5×5 constant matrix that is approximately orthogonal. The approximations in the above equation are due to the fact that $\mathbf{A}'(z)$ is not *exactly* lossless.

For this example, we characterize the constant matrix $\mathbf{A}'_0$ by using the Householder factorization (2.20), and obtain the vectors $\{\mathbf{u}_1, \mathbf{u}_2, \mathbf{u}_3, \mathbf{u}_4\}$. These vectors along with $\{\mathbf{v}_1, \mathbf{v}_2, \mathbf{v}_3, \mathbf{v}_4\}$ give the initialization of all the lattice parameters (total = 34) of the pairwise symmetric lattice (2.28). These initial values are shown in Table 3.6.

The optimization is done to minimize the following objective function,

$$\phi = \int_{\frac{\pi}{5}+\epsilon}^{\pi} |H_0(e^{j\omega})|^2 d\omega + \int_0^{\frac{\pi}{5}-\epsilon} |H_1(e^{j\omega})|^2 d\omega + \int_{\frac{2\pi}{5}+\epsilon}^{\pi} |H_1(e^{j\omega})|^2 d\omega + \int_0^{\frac{2\pi}{5}-\epsilon} |H_2(e^{j\omega})|^2 d\omega. \tag{3.31}$$

As explained in Section 2.3, the other stopband energy terms are not included because of the pairwise symmetry satisfied by the filters. The optimization required $\simeq 14,000$ objective function evaluations to reach convergence. The magnitude responses of the filters of the PR-QMF bank $H_0(z)$, $H_1(z)$ and $H_2(z)$ are shown in Fig. 3.5 (but $H_3(z)$ and $H_4(z)$ are not shown since they can be obtained from $H_1(z)$ and $H_0(z)$ respectively). The length of the PR-QMF filters is 54, whereas the length of the initializing filters (pseudo-QMF) is 46. This increase in the length of the PR-QMF filters is due to the specific form forced by the pairwise symmetric lattice. The filter $H_0(z)$ has stopband attenuation $A_s = 46.81$ dB and stopband edge $\omega_s = 0.316\pi$ radians. The values of all the lattice parameters on completion of the optimization are shown in Table 3.7.

This completes this design example, which illustrates the initialization procedure for PR-QMF design using the pairwise symmetric lattice. In this case also, once the initialization is obtained, we can design a family of PR-QMF banks by choosing different values of the parameter ϵ in (3.31).

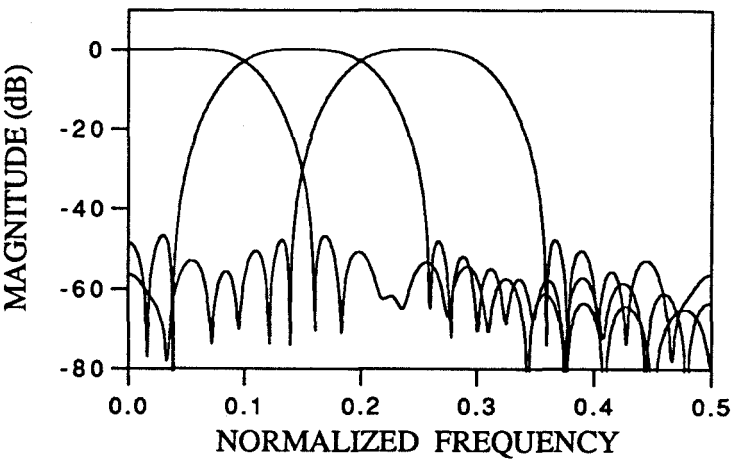

Fig. 3.5. Design example 3.3.
Magnitude responses of three of the filters
of the 5-channel PR-QMF bank (filter length = 54).

3.3 Summary

In this chapter, the lattice-based approaches to PR-QMF design are considered. Since these design methods are based on optimization, obtaining 'good' initialization values for the parameters being optimized plays an important role in yielding good results and in reducing the time for the optimization to converge. Initialization procedures for these PR-QMF design approaches are presented. In the case of two-channel PR-QMF designs, the initialization is obtained from a conventional QMF design whereas in the case of M-channel PR-QMF design ($M \geq 3$), the initialization is obtained from a pseudo-QMF design. Detailed design examples are given to highlight the features of the initialization procedures. Using these design approaches, we are able to design PR-QMF banks very efficiently for $M \leq 7$ channels. For higher values of M, the number of lattice parameters (which must be optimized) becomes large (as shown in Table 4.1) and hence the optimization becomes increasingly difficult. This, in fact, served as a strong motivation to seek alternate methods for PR-QMF design and led to the work presented in the next chapter.

Table 3.6 : Design example 3.3. Initial values of the lattice parameters obtained from a pseudo-QMF design
($\mathbf{v}_k$ – degree-one factors and $\mathbf{u}_k$ – Householder vectors)

$\mathbf{v}_1$	$\mathbf{v}_2$	$\mathbf{v}_3$	$\mathbf{v}_4$
-0.1735048524411 E 00	-0.1338269310171 E 00	-0.2532635023066 E 00	-0.2759948489917 E 00
-0.4542416009039 E 00	-0.3503634540130 E 00	-0.6630524571487 E 00	-0.7225638953802 E 00
0.3970217171326 E 00	0.3062288875698 E 00	0.5795290976483 E 00	0.6315440019386 E 00
-0.4092384958578 E 00	-0.4599950967059 E 00	0.2105322140169 E 00	-2.8215818040862 E-02
0.6621617958028 E 00	0.7442877011284 E 00	-0.3406482780061 E 00	4.5654152610496 E-02

$\mathbf{u}_1$	$\mathbf{u}_2$	$\mathbf{u}_3$	$\mathbf{u}_4$
-0.7511760585052 E 00	0.0000000000000 E 00	0.0000000000000 E 00	0.0000000000000 E 00
-0.2239810296659 E 00	0.7175943237066 E 00	0.0000000000000 E 00	0.0000000000000 E 00
0.1957665982731 E 00	0.2819519608259 E 00	0.7211826482947 E 00	0.0000000000000 E 00
-0.3097990595004 E 00	0.4132397080508 E 00	0.1469618531728 E 00	-0.9619383577839 E 00
0.5012654079544 E 00	0.4845559018942 E 00	0.6769769578875 E 00	-0.2732665289127 E 00

Table 3.7 : Design example 3.3. Final values of the lattice parameters

$\mathbf{v}_1$	$\mathbf{v}_2$	$\mathbf{v}_3$	$\mathbf{v}_4$
0.8032886818602 E 00	0.2013587888479 E 00	-0.3565441866836 E 00	-4.7239858816182 E-02
-6.1573629416919 E-02	2.1108235452691 E-02	-0.7970815490657 E 00	-0.9950069529785 E 00
0.5040796613860 E 00	0.1713044776047 E 00	0.4646884300500 E 00	3.5730249840755 E-02
-0.1829367521508 E 00	-0.9626577524765 E 00	-1.7606324303927 E-02	8.0246315637822 E-02
-0.2517415767117 E 00	-5.4349867518901 E-02	0.1459175363117 E 00	3.6656972664466 E-03

$\mathbf{u}_1$	$\mathbf{u}_2$	$\mathbf{u}_3$	$\mathbf{u}_4$
-0.3471964227661 E 00	0.0000000000000 E 00	0.0000000000000 E 00	0.0000000000000 E 00
-0.2431409534533 E 00	0.8861538861356 E 00	0.0000000000000 E 00	0.0000000000000 E 00
0.7845023826808 E 00	0.3650854659091 E 00	0.6137856407383 E 00	0.0000000000000 E 00
-0.4140705134653 E 00	-0.2849813516361 E 00	-0.4989552054597 E 00	9.4053042734044 E-02
-0.1828626321012 E 00	1.5149979813155 E-02	0.6118095211487 E 00	-0.9955671876636 E 00

Chapter 4

Modulated FIR Filter Banks Satisfying Perfect Reconstruction

Two familiar approaches to M-channel QMF design are the perfect reconstruction QMF banks [Smi84,Vai87a,Vet87,Ngu88b,Koi90] and the pseudo-QMF banks [Roth83, Nus81,Mas85,Cox86]. The tradeoffs between the two are that the latter has an efficient design procedure (only the prototype filter is designed) while the former achieves perfect reconstruction (PR) of the input (i.e., without aliasing, magnitude or phase distortions). Owing to their attractive features, PR-QMF banks are of particular interest. However, the existing approaches for PR-QMF design (which were discussed in the previous chapter) require the optimization of a non-linear objective function of a large number of parameters (particularly for large values of M). In this chapter, we present a method, which while retaining all the attractive features of modulated filter banks (e.g., only the prototype filter is designed), also satisfies the PR property. The analysis and synthesis filters are of equal length (an arbitrary multiple of $2M$).

It is a known result [Prin86,Vet89,Mal90a] that FIR filter banks satisfying PR can be obtained by the modulation of a linear-phase prototype of length $N = 2M$, when certain constraints are imposed on the prototype. In this chapter, we consider linear-phase prototype filters of length $N = 2mM$, where $m \geq 1$. A necessary and sufficient condition for $\mathbf{E}(z)$, the polyphase component matrix of the modulated filter bank, to be lossless, is presented. The losslessness of $\mathbf{E}(z)$ is sufficient to ensure that the

analysis/synthesis system satisfies PR.‡ Our approach throws additional light on the problem and places in evidence its relation to lossless QMF banks [Vai87a]. It also yields an efficient design method, where pairs of polyphase components are designed using the two-channel lossless lattice structure [Vai86b]. This enables the design of a large class of FIR-PR modulated filter banks (with $N = 2mM$). The main advantages of the proposed method are summarized below.

1. These filter banks satisfy the perfect reconstruction (PR) conditions.
2. The method can be used to design filter banks for an arbitrary number of channels.
3. The analysis and synthesis filters are of equal length (N).
4. The analysis and synthesis filters are obtained by cosine modulation of the prototype filter. Hence they can be implemented very efficiently.
5. This method requires half as many parameters to be optimized as compared to the pseudo-QMF method. This is much fewer than the number of parameters optimized in lattice-based PR-QMF designs.
6. The objective function used in the optimization is very simple and it involves only the stopband energy of the prototype. In comparison, the objective function in pseudo-QMF designs, includes the stopband energy of the prototype and a 'flatness constraint' while in lattice-based designs, it includes the stopband energies of all the M filters in the filterbank. Hence, the evaluation of the objective function (which is required at every iteration of the optimization) is simpler.
7. The new scheme is such that the $2M$ polyphase components of the prototype

‡While this work was well under way, Malvar's work [Mal90b] was brought to the author's attention. In [Mal90b], a necessary and sufficient condition for PR is obtained in the time domain, for prototypes of length $N = 2mM$.

$H(z)$ can be grouped into M power complementary pairs. If each pair is implemented in a structurally power complementary manner, then the PR property is retained even in the presence of coefficient quantization. This is achieved by implementing each power complementary pair by a two-channel lossless lattice.

8. The optimization (to obtain the prototype filter) is done directly on the lattice parameters. This enables us to optimize the prototype response (while it is guaranteed that the modulated filter bank will satisfy the PR property).

Losslessness and cosine-modulation

It has been verified by explicit computation that good pseudo-QMF designs [Roth83, Nus81,Mas85,Cox86] are such that the polyphase component matrix $\mathbf{E}(z)$ of the analysis filter bank is 'almost' lossless. This is consistent with the 'almost' perfect reconstruction property of these cosine-modulated filter banks (see Section 4.1.1). We can summarize by saying that this paper incorporates 'exact' losslessness into pseudo-QMF techniques and thereby enables the PR property to be satisfied, while retaining all the attractive features of modulated filter banks.

Outline of the Chapter

In Section 4.1, a brief overview of results in modulated filter banks is given. In Section 4.1.1, a new observation pertaining to pseudo-QMF banks is presented. This result motivates the work presented in the later sections. In Section 4.1.2, the polyphase implementation of modulated filter banks is derived. This also serves to introduce the notation related to the polyphase component matrices and the modulation matrix.

In Section 4.2, we consider the modulated filter banks that satisfy the PR property. In this section, it is shown that for $\mathbf{E}(z)$ (the polyphase component matrix of the modulated filter bank) to be lossless, it is necessary and sufficient that appropriate pairs of polyphase components of the prototype $H(z)$ are power complementary. The losslessness of $\mathbf{E}(z)$ is sufficient to ensure that the analysis/synthesis system satisfies

the perfect reconstruction (PR) property.

The design of prototype filters of modulated PR banks is considered next. Section 4.3.1 contains a description of the two-channel lossless lattice. In Section 4.3.2, it is shown how the two-channel lossless lattice can be used to ensure that the prototype filter satisfies the condition for PR obtained in Section 4.2. Sections 4.3.3–4.3.5 deal with the design procedure (for the prototype filter) based on the two-channel lossless lattice. The advantages of this design approach are discussed in detail. In Section 4.3.6, an efficient implementation of the modulated PR filter banks is presented along with a comparison of its implementation complexity with that of pseudo-QMF banks. Section 4.4 includes design examples to demonstrate the various aspects of the design procedure and a detailed comparison between modulated PR filter banks (designed by the approach proposed in this chapter) and pseudo-QMF banks.

Appendix 4.A contain the proofs of some identities (pertaining to the properties of the cosine-modulation matrix) which are essential in the derivation of the necessary and sufficient conditions in Sections 4.2. In Appendix 4.B, the properties of the two-channel modulated PR filter banks are discussed. It is shown that these filters satisfy the same conditions as the ones in the well-known two-channel PR-QMF designs (presented by Smith-Barnwell).

4.1 Modulated Filter Banks – An Overview

4.1.1 A Key Observation about Pseudo-QMF Banks

Pseudo-QMF banks belong to the family of modulated filter banks. The main results from Pseudo-QMF theory are presented in Chapter 2. Let $\mathbf{h}(z) = [H_0(z)\ H_1(z)\ \cdots\ H_{M-1}(z)]^T$ be the analysis filters of a pseudo-QMF bank. Using Type 1 polyphase decomposition [Vai90], $\mathbf{h}(z)$ can be expressed as

$$\mathbf{h}(z) = \mathbf{E}(z^M)\mathbf{e}_M(z), \tag{4.1}$$

where $\mathbf{E}(z)$ is the polyphase component matrix of the filter bank and $\mathbf{e}_M^T(z) = [1\ z^{-1}\ \cdots\ z^{-(M-1)}]$. The new observation is a property of the matrix $\mathbf{E}(z)$ of pseudo-QMF banks. We have the following result from [Vai87a].

Fact 4.1 : In any perfect reconstruction QMF bank, if the analysis and synthesis filters are related as

$$F_k(z) = cz^{-(N-1)}\widetilde{H}_k(z), \quad 0 \leq k \leq M-1, \tag{4.2}$$

where c is a non-zero constant, then $\mathbf{E}(z)$, the polyphase component matrix of the analysis filter bank is necessarily lossless. $\Diamond$

Based on existing pseudo-QMF design techniques, it is possible to obtain designs that satisfy (4.2). Further, by proper choice of θ_k, the aliasing error and the reconstruction error can be made very small. The overall transfer function $T(z)$ has approximately unit gain at all frequencies. Hence, it is intuitively expected (by using Fact 4.1) that the matrix $\mathbf{E}(z)$ of the pseudo-QMF bank will be 'approximately' lossless, i.e., $\mathbf{E}(z)$ satisfies the condition $\widetilde{\mathbf{E}}(z)\mathbf{E}(z) \simeq \mathbf{I}_M$, with the non-diagonal terms of the LHS being small, but not necessarily zero. This result was verified using a number of design examples, one of which is shown next as an illustration.

Example : Consider a 3-channel pseudo-QMF design. The prototype filter, which is a linear-phase filter of length $N = 36$, is obtained by optimization. It has stopband attenuation $A_s = 51.1$dB and its stopband edge $\omega_s = 0.296\pi$ radians. Each entry of the 3×3 matrix $\mathbf{E}(z)$ is a polynomial of length 12. The product $\widetilde{\mathbf{E}}(z)\mathbf{E}(z)$ was computed, which is also a 3×3 matrix whose elements are polynomials of length 23. The entries of the first row of this product are shown in Table 4.1. (In order to save space, the second and third rows are not shown). Hence, it can be verified that the matrix $\mathbf{E}(z)$ of this pseudo-QMF design is approximately lossless.

Two other related results are :

1. If the matrix $\mathbf{E}(z)$ of a pseudo-QMF bank is lossless, then the pseudo-QMF

Table 4.1. Example in Section 4.1.1. The first row of $\tilde{\mathbf{E}}(z)\mathbf{E}(z)$ of a 3-channel pseudo-QMF design

$\left[\, \tilde{\mathbf{E}}(z)\mathbf{E}(z) \,\right]_{0,0}$	$\left[\, \tilde{\mathbf{E}}(z)\mathbf{E}(z) \,\right]_{0,1}$	$\left[\, \tilde{\mathbf{E}}(z)\mathbf{E}(z) \,\right]_{0,2}$
0.93968 D-21	-0.13235 D-22	-0.89997 D-21
-0.69590 D-05	-0.23399 D-19	0.59822 D-20
0.15585 D-18	-0.63951 D-19	0.81315 D-19
0.21736 D-03	0.69457 D-18	-0.77927 D-19
0.82399 D-17	-0.27376 D-17	-0.67593 D-18
0.60492 D-04	0.56921 D-17	-0.35779 D-17
0.85869 D-16	-0.35020 D-16	0.19516 D-17
-0.70648 D-04	0.43368 D-16	-0.36429 D-16
0.11102 D-15	-0.29490 D-16	-0.46838 D-16
0.68909 D-04	0.20470 D-15	-0.79797 D-16
-0.27756 D-16	0.31225 D-16	0.11796 D-15
0.99994 D+00	0.19429 D-15	0.00000 D+00
-0.27756 D-16	-0.83267 D-16	0.22204 D-15
0.68909 D-04	0.18041 D-15	-0.15266 D-15
0.11102 D-15	-0.48572 D-16	-0.58981 D-16
-0.70648 D-04	0.58981 D-16	-0.69389 D-16
0.85869 D-16	-0.79797 D-16	0.14745 D-16
0.60492 D-04	0.47705 D-17	-0.32960 D-16
0.82399 D-17	-0.10734 D-16	0.43368 D-17
0.21736 D-03	-0.40658 D-19	-0.20600 D-17
0.15585 D-18	-0.76572 D-18	0.93512 D-18
-0.69590 D-05	-0.34305 D-19	0.10164 D-18
0.93968 D-21	0.38066 D-21	-0.13764 D-20

bank (whose filters satisfy (4.2)) will necessarily satisfy the PR property (by using Lemma 3.1 [Vai87a]).

2. In [Prin86,Vet89,Mal90a], it is shown that M channel pseudo-QMF banks can satisfy the PR property, when the length of the linear-phase prototype filter, N, is constrained to be $N = 2M$. For this case, the necessary and sufficient condition for PR is

$$h^2(i) + h^2(M-1-i) = c, \quad 0 \leq i \leq M-1, \tag{4.3}$$

where c is a non-zero constant.

The former result gives the condition that must be satisfied in order for pseudo-QMF banks to satisfy PR and raises the question – "Is it possible for the matrix $\mathbf{E}(z)$ of a pseudo-QMF bank to be lossless ?" The latter result shows that this is possible for the special case when the prototype length $N = 2M$, thus leading to the following questions.

Q1. It has been verified that the matrix $\mathbf{E}(z)$ of any pseudo-QMF bank is 'approximately' lossless. Can we find appropriate constraints on the prototype such that $\mathbf{E}(z)$ is 'exactly' lossless ?

Q2. If such constraints can be found, can they be easily satisfied ?

Q3. Can we design modulated filter banks (satisfying PR property) with the same ease of design as pseudo-QMF banks ? Will they be comparable in performance ?

The answers to all the above questions is in the affirmative and they will be elaborated in the following sections. The first step is to obtain a polyphase component representation of the cosine-modulated filter banks.

4.1.2 Polyphase Implementation of Modulated Filter Banks

As mentioned earlier, we choose the values of θ_k for the cosine-modulated filter bank as in (2.39). If we denote $c_{k,\ell} \triangleq 2\cos\left((2k+1)\frac{\pi}{2M}(\ell - \frac{N-1}{2}) + (-1)^k\frac{\pi}{4}\right)$, then, using the periodicity of the cosine modulation, we get the relation

$$c_{k,(\ell+2pM)} = (-1)^p c_{k,\ell}. \tag{4.4}$$

From this point onwards, the length of the prototype filter (N) will be assumed to be an even multiple of M, i.e., $N = 2mM$, where m is any positive integer (because in this chapter, we will be dealing solely with prototypes satisfying this length constraint).

We shall now obtain a polyphase structure for the analysis filter bank. For this, first we express the prototype $H(z)$ as

$$H(z) = \sum_{q=0}^{2M-1}\sum_{p=0}^{m-1} h(q+2pM)z^{-(q+2pM)} = \sum_{q=0}^{2M-1} z^{-q}G_q(z^{2M}), \tag{4.5}$$

where $G_q(z)$ are the Type 1 polyphase components [Vai90] of $H(z)$. Using (2.34), the analysis filters can then be expressed as

$$H_k(z) = \sum_{n=0}^{N-1} h_k(n)z^{-n} = \sum_{n=0}^{2mM-1} h(n)c_{k,n}z^{-n} = \sum_{q=0}^{2M-1}\sum_{p=0}^{m-1} h(q+2pM)c_{k,(q+2pM)}z^{-(q+2pM)}. \tag{4.6}$$

Using (4.4), we can simplify (4.6) as

$$\begin{aligned} H_k(z) &= \sum_{q=0}^{2M-1} z^{-q}\, c_{k,q}\sum_{p=0}^{m}(-1)^p h(q+2pM)z^{-2pM}, \\ &= \sum_{q=0}^{2M-1} c_{k,q}z^{-q}G_q(-z^{2M}). \end{aligned} \tag{4.7}$$

The analysis filter bank can be expressed in matrix form as

$$\mathbf{h}(z) = \begin{bmatrix} H_0(z) \\ H_1(z) \\ \vdots \\ H_{M-1}(z) \end{bmatrix} = \widehat{\mathbf{C}} \begin{bmatrix} G_0(-z^{2M}) \\ z^{-1}G_1(-z^{2M}) \\ \vdots \\ z^{-(2M-1)}G_{2M-1}(-z^{2M}) \end{bmatrix}, \tag{4.8}$$

where $\widehat{\mathbf{C}}$ is a $M\times 2M$ cosine-modulation matrix and $\left[\widehat{\mathbf{C}}\right]_{k,\ell} = c_{k,\ell}$, $0 \le k \le M-1$, $0 \le \ell \le 2M-1$. This implementation of the analysis filter bank (4.8) is

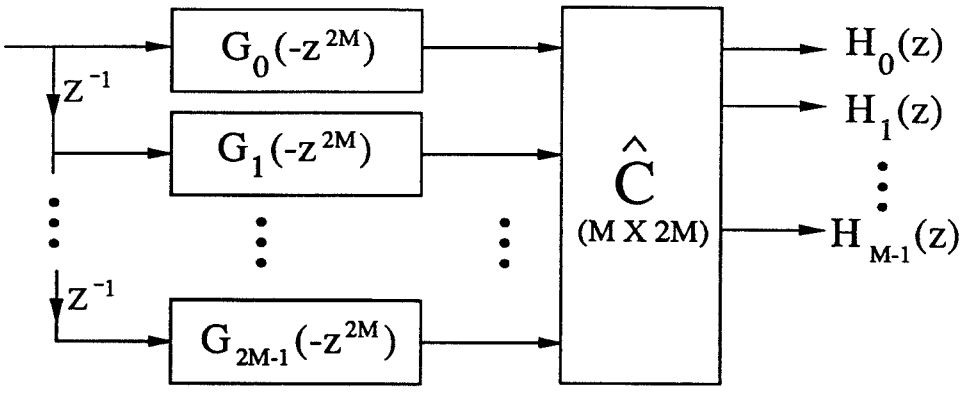

Fig. 4.1. Polyphase implementation of the cosine-modulated analysis filter bank.

shown in Fig. 4.1. An efficient implementation of $\hat{\mathbf{C}}$ will be derived in Section 4.3.6. Using the relationship in (2.36), a similar implementation can be obtained for the synthesis filter bank. Equation (4.8) can be compactly expressed as

$$\mathbf{h}(z) = \hat{\mathbf{C}} \begin{bmatrix} \mathbf{g}_0(z^{2M}) & \mathbf{0} \\ \mathbf{0} & \mathbf{g}_1(z^{2M}) \end{bmatrix} \begin{bmatrix} \mathbf{e}_M(z) \\ z^{-M}\mathbf{e}_M(z) \end{bmatrix}, \tag{4.9}$$

where $\mathbf{e}_M^T(z) = [1 \; z^{-1} \; \cdots \; z^{-(M-1)}]$, and $\mathbf{g}_0(z)$, $\mathbf{g}_1(z)$ are $M \times M$ matrices defined as

$$\begin{aligned} \mathbf{g}_0(z) &\triangleq \text{diag } [G_0(-z), \; G_1(-z), \; \cdots \; G_{M-1}(-z)], \\ \mathbf{g}_1(z) &\triangleq \text{diag } [G_M(-z), \; G_{M+1}(-z), \; \cdots \; G_{2M-1}(-z)]. \end{aligned} \tag{4.10}$$

The results in this section will be used in later sections, where we derive perfect reconstruction filter banks (using the same modulation as pseudo-QMF banks). It must be mentioned that, in pseudo-QMF banks, the AC constraint ensures the cancellation of the significant aliasing terms, but there will always be a residual aliasing error due to the uncanceled aliasing terms. In the same manner, the flatness constraint minimizes the overall distortion (between the output and the input), but does not eliminate it.

On the other hand, in PR filter banks, both these errors are completely eliminated. These facts, while highlighting the differences between pseudo-QMF banks and PR filter banks, also motivate the interest in PR filter banks.

4.2 Modulated PR Filter Banks with $N = 2mM, \quad m \geq 1$

In this section, we derive the conditions on a linear-phase prototype $H(z)$ (length $N = 2mM$, where m is an arbitrary positive integer) such that the M-channel modulated filter bank satisfies the PR property. Substituting $N = 2mM$ in the expression for $c_{k,\ell}$ (defined in Section 4.1.2), we get

$$c_{k,\ell} = 2\cos\left((2k+1)\frac{\pi}{2M}(\ell - mM + \frac{1}{2}) + (-1)^k\frac{\pi}{4}\right). \tag{4.11}$$

The matrix $\widehat{\mathbf{C}}$ (in equation (4.8)) can be expressed as $\widehat{\mathbf{C}} = [\mathbf{A}'_0 \;\; \mathbf{A}'_1]$, where $\mathbf{A}'_0$, $\mathbf{A}'_1$ are given by

$$[\mathbf{A}'_0]_{k,\ell} = c_{k,\ell} \;\text{ and }\; [\mathbf{A}'_1]_{k,\ell} = c_{k,(\ell+M)}, \qquad 0 \leq k,\ell \leq M-1. \tag{4.12}$$

The analysis filter bank (4.9) can then be written in terms of $\mathbf{A}'_0$ and $\mathbf{A}'_1$ as

$$\mathbf{h}(z) = \underbrace{\left[\mathbf{A}'_0\mathbf{g}_0(z^{2M}) + z^{-M}\mathbf{A}'_1\mathbf{g}_1(z^{2M})\right]}_{\mathbf{E}(z^M)}\mathbf{e}_M(z), \tag{4.13}$$

where $\mathbf{E}(z)$ is the polyphase component matrix of the analysis filter bank.

Note that $\mathbf{A}'_0$ and $\mathbf{A}'_1$ depend on the value of m. In Appendix 4.A it has been proved that these matrices satisfy the following properties (for all values of m) :

$$\mathbf{A}_0'^{\dagger}\mathbf{A}'_0 = 2M\left[\mathbf{I}_M + (-1)^{(m-1)}\mathbf{J}_M\right], \tag{4.14}$$

$$\mathbf{A}_1'^{\dagger}\mathbf{A}'_1 = 2M\left[\mathbf{I}_M - (-1)^{(m-1)}\mathbf{J}_M\right], \tag{4.15}$$

$$\mathbf{A}_1'^{\dagger}\mathbf{A}'_0 = \mathbf{A}_0'^{\dagger}\mathbf{A}'_1 = \mathbf{0}, \tag{4.16}$$

where $\mathbf{I}_M$ is the identity matrix and $\mathbf{J}_M$ is the 'reverse operator,' defined in Chapter 1.

From Lemma 3.1 [Vai87a], we know that if $\mathbf{E}(z)$, the polyphase component matrix of the analysis bank is *lossless*, i.e., $\widetilde{\mathbf{E}}(z)\mathbf{E}(z) = \mathbf{I}_M$, then we can always find

a synthesis bank such that the overall analysis/synthesis system satisfies perfect reconstruction (PR). So our aim is to obtain the conditions under which $\mathbf{E}(z)$, the polyphase component matrix of the modulated filter bank, is lossless. We will now prove the following Lemma.

Lemma 4.1 : Let $\mathbf{h}(z)$ be the analysis filter bank (4.8) obtained from $H(z)$, a real coefficient, linear-phase prototype filter of length $N = 2mM$ (where $m \geq 1$). Then, $\mathbf{E}(z)$, the polyphase component matrix of $\mathbf{h}(z)$ is lossless if and only if

$$\tilde{G}_k(z)G_k(z) + \tilde{G}_{M+k}(z)G_{M+k}(z) = \frac{1}{2M}, \quad 0 \leq k \leq M-1. \tag{4.17}$$

where $G_k(z)$ are the Type 1 polyphase components [Vai90] of $H(z)$. ◇

Proof : From (4.13) and (4.16), we can write

$$\tilde{\mathbf{E}}(z)\mathbf{E}(z) = \tilde{\mathbf{g}}_0(z^2)\mathbf{A}_0'^{\dagger}\mathbf{A}_0'\mathbf{g}_0(z^2) + \tilde{\mathbf{g}}_1^{\dagger}(z^2)\mathbf{A}_1'^{\dagger}\mathbf{A}_1'\mathbf{g}_1(z^2). \tag{4.18}$$

Since the prototype $H(z)$ is linear-phase and its length is $N = 2mM$, we have the following relation [Vai87d] between the polyphase components of $H(z)$

$$G_k(z) = z^{-(m-1)}\tilde{G}_{2M-1-k}(z), \quad 0 \leq k \leq M-1. \tag{4.19}$$

Using (4.19), we get $\mathbf{J}_M\mathbf{g}_i(z^2) = (-1)^{(m-1)}z^{-2(m-1)}\tilde{\mathbf{g}}_{(1-i)}(z^2)\mathbf{J}_M$, $i = 0, 1$, which in turn yields the result

$$\tilde{\mathbf{g}}_0(z^2)\mathbf{J}_M\mathbf{g}_0(z^2) = (-1)^{(m-1)}z^{-2(m-1)}\tilde{\mathbf{g}}_0(z^2)\tilde{\mathbf{g}}_1(z^2)\mathbf{J}_M = \tilde{\mathbf{g}}_1(z^2)\mathbf{J}_M\mathbf{g}_1(z^2). \tag{4.20}$$

Substituting (4.14), (4.15) in (4.18) and using (4.20), we get

$$\begin{aligned}\tilde{\mathbf{E}}(z)\mathbf{E}(z) &= 2M\left[\tilde{\mathbf{g}}_0(z^2)\mathbf{g}_0(z^2) + \tilde{\mathbf{g}}_1(z)\mathbf{g}_1(z)\right] + \\ &\qquad (-1)^{(m-1)}2M\underbrace{\left[\tilde{\mathbf{g}}_0(z^2)\mathbf{J}_M\mathbf{g}_0(z^2) - \tilde{\mathbf{g}}_1(z^2)\mathbf{J}_M\mathbf{g}_1(z^2)\right]}_{=0}, \\ &= 2M\left[\tilde{\mathbf{g}}_0(z^2)\mathbf{g}_0(z^2) + \tilde{\mathbf{g}}_1(z^2)\mathbf{g}_1(z^2)\right]. \end{aligned} \tag{4.21}$$

From (4.21) we get

$$\mathbf{E}(z) \text{ is lossless} \Leftrightarrow 2M\left[\tilde{\mathbf{g}}_0(z^2)\mathbf{g}_0(z^2) + \tilde{\mathbf{g}}_1(z^2)\mathbf{g}_1(z^2)\right] = \mathbf{I}_M. \tag{4.22}$$

The matrix equation (4.22) can be re-written as M scalar equations (and since (4.22) holds for all values of z, we can replace $-z^2$ by z), which are precisely the conditions in (4.17). Thus, the lossless property of $\mathbf{E}(z)$ has been shown to be equivalent to the much simpler, power-complementary condition in (4.17). This result can be summarized as, "$\mathbf{E}(z)$ is lossless if and only if appropriate pairs of polyphase components of $H(z)$ are power complementary."

$\nabla\nabla\nabla$

The above lemma covers all cosine-modulated filter banks that are derived from a linear-phase prototype of length $N = 2mM$. Owing to the linear-phase symmetry of $H(z)$, approximately half of the M constraints given in (4.17) are redundant. For example, using (4.19) it can be verified that the condition in (4.17) for $k = k_1$, where $0 \leq k_1 \leq (M-1)$, is the same as the condition for $k = M - 1 - k_1$. Removing the redundant constraints, (4.17) can be expressed as :

1. **for M even**

$$\tilde{G}_k(z)G_k(z) + \tilde{G}_{M+k}(z)G_{M+k}(z) = \frac{1}{2M}, \quad 0 \leq k \leq \frac{M}{2} - 1. \tag{4.23}$$

2. **for M odd**

$$\begin{aligned} \tilde{G}_k(z)G_k(z) + \tilde{G}_{M+k}(z)G_{M+k}(z) &= \frac{1}{2M}, \quad 0 \leq k \leq \lfloor \frac{M}{2} \rfloor - 1. \\ 2\tilde{G}_{\frac{M-1}{2}}(z)G_{\frac{M-1}{2}}(z) &= \frac{1}{2M}. \end{aligned} \tag{4.24}$$

From (4.24), we see that for M odd, the polyphase component $G_{\frac{M-1}{2}}(z)$ is forced to be a pure delay. By symmetry, the polyphase component $G_{M+\frac{M-1}{2}}(z)$ is also a pure delay. The conditions in (4.23) and (4.24) are equivalent to the conditions in (4.17). The total number of independent constraints is $\lfloor \frac{M}{2} \rfloor$, for M even/odd.

Further, for the special case with $N = 2M$, all the $2M$ polyphase components are constants, i.e., $G_k(z) = h(k)$, $0 \leq k \leq 2M - 1$. If $H(z)$ has real coefficients, the

linear-phase symmetry yields $h(k) = h(2M-1-k)$. So we can express (4.17) as

$$h^2(k) + h^2(M+k) = h^2(k) + h^2(M-1-k) = \frac{1}{2M}, \quad 0 \le k \le M-1, \tag{4.25}$$

which is exactly the condition obtained in [Prin86,Vet89,Mal90a]. If $H(z)$ has complex coefficients satisfying $h(n) = h^*(2M-1-n), \ \forall\, n$, then (4.17) becomes

$$|h(k)|^2 + |h(M-1-k)|^2 = \frac{1}{2M}, \quad 0 \le k \le M-1. \tag{4.26}$$

For the rest of this chapter, we will consider prototypes with real coefficients only. The following result, which can be readily verified, will be used later.

Fact 4.2 : Consider a linear-phase prototype of length $N = 2mM$ whose impulse response coefficients are

$$h(k) = \begin{cases} \frac{1}{\sqrt{4M}}, & (mM-M) \le k \le (mM+M-1), \\ 0, & \text{otherwise.} \end{cases} \tag{4.27}$$

This prototype satisfies the conditions given in (4.23), (4.24). ◇

4.3 Design of Prototype ($N = 2mM$)

In this section we focus on the design of the prototype (length $N = 2mM$) for modulated filter banks satisfying the PR property. The approach is to obtain a prototype satisfying the conditions in (4.23), and (4.24) which, by Lemma 4.1, are sufficient to ensure PR for the overall system. Further, the prototype filter $H(z)$ should have high stopband attenuation and a narrow transition bandwidth. So, $H(z)$ must be obtained by optimization.

One way of satisfying the conditions in (4.23), and (4.24) during the optimization is via spectral factorization. Suppose $G_k(z)$, one of the polyphase components of each power complementary pair $\{G_k(z),\ G_{M+k}(z)\}$ is optimized, then $G_{M+k}(z)$ can be computed by spectral factorization. This must be done for each of the power complementary pairs, and the same process must be repeated in every iteration. This would then amount to $\lfloor \frac{M}{2} \rfloor$ spectral factor computations per iteration. However, there

is another way which completely avoids this extensive amount of computation. This is achieved by using the two-channel lossless lattice [Vai86b] which is discussed next. We will fully exploit the advantages of these lattices in our design approach.

4.3.1 Two-Channel Lossless Lattice

We have the following result from [Vai86b], which introduces the two-channel lossless lattice.

Fact 4.3 : A stable digital filter transfer function $P(z)$ with real coefficients is said to be bounded real (BR) if $|P(e^{j\omega})| \leq 1, \quad \forall\omega$. And any FIR BR pair $\{P(z),\ Q(z)\}$ satisfying

$$\tilde{P}(z)P(z) + \tilde{Q}(z)Q(z) = 1, \quad \forall z, \tag{4.28}$$

can always be realized as a non-recursive, cascaded, two-channel lossless lattice structure shown in Fig. 4.2(a),(b). $\Diamond$

In Fig. 4.2(a), the two channel lossless lattice is made up of a cascade of the normalized, four-multiplier lattice sections. Each lattice section is characterized by one parameter θ_j, where the index j refers to the particular lattice section. In Fig. 4.2(b), the lattice is made up of a cascade of the denormalized, two-multiplier lattice sections characterized by the parameter β_j and the overall scaling multiplier α which is defined as $\alpha \triangleq \prod_{j=0}^{q} \frac{1}{\sqrt{1+\beta_j^2}}$.

In this chapter, we use the structure of Fig. 4.2(a) in obtaining the design procedure. However, since the two structures are equivalent [Vai86b], the design procedure can be readily translated to the structure of Fig. 4.2(b). Both lattices have the same number of parameters, but the latter is used in the implementation of the filter bank since it requires approximately half the number of multipliers as the former.

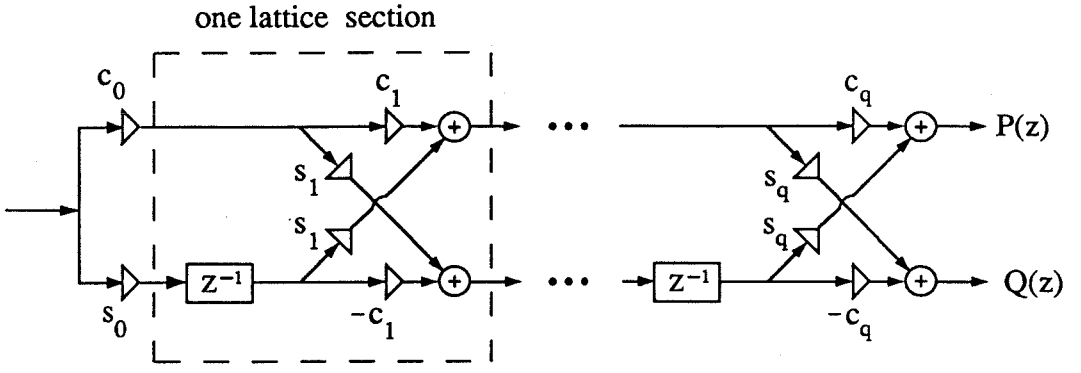

Fig. 4.2(a). The two-channel lossless lattice with four-multiplier lattice sections.
$c_j = \cos\theta_j$ and $s_j = \sin\theta_j$.

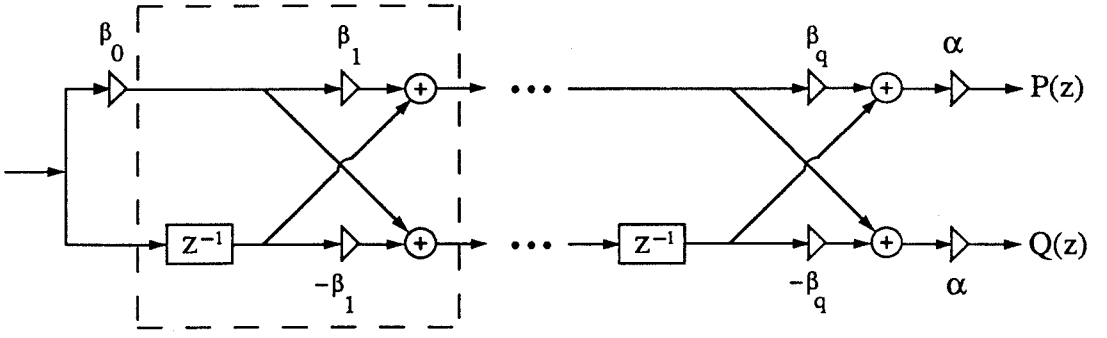

Fig. 4.2(b). The two-channel lossless lattice with two-multiplier lattice sections.
α is the scaling multiplier.

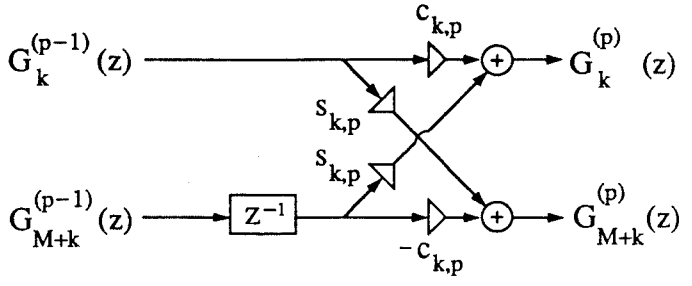

Fig. 4.2(c). Typical four-multiplier implementation of the p^{th} lattice section of the k^{th} lattice.

4.3.2 Satisfying the Pairwise Power Complementary Constraint

From Lemma 4.1, we have the conditions that require pairs of polyphase components to satisfy the power complementary (PC) property. From Fact 4.3, we see that each of these pairs $\{G_k(z),\ G_{M+k}(z)\}$, can be designed (to within a scale factor) by using a separate two-channel lossless lattice. During the optimization of the prototype response, we work directly with the lattice parameters. Hence the polyphase component pairs are guaranteed to satisfy the pairwise PC property which, in turn, ensures PR. The same is true even in the presence of coefficient quantization. So, in other words, the advantage of using the two-channel lossless lattices is that the PR condition is inherently satisfied and hence, it need not be included as one of the constraints in the design of $H(z)$.

For M even (refer equation (4.23)), we design $\frac{M}{2}$ pairs of polyphase components, with the rest being determined by symmetry. For M odd (refer equation (4.24)), we design $\lfloor\frac{M}{2}\rfloor$ pairs of polyphase components, with $G_{\frac{M-1}{2}}(z),\ G_{M+\frac{M-1}{2}}(z)$ being forced to be pure delays and the remaining $\lfloor\frac{M}{2}\rfloor$ pairs of polyphase components being determined by symmetry. So, for any M, the number of two-channel lossless lattices needed for design of the prototype is $\lfloor\frac{M}{2}\rfloor$.

In Fig. 4.2(d), we have a block diagram representation of the $\lfloor\frac{M}{2}\rfloor$ two-channel lattices. The k^{th} lattice yields the PC pair $\{G_k(z),\ G_{M+k}(z)\}$. Its parameters are denoted as $\theta_{k,j}$, where the index j refers to the particular lattice section. The transfer function between the input of the lattice and the output of the p^{th} lattice section is denoted by a superscript p. The lattice transfer functions are initialized as

$$G_k^{(0)}(z) = \cos\theta_{k,0} \quad \text{and} \quad G_{M+k}^{(0)}(z) = \sin\theta_{k,0}, \qquad 0 \le k \le \lfloor\frac{M}{2}\rfloor - 1. \tag{4.29}$$

In Fig. 4.2(c), we have a typical four-multiplier implementation of the p^{th} lattice section of the k^{th} lattice. Let $\{G_k^{(p-1)}(z),\ G_{M+k}^{(p-1)}(z)\}$ be the transfer functions from the input to the output of the $(p-1)^{th}$ section. We can then write down $\{G_k^{(p)}(z),\ G_{M+k}^{(p)}(z)\}$

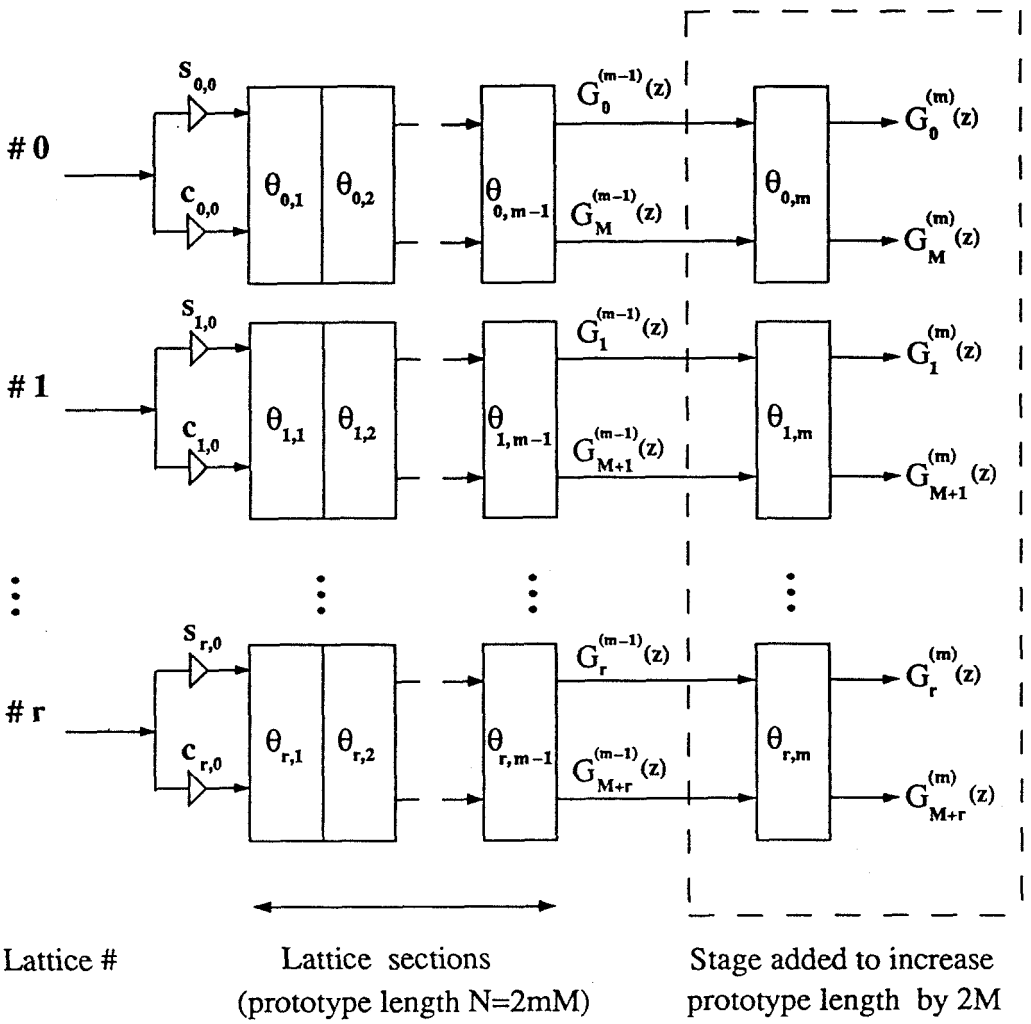

Fig. 4.2(d). A block diagram of the lattices used in the design of an M-channel prototype H(z). The total number of lattices = r+1=$\left\lfloor \frac{M}{2} \right\rfloor$.

as

$$\begin{bmatrix} G_k^{(p)}(z) \\ G_{M+k}^{(p)}(z) \end{bmatrix} = \begin{bmatrix} \cos\theta_{k,p} & \sin\theta_{k,p} \\ \sin\theta_{k,p} & -\cos\theta_{k,p} \end{bmatrix} \begin{bmatrix} G_k^{(p-1)}(z) \\ z^{-1}G_{M+k}^{(p-1)}(z) \end{bmatrix}, \quad p \geq 1,\ 0 \leq k \leq \lfloor \frac{M}{2} \rfloor - 1. \tag{4.30}$$

Hence, we get a recursive relation for the transfer function when a new lattice section is added. From (4.30), it can also be seen that the addition of each lattice section increases the order of the transfer functions by one.

Number of parameters to be optimized

From the preceding discussion, we know that $\lfloor \frac{M}{2} \rfloor$ two-channel lattices are used in the design of the prototype $H(z)$ for an M-channel modulated PR filter bank. If the length of the prototype is $N = 2mM$, then each of $2M$ polyphase components has length m (and hence, order $(m-1)$). This implies that each lattice has $(m-1)$ sections, involving a total of m unknown parameters $[\theta_{k,0},\ \theta_{k,1},\ \cdots\ \theta_{k,(m-1)}]$. Hence the total number of parameters to be optimized is $m\lfloor \frac{M}{2} \rfloor$.

On the other hand, a pseudo-QMF design (same length prototype) involves mM parameters while the lossless lattice approach to PR-QMF design [Vai87a,Vai89, Koi90] requires many more, viz., $[(2m-1)(M-1) + \frac{M(M-1)}{2}]$ parameters. A comparison of the number of parameters to be optimized in each of the three design approaches – the modulated PR bank, pseudo-QMF and lattice-based PR-QMF banks, is shown in Table 4.2. From Table 4.2, we see that the modulated PR filter bank approach requires approximately half the number of parameters as in the pseudo-QMF design and much fewer parameters when compared with the lattice-based PR-QMF approach. This advantage becomes significant, particularly for large M. In the next section (in design example 4.2), we will present design comparisons between the prototypes of modulated PR banks and pseudo-QMF banks.

Table 4.2. Comparison of the number of parameters optimized in the design of Modulated PR banks, Pseudo-QMF banks and traditional PR-QMF banks

		# of parameters optimized		
# channels M	length N	Modulated PR bank	pseudo-QMF	traditional PR-QMF
3-channels	48	8	24	33
	60	10	30	41
5-channels	40	8	20	38
	60	12	30	54
7-channels	42	9	21	51
	84	18	42	87
16-channels	64	16	32	165
	96	24	48	195
17-channels	68	16	34	184
	102	24	51	216

4.3.3 Design Steps

The procedure for designing the M-channel prototype filter (length $N = 2mM$) involves the initialization of the parameters of the $\lfloor \frac{M}{2} \rfloor$ lattices and the optimization of these parameters. We discuss each aspect separately.

I. Initialization : The following is a simple initialization scheme for the parameters of all the $\lfloor \frac{M}{2} \rfloor$ two-channel lattices (each two-channel lattice has $(m-1)$ sections),

$$\theta_{k,p} = \begin{cases} \frac{\pi}{4}, & p = 0, \quad 0 \leq k \leq \lfloor \frac{M}{2} \rfloor - 1, \\ \frac{\pi}{2}, & 1 \leq p \leq (m-1), \quad 0 \leq k \leq \lfloor \frac{M}{2} \rfloor - 1. \end{cases} \tag{4.31}$$

It can be verified that this initialization corresponds to a prototype $H(z)$ satisfying

$$h(k) = \begin{cases} 1, & (mM - M) \leq k \leq (mM + M - 1), \\ 0, & \text{otherwise.} \end{cases} \tag{4.32}$$

With appropriate scaling, this prototype satisfies (4.23), (4.24) (as mentioned earlier in Fact 4.2). This prototype $H(z)$ has stopband attenuation $A_s \simeq 13$ dB and stop-

band edge $\omega_s < \frac{\pi}{M}$ radians. This approach is independent of the value of m (i.e., independent of N) and from (4.32) we see that exactly $2M$ coefficients of $H(z)$ are initialized to be non-zero while the remaining $(2mM - 2M)$ coefficients are set to zero. As a result, this scheme works well for smaller values of m whereas for larger values of m, a different approach (which is described in Section 4.3.5) works better.

II. Optimization : Having initialized all $m\lfloor\frac{M}{2}\rfloor$ parameters, they are then optimized using standard optimization routines (e.g., *e04jaf* [NAG], based on the quasi-Newton algorithm) to minimize the objective function – either Φ_1 **or** Φ_2 given below

$$\Phi_1 = \int_{\frac{\pi}{2M}+\delta}^{\pi} |H(e^{j\omega})|^2 \, d\omega, \qquad \Phi_2 = \max_{\omega\epsilon[\frac{\pi}{2M}+\delta,\pi]} |H(e^{j\omega})|, \tag{4.33}$$

where $\delta < \frac{\pi}{2M}$. Using Φ_1, the problem involves the minimization of the stopband energy (yielding a minimum energy solution) while with Φ_2, it involves the minimization of the maximum of the filter response in the stopband (yielding a minimax solution). In all the examples, it was observed that using Φ_1 produces quicker convergence whereas using Φ_2 gives a prototype with lower stopband attenuation A_s (nearly equiripple solution). In order to combine the advantages of both objective functions Φ_1, Φ_2, the following scheme works well.

Step 1 : After initialization, optimize using Φ_1 and obtain the minimum energy solution.

Step 2 : Using the prototype obtained in Step 1 as the starting point, run the optimization using Φ_2 and obtain the minimax solution.

For Step 2, it was observed that the optimization can be terminated after approximately $100 * m\lfloor\frac{M}{2}\rfloor$ iterations. (**Note** : $m\lfloor\frac{M}{2}\rfloor$ = total number of parameters being optimized.) Doing Step 2 is optional. However, in most cases the prototype obtained by doing Step 2 after Step 1 had higher stopband attenuation than the prototype at the end of Step 1. All the above-mentioned features are demonstrated in the design

examples in Section 4.4.

4.3.4 Increasing the Length of the Prototype

Another attractive feature of this design approach is the ease with which a prototype $H(z)$ of a particular length $N = 2mM$ can be used to obtain a prototype $H'(z)$ of longer length (increments in length are in multiples of $2M$). Let the length of $H'(z)$ be $2mM + 2M$. The increase in the length of the prototype by $2M$ directly translates into a unit increase in the lengths of each of the $2M$ polyphase components. This implies that precisely one lattice section must be added to each of the $\lfloor \frac{M}{2} \rfloor$ two-channel lattices (which are used in the design of the prototype). In this sense, the structure has a hierarchical property. This is shown schematically in Fig. 4.2(c). The procedure to obtain $H'(z)$ is as follows. First, the values of all the $m\lfloor \frac{M}{2} \rfloor$ lattice parameters used to obtain $H(z)$ are retained. Then, for the newly added lattice sections, we set $\theta_{k,m} = \frac{\pi}{2}$, $\forall k$. Finally, all the $(m+1)\lfloor \frac{M}{2} \rfloor$ parameters are optimized to yield the new prototype $H'(z)$.

4.3.5 Two-Stage Design for Long Length Prototypes

The above feature, which allows the length of the prototype to be increased, also gives an approach to design prototypes of long length (i.e, large values of m). Let the desired length of the prototype be $N_1 = 2m_1M$, where $m_1 > 3$. The design steps are summarized below.

(a) Design a prototype for $m = 2$ or 3 by doing Step 1 of the optimization. Use this as an initialization for the next design.

(b) Add $(m_1 - m)$ additional sections to each of the $\lfloor \frac{M}{2} \rfloor$ lattices used in the design and initialize the parameters of these added sections by setting them to $\frac{\pi}{2}$.

(c) Optimize (using Step 1) to obtain the desired prototype filter.

(d) Re-run the optimization (using Step 2), if needed.

The reason for using the above two-stage approach is that the initialization given in (4.31) gives a prototype with $A_s \simeq 13$ dB as the starting point. This initialization works well for the design of prototypes with $m \leq 3$, but is not quite satisfactory for longer length prototypes. The two-stage approach has been found to work well in most cases.

4.3.6 Implementation and Complexity of Modulated PR Banks

We will now obtain an efficient implementation that is applicable to cosine-modulated filter banks satisfying (2.34) obtained from a linear-phase prototype of length $N = 2mM$. (There are no restrictions on M or m.)

The modulation matrix $\hat{\mathbf{C}}$ is expressed as $\hat{\mathbf{C}} = [\mathbf{A}_0' \; \mathbf{A}_1']$ and using the relations in Table 4.8 along with the results in (4A.10) and (4A.11), we have

$$\hat{\mathbf{C}} = \begin{cases} \sqrt{M}\,(-1)^{m_1}\,\mathbf{C}\,[(\mathbf{I}-\mathbf{J}) \;\; -(\mathbf{I}+\mathbf{J})], & \text{for } m \text{ even (i.e., } m = 2m_1), \\ \sqrt{M}\,(-1)^{m_1}\,\mathbf{C}\,[(\mathbf{I}+\mathbf{J}) \;\; (\mathbf{I}-\mathbf{J})], & \text{for } m \text{ odd (i.e., } m = 2m_1+1), \end{cases} \tag{4.34}$$

where $\mathbf{C}$ is the Type IV Discrete Cosine Transform [Yip87] whose definition is given in (4A.6). Using (4.34) in (4.8), we get the implementation in Fig. 4.3(a) (where the constant scale factor $\sqrt{M}(-1)^{m_1}$ has been omitted). For the special case when M is even and m is even, Fig. 4.3(a) can be further simplified to obtain the implementation in [Mas85]. The complexity of the entire modulation section is $3M$ adders along with the complexity of the DCT. Since the modulation part is identical for modulated PR banks and pseudo-QMF banks, in the following comparison, we will consider only the complexity of implementing the polyphase components $[G_0(-z^2),\; G_1(-z^2) \;\cdots\; G_{2M-1}(-z^2)]$.

In pseudo-QMF designs, the $2M$ polyphase components (each of length m) are implemented in direct form requiring $2mM$ multipliers and $2M(m-1)$ adders. For mod-

Table 4.7. Comparison of implementation complexity of Modulated PR Banks and Pseudo-QMF Banks
MPU (APU) - Multiplications (Additions) per unit time

		MPU	APU
Modulated PR Banks	M even	$2(m+1)$	$2(m-1)$
	M odd	$2\alpha(m+1)$	$2\alpha(m-1)$
Pseudo-QMF Banks		$2m$	$2(m-1)$

where $\alpha = \left(\frac{2\lfloor \frac{M}{2} \rfloor}{M}\right) < 1$.

ulated PR banks, the polyphase components are implemented as $2\lfloor \frac{M}{2} \rfloor$ two-channel lossless lattices (Fig. 4.3(b)). Using two-multiplier lattice sections, each lattice requires $(2m+2)$ multipliers (including the two scaling multipliers) and $2(m-1)$ adders. The multiplications per unit time (MPU) and additions per unit time (APU) are two measures of implementation complexity. The corresponding MPU and APU values for modulated PR banks and pseudo-QMF banks are given in Table 4.7.

4.4 Examples of Modulated PR Filter Banks

Design Example 4.1 : This example demonstrates the different aspects of the new approach to design the prototype filter $H(z)$ of a modulated PR filter bank. We will consider the case $M = 17$ channels. (As M is a prime number, the filter bank cannot be implemented as a tree-structure.) Since $\lfloor \frac{M}{2} \rfloor = 8$, we require 8 two-channel lossless lattices in order to design the eight pairs of PC polyphase components (which satisfy (4.24)). Table 4.3 shows the particular polyphase components designed by each of the eight lattices. Since M is odd, two of the polyphase components are forced to be pure delays (as mentioned in Section 4.2). They are $G_8(-z)$ and $G_{25}(-z)$. The remaining eight pairs of polyphase components are obtained by symmetry relations, (given in (4.19)) owing to the linear-phase property of the prototype.

The length of the prototype filter $H(z)$ is $N = 2mM$. We present three designs –

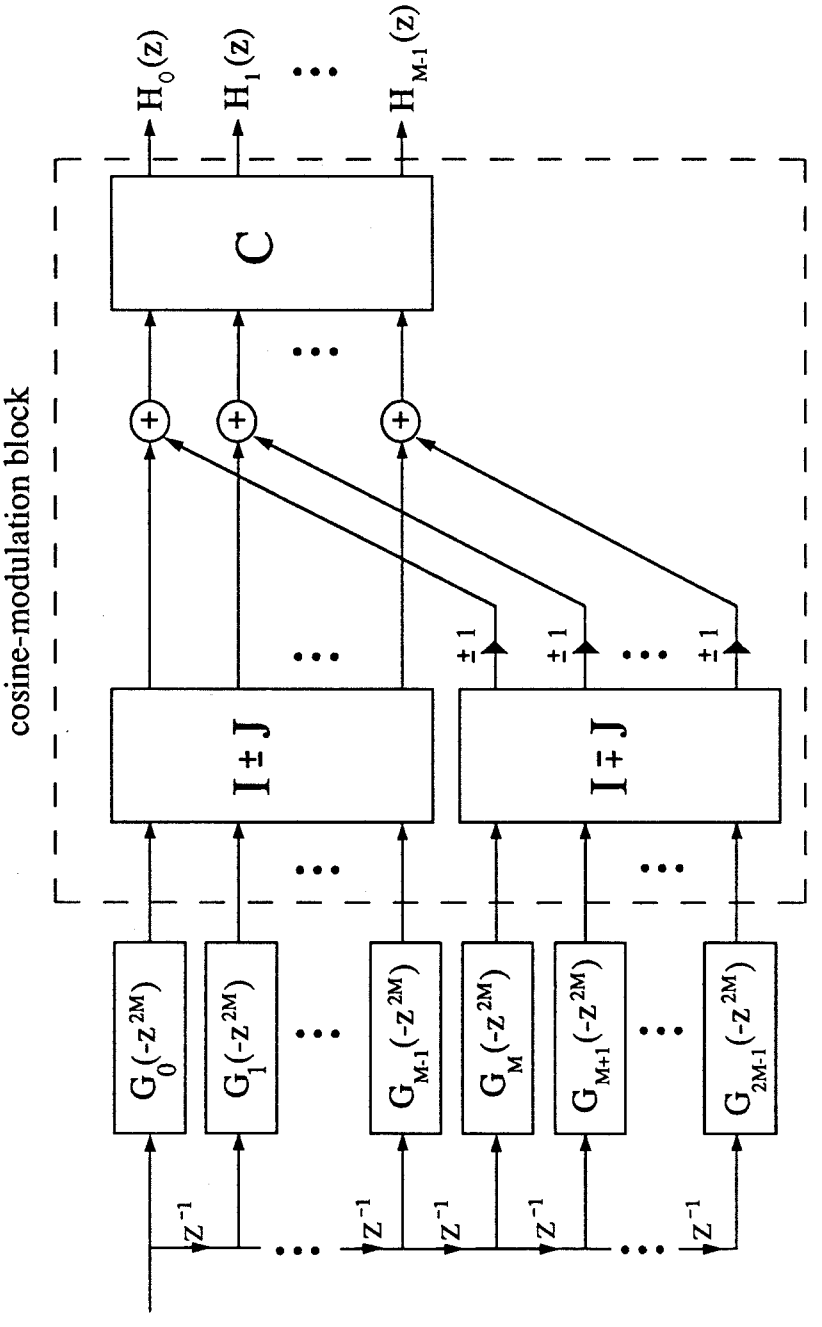

Fig. 4.3(a). Implementation of a cosine-modulated filter bank derived from a linear-phase prototype filter of length N=2mM (including pseudo-QMF banks).
C is the Type IV Discrete Cosine Transform (DCT) matrix.

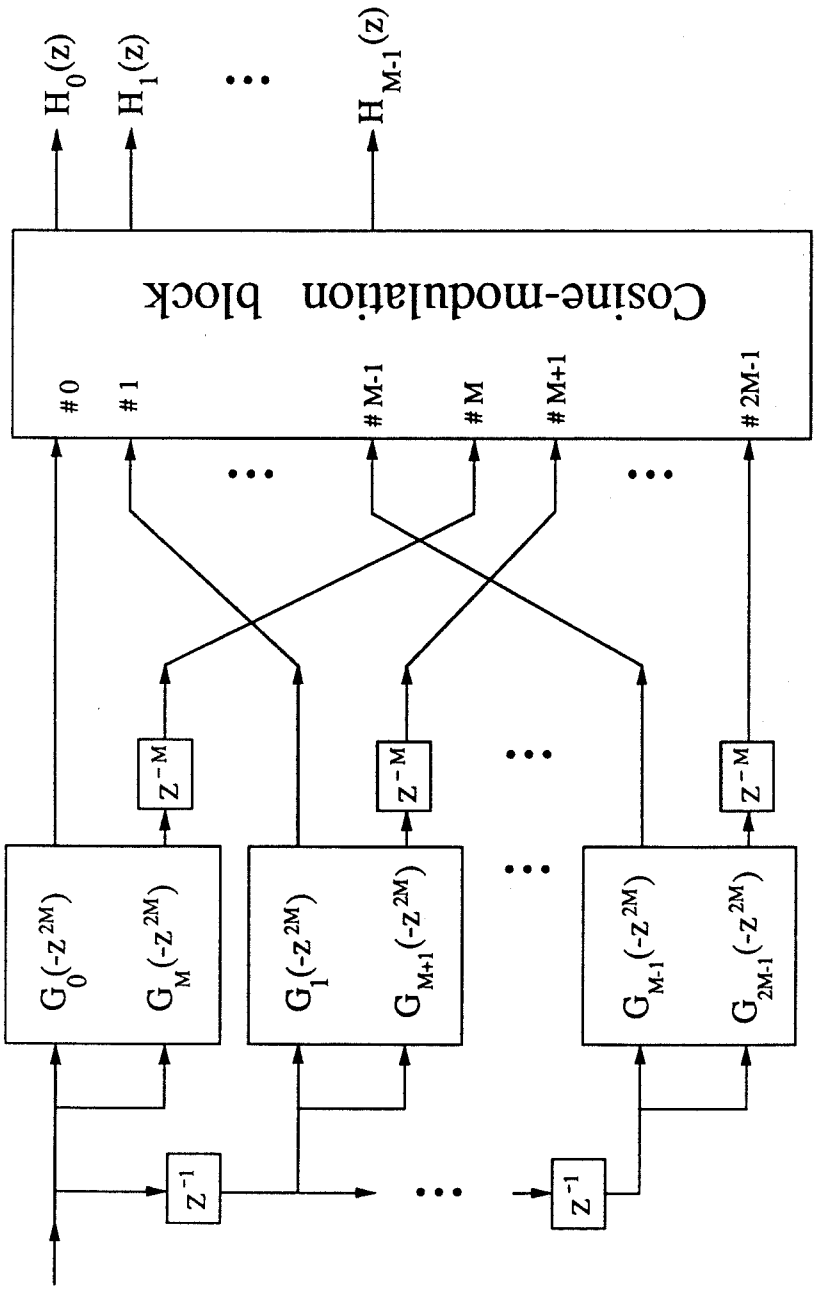

Fig. 4.3(b). Implementation of cosine-modulated PR analysis filter bank. Each polyphase component pair $\{G_k(-z^{2M}), G_{M+k}(-z^{2M})\}$ is implemented by a two-channel lossless lattice. (A total of M lattices are used.) The cosine-modulation block is given in Fig. 4.3(a).

Table 4.3. Design example 4.1. Design of a 17-channel Modulated PR bank prototype

	Lattice number							
	0	1	2	3	4	5	6	7
Polyphase Components	$G_0(z)$, $G_{17}(z)$	$G_1(z)$, $G_{18}(z)$	$G_2(z)$, $G_{19}(z)$	$G_3(z)$, $G_{20}(z)$	$G_4(z)$, $G_{21}(z)$	$G_5(z)$, $G_{22}(z)$	$G_6(z)$, $G_{23}(z)$	$G_7(z)$, $G_{24}(z)$

Table 4.4. Design example 4.1. Comparison of the 17 channel Modulated PR bank prototype after Step 1 and Step 2 of the optimization

Length N	Step 1 (Min. energy)		Step 2 (Minimax)	
	A_s (dB)	ω_s (rads.)	A_s (dB)	ω_s (rads.)
68	30.51	0.0644π	32.45	0.0644π
102	35.72	0.0620π	42.16	0.0644π
136	37.22	0.0614π	44.51	0.0644π

for prototypes of length $N = 68$, $N = 102$ and $N = 136$. The corresponding values of m are $2, 3$ and 4 respectively. The total number of parameters to be optimized in each design is $8m$ $(= m\lfloor\frac{M}{2}\rfloor)$. First we design the prototype with $N = 68$. In this design, the parameters are initialized as in (4.31). After optimization, we obtain the desired prototype filter. Then we increase the length (as explained in Section 4.3.4) to obtain prototypes of length $N = 102$ and 136. In each case, after initialization of the lattice parameters, Step 1 of the optimization was done. Using this design as a starting point, Step 2 of the optimization was also done. For each of the three designs, the magnitude responses of the prototype at the end of Step 1 (Minimum energy solution) and at the end of Step 2 (Minimax solution) are plotted in Fig. 4.4(a)-(c). To facilitate comparison, minimum energy solution is shown by a broken line while the minimax solution is shown by a solid line. The corresponding values of stopband attenuation (A_s) and the stopband edge (ω_s) for each design are presented in Table 4.4.

Hence it can be readily seen that in each instance, doing Step 2 of the optimization (i.e, re-running the optimization with Φ_2 as the objective function) improved the A_s of the prototype. The impulse response coefficients of the prototype filter (with $N = 102$) are given in Table 4.5. It's frequency response is shown in Fig. 4.5(a) and the responses of all the filters in PR bank, obtained by the cosine-modulation of $H(z)$ as in equation (2.34), are plotted in Fig. 4.5(b).

Design Example 4.2 : In this example, we present a comparison between the modulated PR filter banks and pseudo-QMF banks. One of the differences between the two approaches must be mentioned at the outset. That is, in pseudo-QMF banks, an assumption is made that filters belonging to non-adjacent channels do not overlap (i.e., in a seven channel pseudo-QMF bank, $H_3(e^{j\omega})$ has overlaps with $H_2(e^{j\omega})$ and $H_4(e^{j\omega})$. The passbands of all the other filters lie in the stopband of $H_3(e^{j\omega})$). This places a constraint on the transition bandwidth of the prototype filter. Such a constraint is not necessary in the case of modulated PR-banks. But for purposes of comparison, we will look at prototypes (of both methods) with same transition bandwidth.

The performance of a QMF bank is measured by following two quantitative criteria.

1. **The peak-to-peak Reconstruction Error (E_{p-p}) :** The transfer function of the overall analysis/synthesis system is given by $T(z) = \frac{1}{M}\sum_{k=0}^{M-1} H_k(z)F_k(z)$. Using filters whose responses are normalized to unity, we get

$$(1 - \delta_1) \leq M\left|T(e^{j\omega})\right| \leq (1 + \delta_2), \tag{4.35}$$

and E_{p-p} is defined as $E_{p-p} \triangleq \delta_1 + \delta_2$.

2. **The Aliasing Error (E_a) :** The output of the analysis/synthesis system can

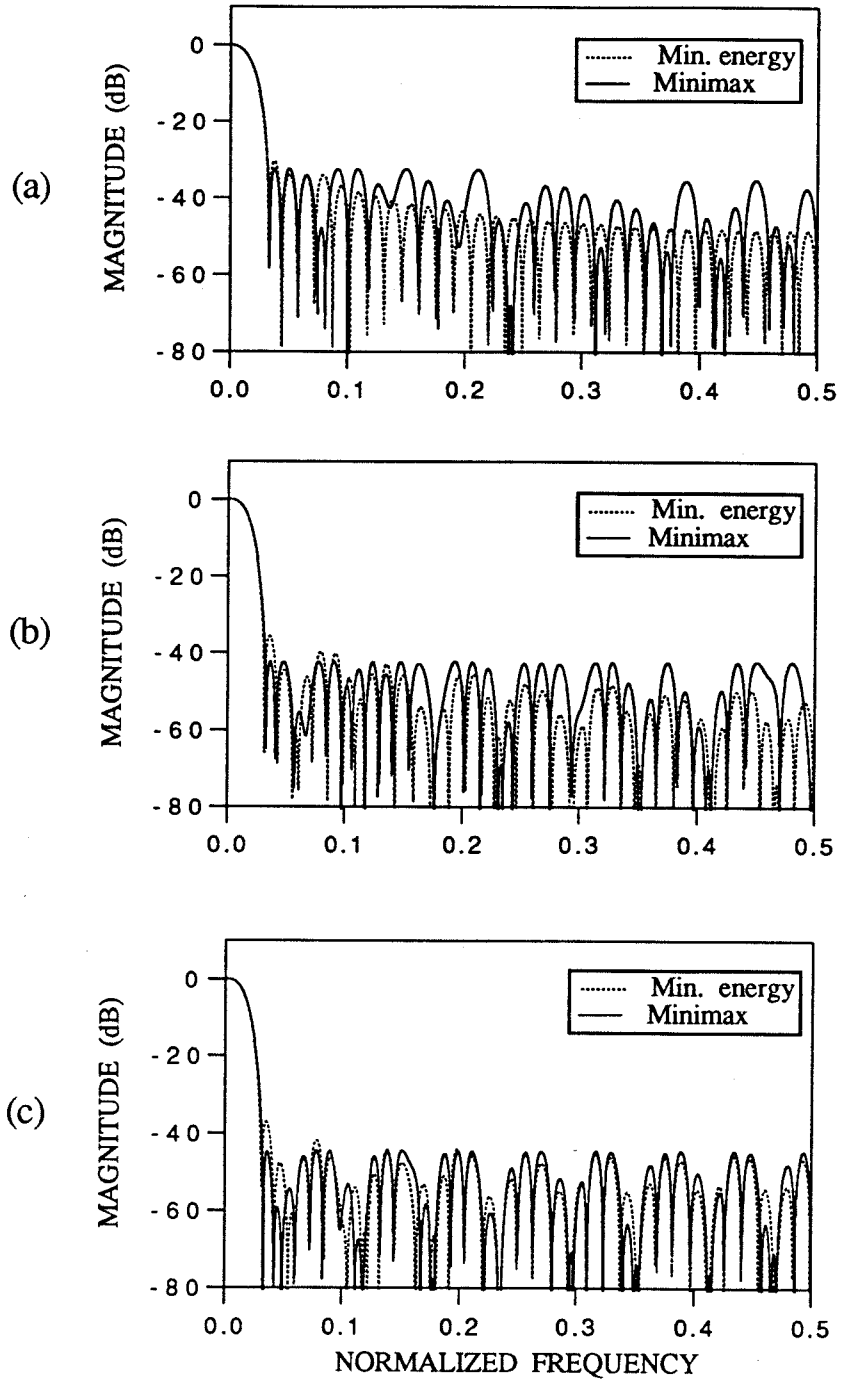

Fig. 4.4 . Design example 4.1. Magnitude responses of 17 channel prototype after Step 1 (Min. energy) and Step 2 (Minimax)
(a). N=68 (b). N=102 (c). N=136

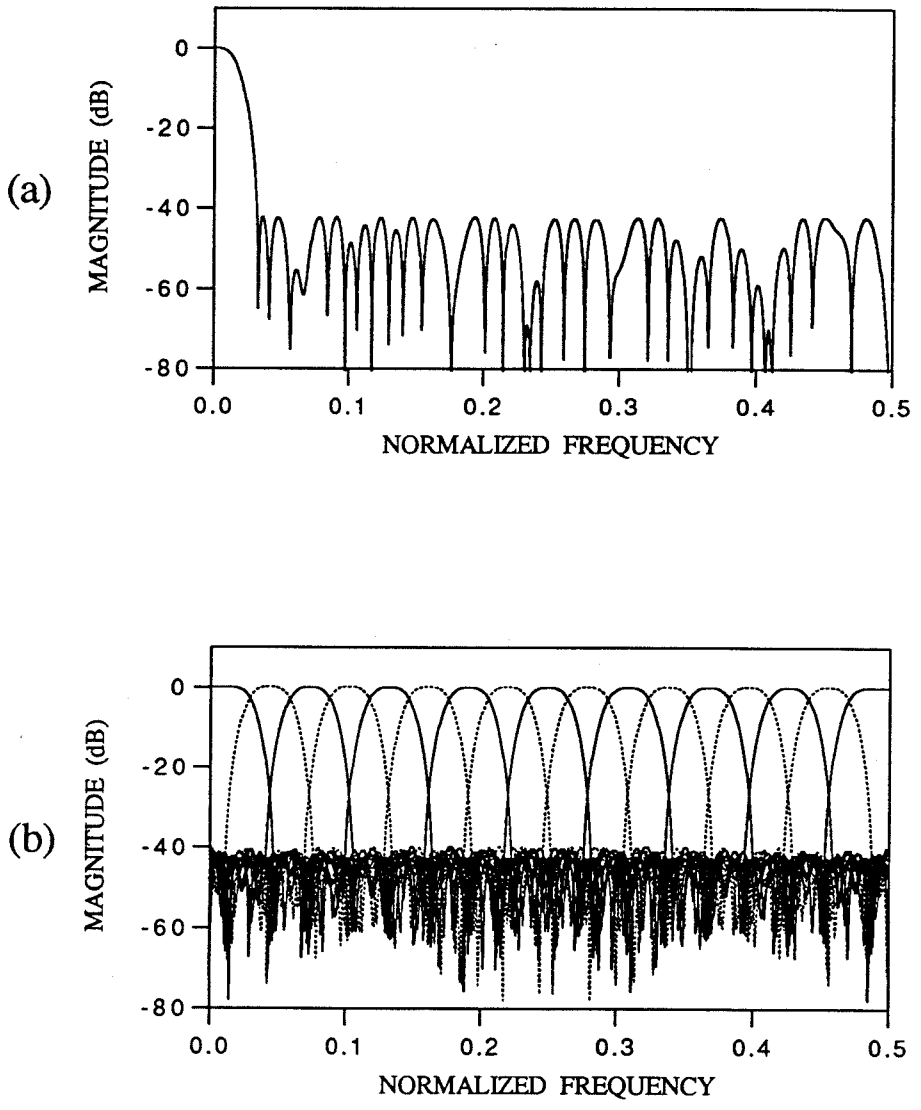

Fig. 4.5. Design example 4.1.
(a) Response of the 17-channel prototype (N=102),
(b) 17-channel cosine-modulated PR filter bank.

Table 4.5. Design example 4.1. Impulse response coefficients of prototype ($N = 102$) of a 17-channel modulated PR filter bank

n	$h(n)$	n	$h(n)$	n	$h(n)$
0	-4.272049E-04	34	1.376675E-02	68	1.316380E-02
1	-4.853395E-04	35	1.633310E-02	69	1.082142E-02
2	-4.997748E-04	36	1.759948E-02	70	9.552895E-03
3	-5.129669E-04	37	2.034467E-02	71	7.256847E-03
4	-5.288108E-04	38	2.191992E-02	72	6.355320E-03
5	-3.490611 E-04	39	2.431080 E-02	73	3.784142 E-03
6	-3.878599 E-04	40	2.595075 E-02	74	3.757966 E-03
7	-2.579029 E-04	41	2.742702 E-02	75	3.160015 E-03
8	1.105338 E-34	42	2.948043 E-02	76	-1.805155 E-18
9	-2.180628 E-03	43	3.116092 E-02	77	-3.737350 E-04
10	-1.960596 E-03	44	3.234317 E-02	78	-7.434289 E-04
11	-1.714884 E-03	45	3.360359 E-02	79	-7.702541 E-04
12	-1.928333 E-03	46	3.478912 E-02	80	-1.742832 E-03
13	-1.959910 E-03	47	3.555154 E-02	81	-1.899333 E-03
14	-2.102945 E-03	48	3.643303 E-02	82	-2.270290 E-03
15	-2.075392 E-03	49	3.665203 E-02	83	-2.530636 E-03
16	-2.265407 E-03	50	3.693109 E-02	84	-2.482397 E-03
17	-2.482397 E-03	51	3.693109 E-02	85	-2.265407 E-03
18	-2.530636 E-03	52	3.665203 E-02	86	-2.075392 E-03
19	-2.270290 E-03	53	3.643303 E-02	87	-2.102945 E-03
20	-1.899333 E-03	54	3.555154 E-02	88	-1.959910 E-03
21	-1.742832 E-03	55	3.478912 E-02	89	-1.928333 E-03
22	-7.702541 E-04	56	3.360359 E-02	90	-1.714884 E-03
23	-7.434289 E-04	57	3.234317 E-02	91	-1.960596 E-03
24	-3.737350 E-04	58	3.116092 E-02	92	-2.180628 E-03
25	-1.805155 E-18	59	2.948043 E-02	93	1.105338 E-34
26	3.160015 E-03	60	2.742702 E-02	94	-2.579029 E-04
27	3.757966 E-03	61	2.595075 E-02	95	-3.878599 E-04
28	3.784142 E-03	62	2.431080 E-02	96	-3.490611 E-04
29	6.355320 E-03	63	2.191992 E-02	97	-5.288108 E-04
30	7.256847 E-03	64	2.034467 E-02	98	-5.129669 E-04
31	9.552895 E-03	65	1.759948 E-02	99	-4.997748 E-04
32	1.082142 E-02	66	1.633310 E-02	100	-4.853395 E-04
33	1.316380 E-02	67	1.376675 E-02	101	-4.272049 E-04

be expressed in terms of the input as

$$\widehat{X}(z) = \frac{1}{M}X(z)\sum_{k=0}^{M-1} H_k(z)F_k(z) + \underbrace{\frac{1}{M}\sum_{\ell=1}^{M-1} X(zW^{\ell})\sum_{k=0}^{M-1} H_k(zW^{\ell})F_k(z)}_{\text{Alias terms}}, \qquad (4.36)$$

and the total aliasing error is given by

$$E(\omega) = \frac{1}{M}\left[\sum_{\ell=1}^{M-1}\left|A_\ell(e^{j\omega})\right|^2\right]^{\frac{1}{2}}, \qquad (4.37)$$

where $A_\ell(z) = \sum_{k=0}^{M-1} H_k(zW^{\ell})F_k(z)$ and $E_a \triangleq \max_\omega E(\omega)$. In the design comparisons, the stopband attenuation (A_s) and stopband edge (ω_s) of each prototype (modulated-PR and pseudo-QMF) are tabulated along with their respective E_{p-p} and E_a values. This is done for a 7-channel design and also for a 17-channel design.

In the 7-channel design, the length of the prototype is $N = 42$ (the corresponding value of m is 3). For the design of the modulated PR prototype, 3 two-channel lossless lattices are used. The lattice parameters (total = 9) are initialized as in (4.31) and the prototype is obtained by doing both Step 1 and Step 2 of the optimization. The resulting prototype filter has stopband attenuation $A_s = 34.13$ dB and stopband edge $\omega_s = 0.1426\pi$ rads. The values of E_{p-p} and E_a are 1.998 E-15 and 8.517 E-16 respectively. In pseudo-QMF designs, relative weighting is used in the objective function to trade off between the flatness constraint (affecting E_{p-p}) and the prototype filter stopband energy (affecting E_a). The three designs are obtained with different values of the relative weights. The parameters of the different designs are shown in Table 4.6(a).

In the 17-channel comparison, the modulated PR prototype has $N = 102$ with $A_s = 35.72$ dB and $\omega_s = 0.0586\pi$ rads. Its values of E_{p-p} and E_a are 8.216 E-15 and 1.041 E-15 respectively. As in the previous comparison, the modulated PR prototype is compared with three different pseudo-QMF prototypes and the results are given in Table 4.6(b). In both of the above design examples, we see that approximately 5 dB (in stopband attenuation) is the price paid to obtain PR. It must also be mentioned

Table 4.6(a). Design example 4.2. Comparison between Modulated PR-Banks and Pseudo-QMF Banks – 7 Channel $(N = 42)$

	Prototype		Reconstruction	Aliasing
	A_s (dB)	ω_s (rads.)	Error (E_{p-p})	Error (E_a)
Pseudo-QMF bank	39.03	0.1424π	1.296 E-03	8.848 E-04
	38.55	0.1420π	2.095 E-04	9.198 E-04
	38.14	0.1414π	9.459 E-05	1.022 E-03
modulated PR bank	34.13	0.1426π	1.998 E-15	8.517 E-16

Table 4.6(b). Design example 4.2. Comparison between Modulated PR-Banks and Pseudo-QMF Banks – 17 Channel $(N = 102)$

	Prototype		Reconstruction	Aliasing
	A_s (dB)	ω_s (rads.)	Error (E_{p-p})	Error (E_a)
Pseudo-QMF bank	40.65	0.0590π	6.790 E-03	3.794 E-04
	38.68	0.0585π	2.139 E-04	3.193 E-04
	38.42	0.0581π	8.749 E-05	8.113 E-04
modulated PR bank	35.72	0.0586π	8.216 E-15	1.041 E-15

that it is not possible to choose the relative weights (for the objective function) in pseudo-QMF designs such that either E_{p-p} or E_a can be made arbitrarily small or comparable to the corresponding values in the modulated PR designs.

4.5 Summary

In this chapter, we have presented a derivation of the necessary and sufficient condition on the polyphase components of a linear-phase prototype filter $H(z)$ (length $N = 2mM$, where $m \geq 1$) such that $\mathbf{E}(z)$, the polyphase component matrix of the cosine-modulated filter bank, is lossless. The losslessness of $\mathbf{E}(z)$, in turn, ensures that the analysis/synthesis system (using modulated filter banks for analysis

and synthesis) satisfies the perfect reconstruction (PR) property. An efficient procedure to design the prototype (satisfying the above necessary and sufficient condition) is presented. This design procedure, based on the two-channel lossless lattice, involves fewer parameters to be optimized than pseudo-QMF designs and much fewer than lattice-based PR-QMF designs. This advantage becomes significant for large M (number of channels) and for long length prototypes. Using this approach, PR filter banks (FIR) can be designed for an arbitrary number of channels. Further, since both the analysis and synthesis filter banks are obtained by cosine modulation, an efficient is derived implementation using the $2M$ polyphase components of the prototype filter and the Discrete Cosine Transform (DCT) matrix. The details of design procedure and complexity of implementation are discussed and all the above-mentioned aspects are demonstrated by the examples and the detailed comparisons.

Appendix 4.A
Properties of Modulated PR Filter Banks

In this appendix, we present a proof for the results in equations (4.14), (4.15) and (4.16). The proof is given in two parts.

Part I : Let $\mathbf{A}_0$ and $\mathbf{A}_1$ be equal to $\mathbf{A}'_0$ and $\mathbf{A}'_1$ respectively, for the particular case when $m = 1$. Hence, using (4.11) and (4.12) we get

$$[\mathbf{A}_0]_{k,\ell} = 2\cos\left((2k+1)\frac{\pi}{2M}\left(\ell - M + \frac{1}{2}\right) + (-1)^k\frac{\pi}{4}\right), \quad 0 \le k,\ell \le M-1, \tag{4A.1}$$

$$[\mathbf{A}_1]_{k,\ell} = 2\cos\left((2k+1)\frac{\pi}{2M}\left(\ell + \frac{1}{2}\right) + (-1)^k\frac{\pi}{4}\right), \quad 0 \le k,\ell \le M-1. \tag{4A.2}$$

Now, we prove the following results

$$\mathbf{A}_0^\dagger\mathbf{A}_0 = 2M\left[\mathbf{I}_M + \mathbf{J}_M\right], \tag{4A.3}$$

$$\mathbf{A}_1^\dagger\mathbf{A}_1 = 2M\left[\mathbf{I}_M - \mathbf{J}_M\right], \tag{4A.4}$$

$$\mathbf{A}_1^\dagger\mathbf{A}_0 = \mathbf{A}_0^\dagger\mathbf{A}_1 = \mathbf{0}. \tag{4A.5}$$

Proof of (4A.3), (4A.4) and (4A.5) :

Let $\mathbf{C}$ and $\mathbf{S}$ be the Type IV Discrete Cosine Transform (DCT) and Type IV Discrete Sine Transform (DST) [Yip87] respectively, whose definitions are given below.

$$[\mathbf{C}]_{k,\ell} \triangleq c(k,\ell) = \sqrt{\frac{2}{M}}\cos\left(\frac{\pi}{M}(k+\frac{1}{2})(\ell+\frac{1}{2})\right), \quad 0 \le k,\ell \le M-1, \tag{4A.6}$$

$$[\mathbf{S}]_{k,\ell} \triangleq s(k,\ell) = \sqrt{\frac{2}{M}}\sin\left(\frac{\pi}{M}(k+\frac{1}{2})(\ell+\frac{1}{2})\right), \quad 0 \le k,\ell \le M-1. \tag{4A.7}$$

From [Yip87], we have the following identities (stating the Unitary and Hermitian properties of $\mathbf{C}$ and $\mathbf{S}$),

$$[\mathbf{C}]^{-1} = \mathbf{C} = [\mathbf{C}]^\dagger, \tag{4A.8}$$

$$[\mathbf{S}]^{-1} = \mathbf{S} = [\mathbf{S}]^\dagger. \tag{4A.9}$$

The matrices $\mathbf{A}_0$ and $\mathbf{A}_1$ can be expressed in terms of $\mathbf{C}$ and $\mathbf{S}$ as given below :

$$\mathbf{A}_0 = \sqrt{M}\,[\mathbf{C} + \mathbf{\Lambda S}], \tag{4A.10}$$

$$\mathbf{A}_1 = \sqrt{M}\,[\mathbf{C} - \mathbf{\Lambda S}], \tag{4A.11}$$

where $\mathbf{\Lambda}$ is an $M \times M$ diagonal matrix whose diagonal elements are given by $[\mathbf{\Lambda}]_{k,k} = (-1)^k$, $0 \leq k \leq M-1$. For example, for $M = 4$, $\mathbf{\Lambda} = \text{diag}[1, -1, 1, -1]$. Using (4A.8) - (4A.11), we get

$$\mathbf{A}_0^\dagger \mathbf{A}_0 = M\,[2\mathbf{I} + \mathbf{C\Lambda S} + \mathbf{S\Lambda C}], \tag{4A.12}$$

$$\mathbf{A}_1^\dagger \mathbf{A}_1 = M\,[2\mathbf{I} - \mathbf{C\Lambda S} - \mathbf{S\Lambda C}], \tag{4A.13}$$

$$\mathbf{A}_0^\dagger \mathbf{A}_1 = M\,[-\mathbf{C\Lambda S} + \mathbf{S\Lambda C}] = -\mathbf{A}_1^\dagger \mathbf{A}_0 \tag{4A.14}$$

From the definitions of $\mathbf{C}$, $\mathbf{S}$, $\mathbf{\Lambda}$ and $\mathbf{J}$, we can write

$$[\mathbf{\Lambda SJ}]_{k,\ell} = (-1)^k\,[\mathbf{SJ}]_{k,\ell} = (-1)^k\,[\mathbf{S}]_{k,(M-1-\ell)}, \quad 0 \leq k, \ell \leq M-1, \tag{4A.15}$$

$$= (-1)^k \sqrt{\frac{2}{M}}\,\sin\left(\frac{\pi}{2}(2k+1) - \frac{\pi}{M}(k+\frac{1}{2})(\ell+\frac{1}{2})\right),$$

$$= \sqrt{\frac{2}{M}}\,\cos\left(\frac{\pi}{M}(k+\frac{1}{2})(\ell+\frac{1}{2})\right) = [\mathbf{C}]_{k,\ell}. \tag{4A.16}$$

Thus we get $\mathbf{\Lambda SJ} = \mathbf{C}$, which can also be expressed as (by using the Hermitian property)

$$\mathbf{\Lambda S} = \mathbf{CJ} \qquad \text{and} \qquad \mathbf{S\Lambda} = \mathbf{JC}, \tag{4A.17}$$

Substituting (4A.17) in (4A.12) - (4A.14), and using the unitary property of $\mathbf{C}$ and $\mathbf{S}$ (given in equations (4A.8), (4A.9)), we get (4A.3) - (4A.5). ▽▽▽

Part II : Proof of (4.14), (4.15) and (4.16)

In this proof, we will use the results proved in part I. Table 4.8 is obtained from the definitions of $\{\mathbf{A}_0', \mathbf{A}_1'\}$ and $\{\mathbf{A}_0, \mathbf{A}_1\}$. Using the relations in Table 4.8 along with (4A.3)-(4A.5), the results in equations (4.14), (4.15) and (4.16) can be readily verified. ▽▽▽

Table 4.8. Appendix 4.A. Relation between the matrices $\{\mathbf{A}'_0, \mathbf{A}'_1\}$ and $\{\mathbf{A}_0, \mathbf{A}_1\}$

m even $(m = 2m_1)$	$\mathbf{A}'_0 = (-1)^{m_1}\mathbf{A}_1$ $\mathbf{A}'_1 = (-1)^{(m_1-1)}\mathbf{A}_0$
m odd $(m = 2m_1 + 1)$	$\mathbf{A}'_0 = (-1)^{m_1}\mathbf{A}_0$ $\mathbf{A}'_1 = (-1)^{m_1}\mathbf{A}_1$

Appendix 4.B
Two-channel Modulated PR Filter Banks

In this appendix, we consider the cosine-modulated filter banks satisfying the PR property, for the special case $M = 2$, i.e., two-channel designs. We will show that these filters satisfy the same relations/properties as the filters of the two-channel PR-QMF solution given by Smith-Barnwell [Smi84].

As mentioned in Section 4.2, the constraint on the length of the linear-phase prototype filter is $N = 2mM$, where $m > 0$. In this case, it becomes $N = 4m$. From (2.34) and (2.39), we obtain the modulation equations for the analysis filters,

$$h_0(n) = 2h(n)\cos\left(\frac{\pi}{4}(n - \frac{N-1}{2}) + \frac{\pi}{4}\right), \quad 0 \le n \le N-1, \tag{4B.1}$$

$$h_1(n) = 2h(n)\cos\left(\frac{3\pi}{4}(n - \frac{N-1}{2}) - \frac{\pi}{4}\right), \quad 0 \le n \le N-1. \tag{4B.2}$$

Using (4B.1) and (4B.2) it can be verified that

$$H_1(z) = -z^{-(N-1)}\widetilde{H}_0(-z). \tag{4B.3}$$

As given in (2.36), the synthesis filters are related to the analysis filters by

$$F_0(z) = z^{-(N-1)}\widetilde{H}_0(z), \tag{4B.4}$$

$$F_1(z) = z^{-(N-1)}\widetilde{H}_1(z). \tag{4B.5}$$

Further, since the modulated PR bank prototype is designed to satisfy (4.17), then by Lemma 4.1, the polyphase component matrix $\mathbf{E}(z)$ is lossless. We have the following

result from [Vai89].

Fact 4B.1 : Let $\mathbf{E}(z)$ be the polyphase component matrix of the analysis filter bank $\{H_0(z),\ H_1(z),\ \cdots\ H_{M-1}(z)\}$. If $\mathbf{E}(z)$ is lossless, then each of the filters $H_k(z),\ 0 \leq k \leq M-1$, is a spectral factor of an M^{th} band filter and satisfies

$$\sum_{\ell=0}^{M-1} H_k(zW_M^{\ell})\widetilde{H}_k(zW_M^{\ell}) = c, \quad \forall z, \tag{4B.6}$$

where c is a nonzero constant and $W_M = e^{-j\frac{2\pi}{M}}$. $\diamondsuit$

Using Fact 4B.1, it can be concluded that the filter $H_0(z)$, of a two-channel modulated PR bank, is a spectral factor of a half-band filter. Hence, it satisfies

$$H_0(z)\widetilde{H}_0(z) + H_0(-z)\widetilde{H}_0(-z) = c, \quad \forall z. \tag{4B.7}$$

From (4B.3)-(4B.5) and (4B.7), it can be verified that the filters of a two-channel modulated PR bank satisfy the same conditions as the designs in [Smi84]. However, owing to the constraints imposed on the prototype, the two-channel cosine-modulated PR banks are only a subset of all the possible two-channel Smith-Barnwell designs (with filter length $N = 4m$).

Chapter 5

A Spectral Factorization Approach to Pseudo-QMF Design

The main results from pseudo-QMF theory [Roth83,Nus81,Mas85,Cox86] are summarized in Chapter 2. These results are well known and pseudo-QMF designs have been widely used in subband coding of speech and other applications like analog voice privacy systems [Cro83,Vai90]. Pseudo-QMF banks can be designed for an arbitrary number of channels, as shown in Appendix B. In conventional pseudo-QMF designs [Roth83,Cox86], we first design a linear-phase prototype filter $H(z)$ by optimization. The objective function used in the optimization is a weighted sum of the stopband energy and a 'flatness constraint' (which must be computed by numerical integration). Once the prototype is obtained, the analysis and synthesis filters are obtained by suitable cosine-modulation (incorporating the aliasing cancellation (AC) constraint), as given in (2.34) and (2.35). So, the main computational effort in conventional pseudo-QMF designs lies in the optimization of the prototype.

In this chapter we present a new approach to pseudo-QMF design which does not involve any optimization. In this approach, the prototype filter of an M channel filter bank is obtained as a spectral factor of a $2M^{th}$ band filter. The AC constraint is derived such that all the significant aliasing terms are canceled. The new approach to pseudo-QMF design and the conventional one are similar in regard to the derivation of the AC condition but are different in the way that the analysis and synthesis filters

are obtained from the prototype filter. The main features of the proposed method are :

1. The prototype filter $H(z)$ is obtained, without need for any optimization, by the spectral factorization of $G(z)$, a $2M^{th}$ band filter. $G(z)$ can be designed by using the standard filter design techniques such as (a) window-based filter design [Vai87a], or (b) the method in [Min82] which uses the McClellan-Parks design program [Mcc73] or (c) the eigenfilter approach [Vai87b]. Hence, the coefficients of $G(z)$ are readily obtained.

2. As in conventional pseudo-QMF designs, the prototype is designed such that non-adjacent filters of the filter bank do not overlap.

3. The aliasing cancellation (AC) constraint is obtained by using a similar approach as in conventional pseudo-QMF designs. The AC constraint ensures that all the significant aliasing terms are canceled.

4. The overall transfer function $T(z)$ of the analysis/synthesis system has linear phase. Hence, the QMF circuit is free from phase distortion. However, the prototype filter $H(z)$ does not have linear phase.

5. The magnitude response $|T(e^{j\omega})|$ is 'flat' in the frequency region $\epsilon \leq \omega \leq (\pi - \epsilon)$, where the value of ϵ depends on the transition bandwidth of the prototype filter, and we always have $0 < \epsilon < \frac{\pi}{2M}$. In this region, the extent of amplitude distortion (i.e., the deviation from flatness) depends on the stopband attenuation of the prototype. The flat response is due to the fact that $H(z)$ is a spectral factor of a $2M^{th}$ band filter. Consequently, there is no need for a separate flatness constraint. Around $\omega = 0$ and $\omega = \pi$, the response $|T(e^{j\omega})|$ has dips/bumps. So, except in these frequency regions, the amplitude distortion is very small.

6. The M analysis and synthesis filters are of equal length. We will assume that

$(N-1)$, the order of the prototype is a multiple of M (the number of channels) i.e., $(N-1) = mM$. This assumption is made in order to simplify the derivation of the AC constraint.

Conventional pseudo-QMF designs : The expressions for the impulse responses of the analysis and synthesis filters are given in (2.34) and (2.35). As mentioned in Section 2.4, the choice of θ_ks (in these equations) is made such that the AC condition is satisfied. One possible choice is $\theta_k = (-1)^k \frac{\pi}{4}$, $0 \leq k \leq M-1$, which yields an overall transfer function $T(z)$ with a 'flat' magnitude response (i.e., close to unity gain) at all frequencies. Another possible choice is

$$\theta_k = \begin{cases} 0, & \text{for } k \text{ even}, \\ \frac{\pi}{2}, & \text{for } k \text{ odd}. \end{cases} \tag{5.1}$$

In [Roth83], it has been shown that this particular choice of θ_ks yields a $T(z)$ with a magnitude response that is close to unity at all frequencies except around $\omega = 0$ and $\omega = \pi$, where it may have a dip or a bump. Such filter banks find use in applications where the regions around $\omega = 0$ and $\omega = \pi$ are treated as *don't care* bands [Roth83,Rab78].

Outline of the Chapter

In Section 5.1, the spectral factorization approach to pseudo-QMF bank design is introduced. The modulation by which the analysis and synthesis filters are derived from the prototype filter is given. Along with that, the relations between the analysis and synthesis filters are stated. Based on this, we get expressions for the channel signals in each of the M branches of the QMF circuit (using approximations to retain only the significant terms). The approximations, that are used, are explained. Then we derive the AC condition that ensures that all the significant aliasing terms are canceled. After that, the expression for $T(z)$, the overall transfer function of the analysis/synthesis system, is obtained. It is shown that $T(z)$ has an approximately flat response in the region $\epsilon \leq \omega \leq (\pi - \epsilon)$ due to the fact that $H(z)$ is a spectral

factor of a $2M^{th}$ band filter.

Section 5.2 deals with the design details of the prototype filter that involves spectral factorization. Two design examples are presented. Both designs were obtained by using a new spectral factorization algorithm which is based on the inverse Linear Predictive Coding (LPC) technique. The details of this algorithm are given in Appendix A.

Notations : As given in Chapter 1, the complex constant W_k is defined as $W_k \triangleq e^{-j\frac{2\pi}{k}}$, for any k. In this chapter, if W is unsubscripted, then $W = W_M = e^{-j\frac{2\pi}{M}}$, where M is the number of channels.

5.1 Spectral Factorization Approach

Let $H(z) = \sum_{n=0}^{N-1} h(n)z^{-n}$ be the prototype filter (with real coefficients). In this approach, since $H(z)$ is obtained by spectral factorization, it does not have linear-phase symmetry. Assume that $(N-1)$, the order of $H(z)$, is a multiple of M, the number of channels, i.e., $(N-1) = mM$. (There are no restrictions on M or m.) Let $S_k(z)$ be defined as follows

$$S_k(z) \triangleq a_k H(zW_{2M}^{(k+\frac{1}{2})}) + a_k^* H(zW_{2M}^{-(k+\frac{1}{2})}), \quad 0 \le k \le M-1, \tag{5.2}$$

where a_k are complex constants of unit magnitude and W_{2M} is a complex constant as specified in Chapter 1. $H_k(z)$ and $F_k(z)$, the analysis and synthesis filter respectively of the pseudo-QMF bank are obtained as shown next.

$$H_k(z) = \begin{cases} S_k(z), & \text{for } k \text{ even}, \\ z^{-(N-1)}\widetilde{S}_k(z), & \text{for } k \text{ odd}, \end{cases} \quad 0 \le k \le M-1, \tag{5.3}$$

$$F_k(z) = z^{-(N-1)}\widetilde{H}_k(z), \quad 0 \le k \le M-1. \tag{5.4}$$

As will become evident later on, the above choices for the analysis/synthesis filters are essential in the derivation of the AC constraint. Letting $a_k = e^{j\theta_k}$, we can write

(5.2) (in time domain) as

$$s(n) = 2h(n)\cos\left(\frac{\pi}{M}(k+\frac{1}{2})n + \theta_k\right), \tag{5.5}$$

and hence, we get

$$h_k(n) = \begin{cases} s_k(n), & \text{for } k \text{ even}, \\ s_k(N-1-n), & \text{for } k \text{ odd}, \end{cases} \qquad 0 \le k \le M-1. \tag{5.6}$$

$$f_k(n) = h_k(N-1-n), \quad 0 \le k \le M-1. \tag{5.7}$$

Next, we define $U_k(z)$ and $V_k(z)$, which are complex-modulated versions of the prototype $H(z)$. For $0 \le k \le M-1$,

$$U_k(z) \triangleq H(zW_{2M}^{(k+\frac{1}{2})}) \qquad \text{and} \qquad V_k(z) \triangleq H(zW_{2M}^{-(k+\frac{1}{2})}). \tag{5.8}$$

Using (5.8) in (5.2), $S_k(z)$ can be expressed as

$$S_k(z) = a_k U_k(z) + a_k^* V_k(z), \quad 0 \le k \le M-1. \tag{5.9}$$

The signals $Y_k(z)$, which are the output of the synthesis filters in Fig. 5.1(a) can be expressed as

$$\begin{aligned} Y_k(z) &= \frac{1}{M}F_k(z)\sum_{\ell=0}^{M-1} H_k(zW^\ell)X(zW^\ell), \quad 0 \le k \le M-1, \\ &= \begin{cases} \frac{1}{M}F_k(z)\sum_{\ell=0}^{M-1}[a_k U_k(zW^l) + a_k^* V_k(zW^l)]X(zW^\ell), & \text{if } k \text{ even}, \\ \frac{z^{-(N-1)}}{M}F_k(z)\sum_{\ell=0}^{M-1}[a_k^* \tilde{U}_k(zW^\ell) + a_k \tilde{V}_k(zW^\ell)]X(zW^\ell), & \text{if } k \text{ odd}. \end{cases} \end{aligned} \tag{5.10}$$

Note : $(N-1)$ is assumed to be a multiple of M.

A key assumption in all pseudo-QMF designs is that filters belonging to non-adjacent channels do not overlap. For example, in a seven channel pseudo-QMF bank, $|H_3(e^{j\omega})|$ has an overlap only with $|H_2(e^{j\omega})|$ and $|H_4(e^{j\omega})|$. The passbands of all the other filters lie in the stopband of $H_3(z)$. In this section, we will repeatedly use this assumption. The following brief discussion will help to clarify the notation and the approximations used in this section. The magnitude response of a typical prototype filter is given in Fig. 5.1(b).

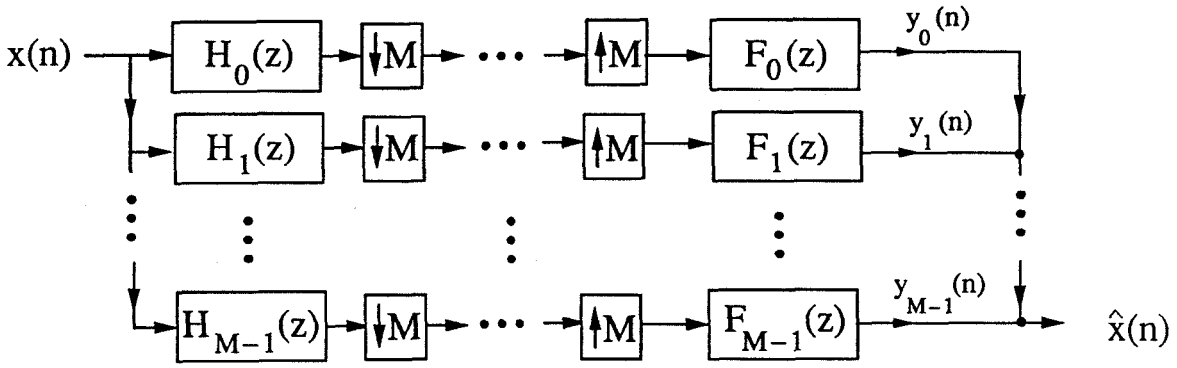

Fig. 5.1(a). The M-channel maximally decimated QMF circuit.

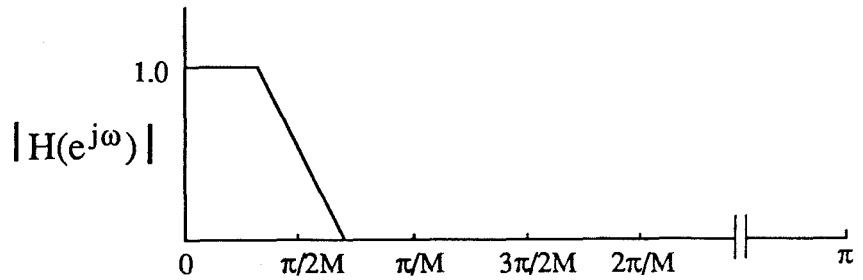

Fig. 5.1(b). The desired response of the prototype H(z) of an M-channel pseudo-QMF bank.

Consider for example, the case when $M = 4$. In Fig. 5.2(a),(b) we have the typical magnitude responses of the analysis and synthesis filters of a four-channel pseudo-QMF bank (which satisfies the above assumption). In the above figure, $U_k(z)$ and $V_k(z)$, the modulated versions of the prototype filter, have also been shown. For this case,

$$Y_k(z) = \frac{1}{4}F_k(z)\sum_{\ell=0}^{3} H_k(zW_4^{\ell})X(zW_4^{\ell}), \qquad 0 \le k \le 3. \tag{5.11}$$

In particular, for $k = 2$,

$$Y_2(z) = \frac{1}{4}F_2(z)\sum_{\ell=0}^{3}[a_2U_2(zW_4^{\ell}) + V_2(zW_4^{\ell})]X(zW_4^{\ell}). \tag{5.12}$$

Fig. 5.3(a),(b) show $U_2(z)$, $V_2(z)$ and their respective frequency shifted versions. In Fig. 5.3(c), we have the magnitude response of $F_2(z)$. From these figures, it can be seen that $V_2(z)$ and $U_2(z)$ overlap with $F_2(z)$. Also, the modulated versions $V_2\left(zW_4^2\right)$ and $U_2\left(zW_4^{-2}\right)$ overlap with the low frequency edges of the filter $F_2(z)$ while $V_2\left(zW_4^3\right)$ and $U_2\left(zW_4^3\right)$ overlap with the high frequency edges of $F_2(z)$. So, $Y_2(z)$ has a total of six significant terms, as shown in Fig. 5.3(d).

$$\begin{aligned} Y_2(z) = \frac{1}{4}F_2(z)\Big[&a_2U_2(z)X(z) + a_2^*V_2(z)X(z) + a_2^*V_2(zW_4^2)X(zW_4^2) + \\ &a_2U_2(zW_4^{-2})X(zW_4^{-2}) + a_2^*V_2(zW_4^3)X(zW_4^3) + a_2U_2(zW_4^{-3})X(zW_4^{-3})\Big]. \end{aligned} \tag{5.13}$$

Using similar reasoning, the expressions in (5.10) can be simplified as shown next. Neglecting those terms that do not have significant overlap with $F_k(z)$, we obtain :

(a) for $1 \le k \le M-2$ and k even :

$$\begin{aligned} Y_k(z) = \frac{1}{M}F_k(z)\,&[a_kU_k(z)X(z) + a_k^*V_k(z)X(z) \\ &+a_k^*V_k(zW^k)X(zW^k) + a_kU_k(zW^{-k})X(zW^{-k}) + \\ &+a_k^*V_k(zW^{(k+1)})X(zW^{(k+1)}) + a_kU_k(zW^{-(k+1)})X(zW^{-(k+1)})\Big]. \end{aligned} \tag{5.14}$$

(b) for $1 \le k \le M-2$ and k odd :

$$Y_k(z) = \frac{z^{-(N-1)}}{M}F_k(z)\left[a_k^*\tilde{U}_k(z)X(z) + a_k\tilde{V}_k(z)X(z)\right.$$

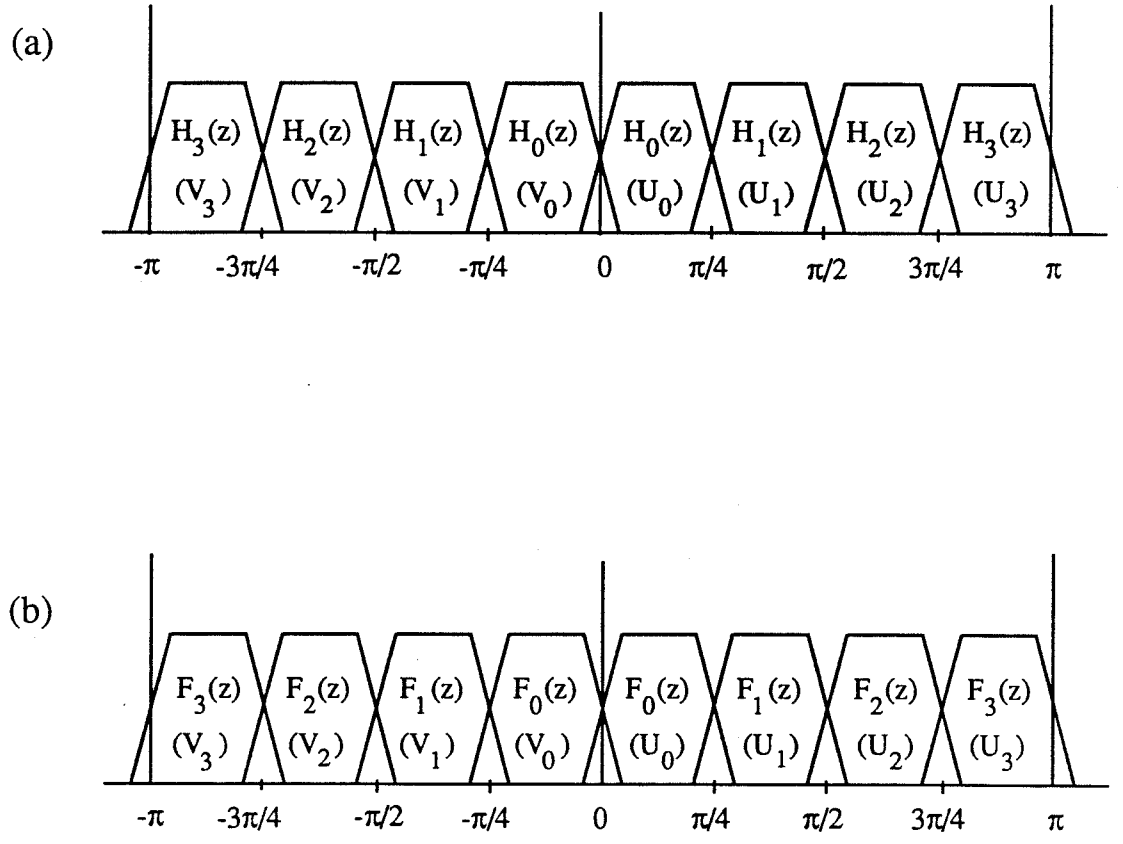

Fig. 5. 2. A typical four-channel pseudo-QMF bank
(a). The analysis filters $H_k(z)$,
(b). The synthesis filters $F_k(z)$.

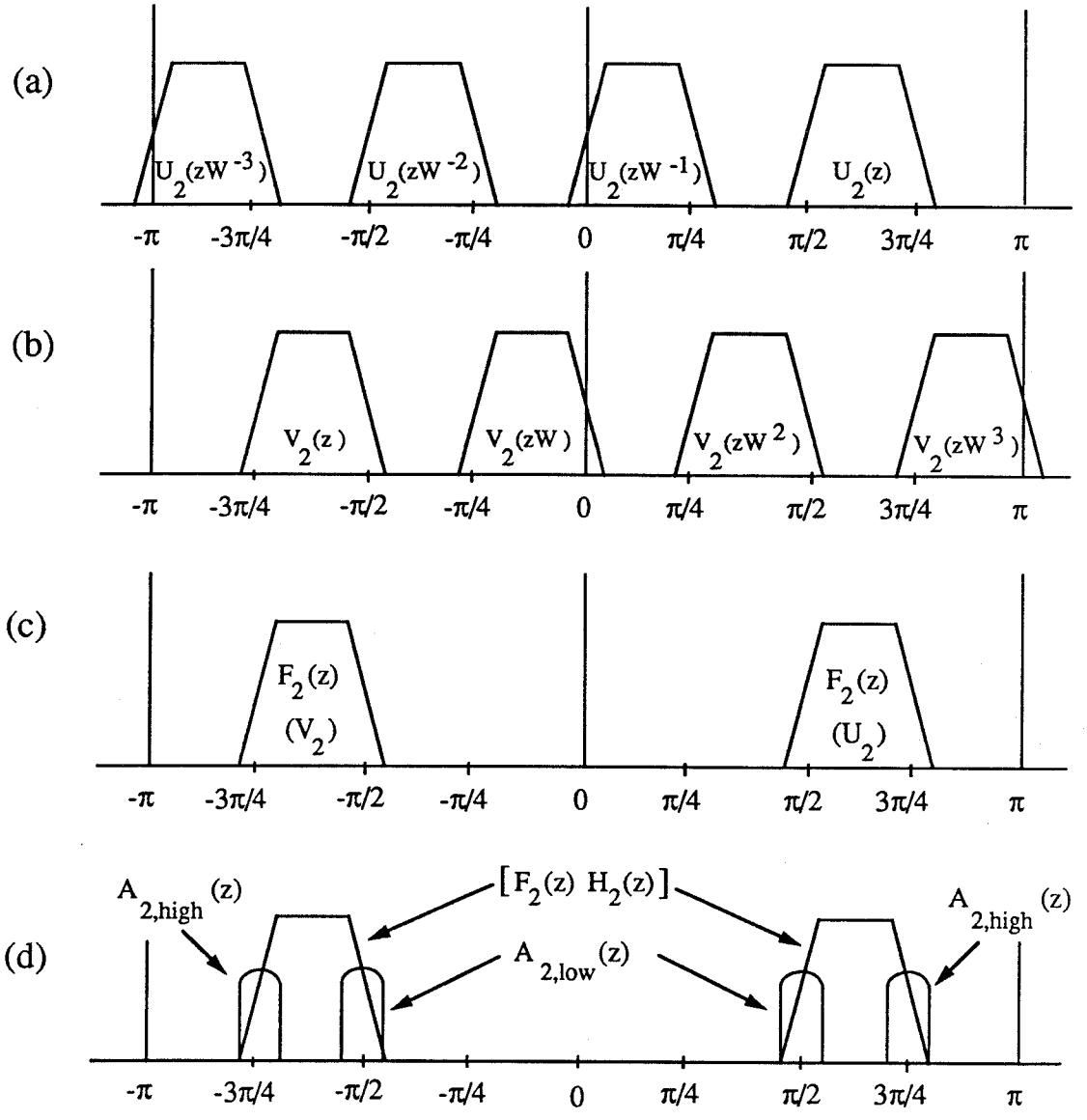

Fig. 5. 3. The four-channel pseudo-QMF bank ($W=W_4$)
(a). $U_2(z)$ and its shifted versions,
(b). $V_2(z)$ and its shifted versions,
(c). The synthesis filter $F_2(z)$,
(d). The six significant terms in $Y_2(z)$.

$$+a_k^*\tilde{U}_k(zW^{-k})X(zW^{-k}) + a_k\tilde{V}_k(zW^k)X(zW^k)$$
$$+a_k^*\tilde{U}_k(zW^{-(k+1)})X(zW^{-(k+1)}) + a_k\tilde{V}_k(zW^{(k+1)})X(zW^{(k+1)})\Big]. \quad (5.15)$$

It can be readily verified that for the special case when $M = 4$ and $k = 2$, equation (5.14) reduces to (5.13). From (5.14) and (5.15), we see that the expressions for $Y_k(z)$ have four aliasing terms. Of the four terms, two are due to overlap of modulated versions of the input (called *images*) with the low frequency edge of $F_k(z)$ and two are due to overlap of images with the high frequency edge of $F_k(z)$. Let them be denoted as $A_{k,low}(z)$ and $A_{k,high}(z)$ respectively (as demonstrated in Fig. 5.3(d)). For $1 \leq k \leq (M-2)$ we can write :

For k even :

$$A_{k,low}(z) = F_k(z)\left[a_k^*V_k(zW^k)X(zW^k) + a_kU_k(zW^{-k})X(zW^{-k})\right], \quad (5.16)$$
$$A_{k,high}(z) = F_k(z)\left[a_k^*V_k(zW^{(k+1)})X(zW^{(k+1)}) + a_kU_k(zW^{-(k+1)})X(zW^{-(k+1)})\right]. \quad (5.17)$$

For k odd :

$$A_{k,low}(z) = z^{-(N-1)}F_k(z)\left[a_k^*\tilde{U}_k(zW^{-k})X(zW^{-k}) + a_k\tilde{V}_k(zW^k)X(zW^k)\right], \quad (5.18)$$
$$A_{k,high}(z) = z^{-(N-1)}F_k(z)\left[a_k^*\tilde{U}_k(zW^{-(k+1)})X(zW^{-(k+1)}) + a_k\tilde{V}_k(zW^{(k+1)})X(zW^{(k+1)})\right]. \quad (5.19)$$

So we can express $Y_k(z)$ as

$$Y_k(z) = \frac{1}{M}F_k(z)H_k(z)X(z) + \frac{1}{M}A_{k,low}(z) + \frac{1}{M}A_{k,high}(z), \quad 1 \leq k \leq M-2. \quad (5.20)$$

$Y_0(z)$ has aliasing terms only due to the overlap of images with the high frequency edge of $F_0(z)$, which are denoted as $A_{0,high}(z)$. On the other hand, $Y_{M-1}(z)$ has aliasing terms only due to the overlap of images with the low frequency edge of $F_{M-1}(z)$, which are denoted as $A_{M-1,low}(z)$. Hence we get the expressions

$$Y_0(z) = \frac{1}{M}F_0(z)H_0(z)X(z) + \frac{1}{M}A_{0,high}(z), \quad (5.21)$$
$$Y_{M-1}(z) = \frac{1}{M}F_k(z)H_{M-1}(z)X(z) + \frac{1}{M}A_{M-1,low}(z). \quad (5.22)$$

Aliasing Cancellation

In the new design approach, we will derive the aliasing cancellation (AC) condition (which ensures that all the significant aliasing terms are canceled) in a manner similar to the conventional pseudo-QMF designs [Roth83], and we will obtain the conditions that ensure that all the significant aliasing terms are canceled. From the definitions in (5.16) and (5.17), we can verify that the magnitude responses of $A_{k,high}(z)$ and $A_{k+1,low}(z)$ overlap each other. Hence the condition

$$A_{k+1,low}(z) = -A_{k,high}(z), \qquad 0 \leq k \leq M-2, \tag{5.23}$$

achieves the cancellation of the aliasing terms between the signals in adjacent channels. If (5.23) is satisfied, the analysis/synthesis system is said to be 'approximately' alias-free, since all the significant aliasing terms have been eliminated. We now derive the conditions under which (5.23) can be satisfied.

Consider the range $0 \leq k \leq M-2$. Without loss of generality, assume that k is even. The expression for $A_{k,high}(z)$ is given in (5.17). Since $(k+1)$ is odd, we get (from (5.18))

$$\begin{aligned} A_{k+1,low}(z) \;=\; & z^{-(N-1)}F_{k+1}(z)\left[a^*_{k+1}\tilde{U}_{k+1}(zW^{-(k+1)})X(zW^{-(k+1)})+\right. \\ & \left. a_{k+1}\tilde{V}_{k+1}(zW^{(k+1)})X(zW^{(k+1)})\right]. \end{aligned} \tag{5.24}$$

Substituting for $A_{k,high}(z)$ and $A_{k+1,low}(z)$ in (5.23), we obtain the following two conditions :

$$a_k F_k(z)U_k(zW^{-(k+1)}) = -z^{-(N-1)}a^*_{k+1}F_{k+1}(z)\tilde{U}_{k+1}(zW^{-(k+1)}), \tag{5.25}$$

and

$$a^*_k F_k(z)V_k(zW^{(k+1)}) = -z^{-(N-1)}a_{k+1}F_{k+1}(z)\tilde{V}_{k+1}(zW^{(k+1)}). \tag{5.26}$$

In other words, (5.23) holds if (5.25) and (5.26) are satisfied. Substituting for $F_k(z)$, the LHS of (5.25) becomes

$$a_k F_k(z)U_k(zW^{-(k+1)}) = z^{-(N-1)}a_k\left[a^*_k\tilde{U}_k(z)+a_k\tilde{V}_k(z)\right]U_k(zW^{-(k+1)}), \tag{5.27}$$

$$\simeq z^{-(N-1)} a_k^2 \tilde{V}_k(z) U_k(zW^{-(k+1)}), \tag{5.28}$$

which is obtained by retaining only the significant term (the omitted term is a product whose components do not have significant overlap with each other). In the same manner, substituting for $F_{k+1}(z)$ in the RHS of (5.25) and simplifying, we get

$$z^{-(N-1)} a_{k+1}^* F_{k+1}(z) \tilde{U}_{k+1}(zW^{-(k+1)}) = z^{-(N-1)} a_{k+1}^{*2} V_{k+1}(z) \tilde{U}_{k+1}(zW^{-(k+1)}). \tag{5.29}$$

Substituting (5.28) and (5.29) in (5.25), it becomes

$$z^{-(N-1)} a_k^2 \tilde{V}_k(z) U_k(zW^{-(k+1)}) = -z^{-(N-1)} a_{k+1}^{*2} V_{k+1}(z) \tilde{U}_{k+1}(zW^{-(k+1)}). \tag{5.30}$$

From the definitions of $U_k(z)$ and $V_k(z)$ (from (5.8)) we have

$$\tilde{V}_k(z) = \tilde{U}_{k+1}(zW^{(k+1)}) \quad \text{and} \quad U_k(zW^{-(k+1)}) = V_{k+1}(z). \tag{5.31}$$

Hence, (5.30) reduces to

$$a_k^2 + a_{k+1}^{*2} = 0, \qquad 0 \leq k \leq (M-2). \tag{5.32}$$

The above condition is obtained by starting with equation (5.25). It can be verified that if we start with equation (5.26), we obtain the same condition as in (5.32). This result is summarized as follows.

Fact 5.1 : In the proposed approach to pseudo-QMF design, wherein the prototype is a spectral factor of a $2M^{th}$ band filter with analysis and synthesis filters being obtained by the modulation of the prototype given in (5.3) and (5.4) respectively, the condition in (5.32) is sufficient to ensure that all the significant aliasing terms are canceled. Since $a_k = e^{j\theta_k}$, the same condition can be expressed in terms of θ_ks as

$$\theta_{k+1} = \pm(2i+1)\frac{\pi}{2} - \theta_k, \qquad 0 \leq k \leq M-2, \tag{5.33}$$

where i is an integer. $\diamondsuit$

Choice of θ_k : Two of the several possible choices that satisfy (5.33) are

$$\theta_k = \frac{\pi}{4}, \ \forall\, k, \tag{5.34}$$

and

$$\theta_k = \begin{cases} 0, & \text{if } k \text{ is even,} \\ \frac{\pi}{2}, & \text{if } k \text{ is odd.} \end{cases} \tag{5.35}$$

The Overall Transfer Function

With the θ_k chosen to satisfy (5.33), the analysis/synthesis system is 'approximately' alias-free and the input-output equation is given by

$$\widehat{X}(z) = \sum_{k=0}^{M-1} Y_k(z) \simeq \frac{1}{M} X(z) \sum_{k=0}^{M-1} F_k(z) H_k(z). \tag{5.36}$$

Hence the overall transfer function $T(z)$ can be expressed as

$$\frac{\widehat{X}(z)}{X(z)} \simeq T(z) = \frac{z^{-(N-1)}}{M} \sum_{k=0}^{M-1} H_k(z) \widetilde{H}_k(z). \tag{5.37}$$

Substituting in (5.37) from (5.3) and (5.4), we get

$$T(z) = \frac{z^{-(N-1)}}{M} \sum_{k=0}^{M-1} [a_k U_k(z) + a_k^* V_k(z)][a_k^* \tilde{U}_k(z) + a_k \tilde{V}_k(z)]. \tag{5.38}$$

Retaining only the significant terms in (5.38),

$$\begin{aligned} T(z) \;=\; & \underbrace{\frac{z^{-(N-1)}}{M} \sum_{k=0}^{M-1} \left[U_k(z)\tilde{U}_k(z) + V_k(z)\tilde{V}_k(z) \right]}_{T_1(z)} \\ & + \frac{z^{-(N-1)}}{M} \Big[\underbrace{a_0^2 U_0(z)\tilde{V}_0(z) + a_0^{*2} V_0(z)\tilde{U}_0(z)}_{P_1(z)} \\ & + \underbrace{a_{M-1}^2 U_{M-1}(z)\tilde{V}_{M-1}(z) + a_{M-1}^{*2} V_{M-1}(z)\tilde{U}_{M-1}(z)}_{P_2(z)} \Big]. \end{aligned} \tag{5.39}$$

Substituting for $U_k(z)$ and $V_k(z)$ (from(5.8)), in the expression for $T_1(z)$, we obtain,

$$\begin{aligned} T_1(z) \;&=\; \frac{z^{-(N-1)}}{M} \sum_{k=0}^{M-1} \left[H(zW_{2M}^{(k+\frac{1}{2})}) \widetilde{H}(zW_{2M}^{(k+\frac{1}{2})}) + H(zW_{2M}^{-(k+\frac{1}{2})}) \widetilde{H}(zW_{2M}^{-(k+\frac{1}{2})}) \right], \\ &=\; \frac{z^{-(N-1)}}{M} \sum_{k=0}^{2M-1} H(zW_{2M}^{(k+\frac{1}{2})}) \widetilde{H}(zW_{2M}^{(k+\frac{1}{2})}). \end{aligned} \tag{5.40}$$

Fact 5.2 : Let $G(z)$ be a zero-phase, $2M^{th}$ band filter. Then it satisfies

$$\sum_{k=0}^{2M-1} G(zW_{2M}^k) = c, \qquad \forall\, z, \tag{5.41}$$

where c is a constant. $\Diamond$

The prototype filter $H(z)$ is obtained as a spectral factor of $G(z)$, i.e., satisfying $G(z) = H(z)\widetilde{H}(z)$. So we have the following property (by Fact 5.2),

$$\sum_{k=0}^{2M-1} H(zW_{2M}^{k})\widetilde{H}(zW_{2M}^{k}) = c, \qquad \forall\, z. \tag{5.42}$$

Using (5.42) in (5.40), we obtain

$$T_1(z) = \frac{z^{-(N-1)}}{M} * c. \tag{5.43}$$

Substituting (5.43) in (5.39), we get

$$T(z) \simeq \frac{z^{-(N-1)}}{M} * c + \frac{z^{-(N-1)}}{M}\left[P_1(z) + P_2(z)\right], \tag{5.44}$$

where $P_j(z)$ are the cross terms (defined in (5.39)), which cannot be eliminated for any choice of of θ_k. The magnitude response of $P_1(z)$ is significant only in the region $|\omega| < \epsilon$ while that of $P_2(z)$ is significant only in the region $(\pi - \epsilon) < |\omega| < (\pi + \epsilon)$, where ϵ depends on the transition bandwidth of $H(z)$ and its value lies in the range $(0, \frac{\pi}{2M})$. As a direct consequence, we see that

$$|T(e^{j\omega})| \simeq constant, \quad \epsilon \leq \omega \leq (\pi - \epsilon). \tag{5.45}$$

In the regions around $\omega = 0$ and $\omega = \pi$, $|T(e^{j\omega})|$ can have bumps/dips. The response in these regions depends on the two crossterms. So the main results are

* The 'flat' response, mentioned in (5.45), is an inherent feature of the proposed design due to the fact that the prototype $H(z)$ is a spectral factor of a $2M^{th}$ band filter.

* No optimization is involved in the design of $H(z)$, which is the main advantage of this method over conventional pseudo-QMF designs.

* The overall transfer function of the analysis/synthesis system, $T(z)$, has linear phase and hence it does not have phase distortion. This can be verified from (5.37) and (5.44).

5.2 Design of the Prototype Filter

In this approach, the prototype $H(z) = \sum_{n=0}^{N-1} h(n)z^{-n}$ is obtained by the spectral factorization of $G(z)$, a $2M^{th}$ band filter, i.e., $H(z)$ satisfies $G(z) = H(z)\widetilde{H}(z)$. Hence, it does not involve any optimization. The order of $H(z)$ is $(N-1)$, i.e., $H(z) = \sum_{n=0}^{N-1} h(n)z^{-n}$. The design involves the following three steps.

1. **Design of $G'(z)$:** Let $G'(z) = \sum_{n=-(N-1)}^{(N-1)} g'(n)z^{-n}$, be a zero-phase, FIR low pass filter (non-causal) which is a $2M^{th}$ band filter, i.e., it satisfies

$$\sum_{k=0}^{2M-1} G'(zW_{2M}^{k}) = constant. \tag{5.46}$$

This condition can be expressed in the time domain as

$$g'(2pM) = \begin{cases} \frac{1}{2M}, & p = 0, \\ 0, & p \neq 0. \end{cases} \tag{5.47}$$

The filter $G'(z)$, (satisfying the above conditions), can be readily designed by the standard window-based filter design techniques [Vai87a]. In our design, we will use the Kaiser window [Vai87a]. The coefficients of $G'(z)$ are obtained as follows :

$$g'(n) = h_i(n)w(n), \qquad -(N-1) \leq n \leq (N-1), \tag{5.48}$$

where $h_i(n)$ are the impulse response coefficients of an ideal lowpass filter (with cutoff frequency $= \frac{\pi}{2M}$ rads.), which are given by $h_i(n) = \frac{1}{\pi n}\sin(\frac{\pi}{2M}n)$, and $w(n)$ are the coefficients of a Kaiser window of length $2N-1$. The values of $w(n)$ depend on the value of the parameter β. The main considerations in the choice of β are

   (a) If A_s is the desired stopband attenuation (in dB) of the prototype filter, then the stopband attenuation of $G'(z)$ must be $\geq (2A_s + 6)$ dB.

   (b) $G'(z)$ should have the same transition bandwidth as $H(z)$.

Having chosen the value of β, the coefficients of the Kaiser window are easily computed.

2. **Design of $G(z)$:** Let δ_2 be the stopband ripple of $G'(z)$.Then $G(z)$ is obtained as $G(z) = G'(z) + \delta_2 + \delta$, where δ is a positive, real constant which 'lifts' the zeros of the spectrum which are on the unit circle (as required by the spectral factorization algorithm in Appendix B). $G(z)$ can also be expressed as

$$\begin{aligned} g(0) &= g'(0) + \delta_2 + \delta, \\ g(n) &= g'(n), \quad n \neq 0. \end{aligned} \tag{5.49}$$

Since $G'(z)$ is a $2M^{th}$ band filter, $G(z)$ is also a $2M^{th}$ band filter.

3. **Design of $H(z)$ by Spectral Factorization :** From its definition in (5.49), $G(e^{j\omega})$ has a real, non-negative spectrum, i.e., $G(e^{j\omega}) \geq 0$. Hence its spectral factor can be computed by the algorithm given in Appendix A or by one of the other spectral factorization methods [Mia82,Fri83]. Thus we obtain the desired prototype $H(z)$ satisfying $G(z) = H(z)\widetilde{H}(z)$.

Design example 5.1 : Using the proposed method, a design example for an 8-channel pseudo-QMF bank is presented here. Consider a prototype of length $N = 97$. (Its order is 96, which is a multiple of M.) First, we obtain the $2M^{th}$ band filter $G'(z)$, whose length $N_1 = 193$. $G'(z)$ is designed as a Kaiser-window based lowpass filter (LPF) in which the cutoff frequency of the ideal LPF is $\frac{\pi}{16}$ radians and the Kaiser window parameter $\beta = 15.56$. The resultant filter $G'(z)$ has stopband attenuation = 147.91 dB and stopband edge = 0.1138π radians. The value of the peak stopband ripple of $G'(z)$ is $\delta_2 = 4.023$ E-08. Using $\delta = \frac{\delta_2}{2}$ in (5.49), we obtain the impulse response coefficients of $G(z)$. Hence, the spectrum $G(e^{j\omega})$ does not have any zeros on the unit circle.

The prototype filter $H(z)$ is then obtained as a spectral factor of $G(z)$, by using the Inverse LPC-based spectral factorization technique (outlined in Appendix B). The resultant prototype $H(z)$ has stopband attenuation $A_s = 70.94$ dB and the stopband edge $\omega_s = 0.1138\pi$ rads. Its magnitude response is shown in Fig. 5.4(a). The analysis filter bank is obtained by the cosine modulation given in (5.3), (5.6) with θ_k chosen as in (5.34). The responses of all the analysis filters are shown in Fig. 5.4(b).

For this choice of analysis and synthesis filters, $T(z)$, the overall transfer function of the analysis/synthesis system is obtained using (5.37). Its magnitude response, $|T(e^{j\omega})|$, is plotted in Fig. 5.4(c), with an expanded view of the 'flat' portion shown in (d). For this example, $|T(e^{j\omega})|$ has an approximately flat response in the frequency region $\epsilon \leq \omega \leq (\pi - \epsilon)$, where $\epsilon = 0.05\pi$ radians. In this region, the peak-to-peak error E_{p-p}=2.288 E-02 dB. From Fig. 5.4(c), it can be seen that $|T(e^{j\omega})|$ has a dip around $\omega = 0$ and a bump around $\omega = \pi$. The total aliasing error is defined as $E(\omega) \triangleq \frac{1}{M}\left[\sum_{\ell=1}^{M-1} |A_\ell(e^{j\omega})|^2\right]^{\frac{1}{2}}$ where $A_\ell(z) = \sum_{k=0}^{M-1} H_k(zW_M^\ell)F_k(z)$. This error is plotted in Fig. 5.4(e). Its peak value is $E_a = 1.543$ E-04, which confirms that all the significant aliasing terms are indeed canceled.

As mentioned in Section 5.1, the value of ϵ (and hence, the extent of the region of flat response of $|T(e^{j\omega})|$) depends on the transition bandwidth of the prototype filter. On the other hand, the errors E_{p-p} and E_a depend on the A_s of the prototype (i.e., the higher the stopband attenuation, the lower the values of E_{p-p} and E_a). So for a given length of the prototype filter, the tradeoff between the transition bandwidth and A_s is reflected as a tradeoff (for the overall analysis/synthesis system) between ϵ and the errors E_{p-p}, E_a. To illustrate this fact, we present another design example.

Design example 5.2 : This is also an 8-channel pseudo-QMF bank designed in an identical manner to the previous example, using the same filter length but the prototype filter in this example has a narrower transition bandwidth and lower

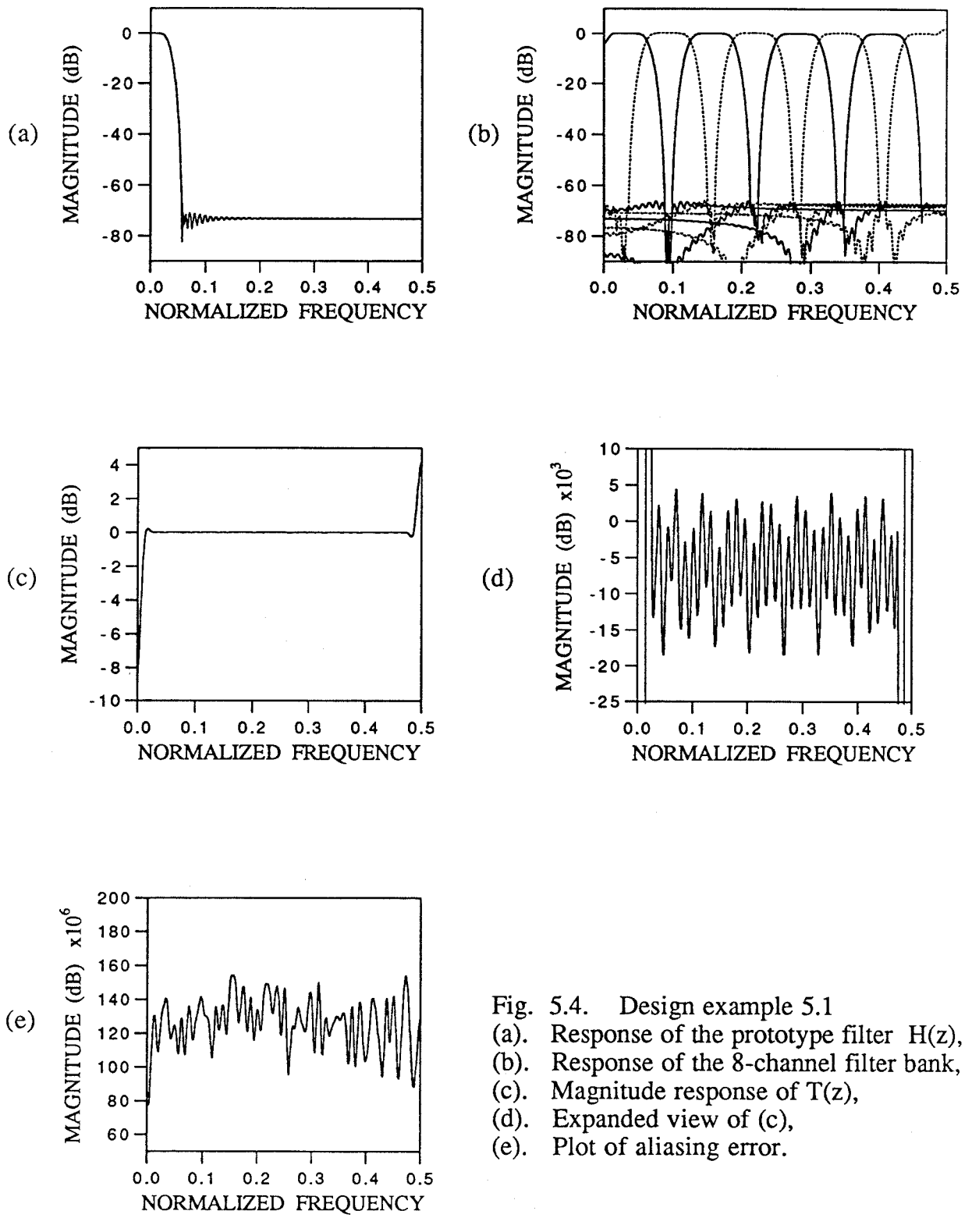

Fig. 5.4. Design example 5.1
(a). Response of the prototype filter H(z),
(b). Response of the 8-channel filter bank,
(c). Magnitude response of T(z),
(d). Expanded view of (c),
(e). Plot of aliasing error.

stopband attenuation (when compared with the prototype of example 5.1). $G'(z)$, of length $N = 193$, is designed by using a Kaiser widow parameter $\beta = 10.5$. It has stopband attenuation = 104.19 dB and stopband edge = 0.0976 π radians. The value of $\delta_2 = 6.174$ E-06 and the impulse response coefficients of $G(z)$ are obtained by using $\delta = \frac{\delta_2}{2}$ in (5.49). Using the same spectral factorization algorithm, we obtain the prototype $H(z)$ which has $A_s = 48.82$ dB and $\omega_s = 0.0976\pi$ radians. Its magnitude response is shown in Fig. 5.5(a). Comparing this prototype with that of the previous example, the tradeoff between the transition bandwidth and A_s is evident. The responses of all the analysis/synthesis filters are shown in Fig. 5.5(b). The magnitude response $|T(e^{j\omega})|$ is plotted in Fig. 5.5(c),(d) and the total aliasing error is given in Fig. 5.5(e). For this example, $\epsilon = 0.0348\pi$ radians, while $E_{p-p} = 0.1407$ dB and $E_a = 2.77$ E-03. So, in this example $|T(e^{j\omega})|$ has an approximately flat response over a wider region than in the previous example, but the errors E_{p-p}, E_a are noticeably bigger. In general, it has been observed that choosing the prototype with the higher stopband attenuation yields a better pseudo-QMF design.

5.3 Summary

In this chapter, a new approach to pseudo-QMF design, based on spectral factorization, is presented. The main advantage of this approach over conventional pseudo-QMF designs is that no optimization is involved in the design of the prototype. The AC constraint ensures that all the significant aliasing terms are canceled. The overall transfer function of the analysis/synthesis system has a 'flat' response in the frequency region $\epsilon \leq \omega \leq (\pi - \epsilon)$ where ϵ depends on the transition bandwidth of the prototype filter and $0 < \epsilon < \frac{\pi}{2M}$. Examples of pseudo-QMF banks, designed by the spectral factorization approach, are included.

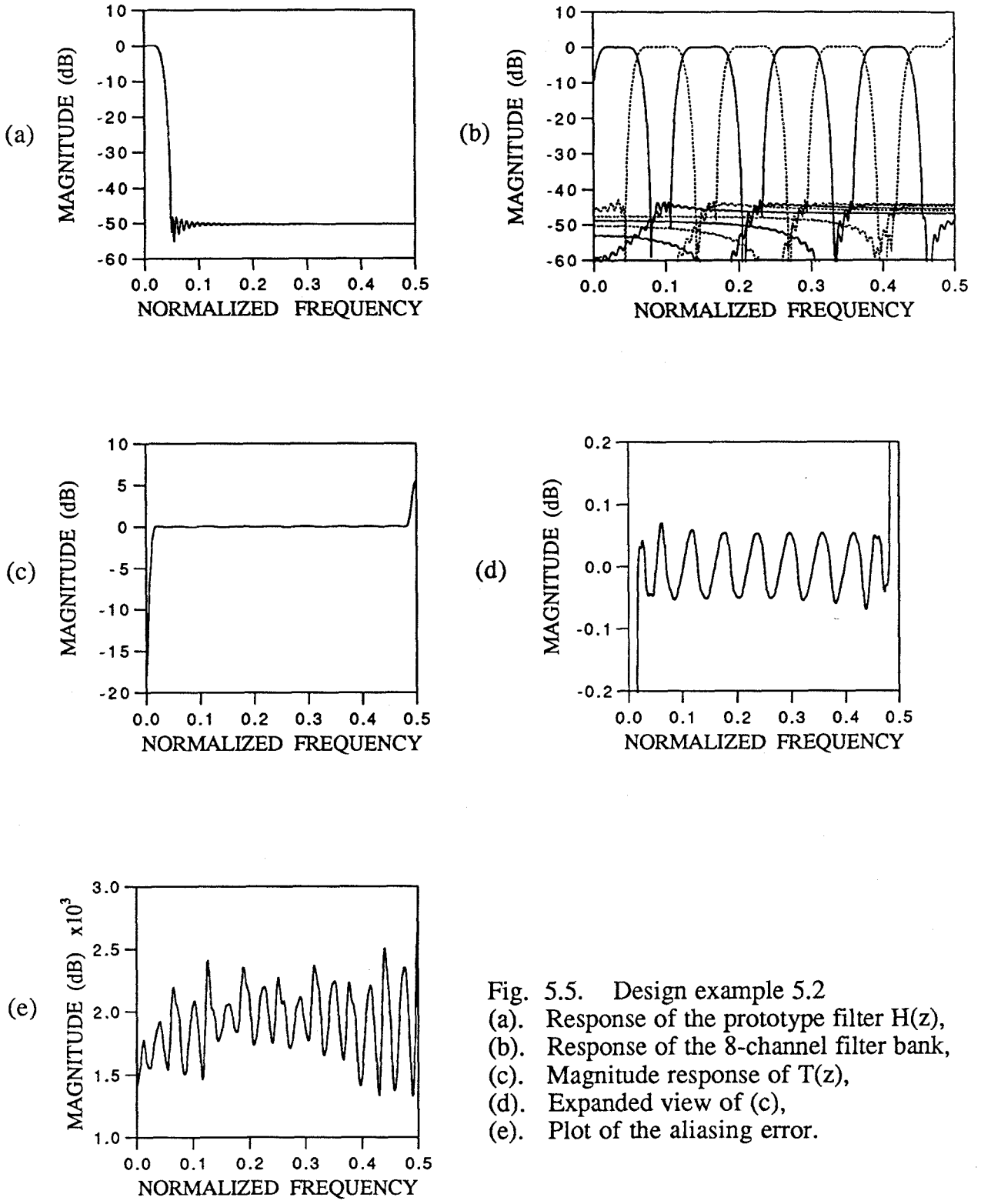

Fig. 5.5. Design example 5.2
(a). Response of the prototype filter H(z),
(b). Response of the 8-channel filter bank,
(c). Magnitude response of T(z),
(d). Expanded view of (c),
(e). Plot of the aliasing error.

Chapter 6

New Results on Crosstalk-free Transmultiplexers

Transmultiplexers are used for interconversion between the Time Division Multiplexing (TDM) format and the Frequency Division Multiplexing (FDM) format. This topic has received widespread attention and hence, there exists a considerable amount of literature [Sch81,Fre80,Vet86,Com78,Com82,Bel82] covering the theory, design and implementation details of transmultiplexers. The main problem in transmultiplexers is the leakage of signal from one channel to another in the TDM $\rightarrow$ FDM $\rightarrow$ TDM conversion, which is known as Crosstalk [Sch81]. The focus of transmultiplexer designs is to minimize the crosstalk.

A schematic of the digital transmultiplexer system is presented in Fig. 6.1. The M input signals are $[x_0(n), x_1(n), \cdots x_{M-1}(n)]$ (which are also the M components of the TDM signal). $[F_0(z), F_1(z), \cdots F_{M-1}(z)]$ are the filters used in TDM $\rightarrow$ FDM conversion and will be called *synthesis filters.* The M input signals are interpolated and passed through the synthesis filter bank and combined to produce the FDM signal. At the other end, $[H_0(z), H_1(z), \cdots H_{M-1}(z)]$ are the filters used in FDM $\rightarrow$ TDM conversion and will be called *analysis filters.* The FDM signal $y(n)$ is passed through the analysis filter bank and then decimated to get back the TDM signals, $\hat{x}_i(n)$, $0 \leq i \leq M-1$.

Fig. 6.2(a),(b) show the frequency spectra of a typical input $x_i(n)$ and the FDM signal $y(n)$ respectively. The voiceband channels are placed adjacent to one another

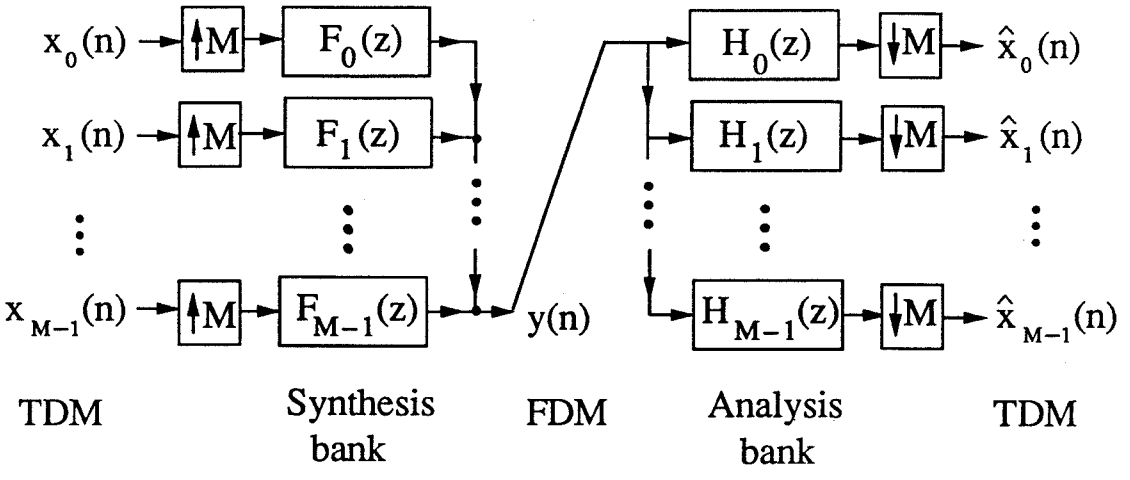

Fig. 6.1 The transmultiplexer system.

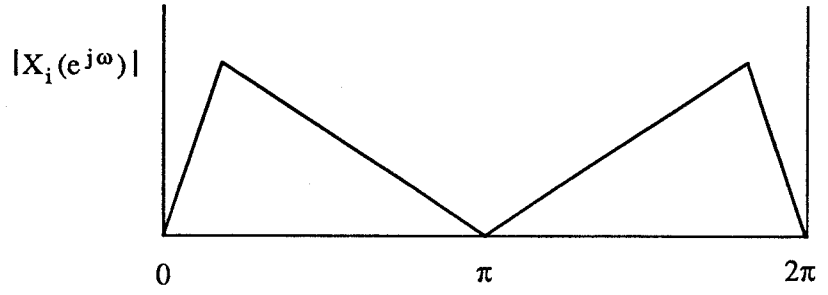

Fig. 6.2(a). Spectrum of input signal $x_i(n)$

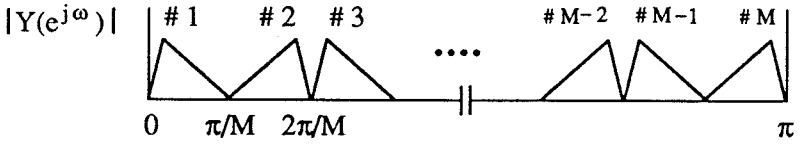

Fig. 6.2(b). Spectrum of the FDM signal y(n)

and hence the bandwidth of the FDM signal is equal to the sum of the bandwidths of the component signals. Since the synthesis and analysis filters are non-ideal, crosstalk occurs between the different channels of the transmultiplexer. The crosstalk decreases as the transition bandwidth (Δf) of the channel filters decreases and as their stopband attenuation (A_s) increases. These are the only handles on the crosstalk that are available in the traditional transmultiplexer design approaches.

The aim of this chapter is to present new results on crosstalk-free transmultiplexers. This novel method, originally presented in [Vet86,Vet87], focuses on *Crosstalk Cancellation* (CC) rather than suppressing it. Using this approach, the crosstalk can be reduced to very low values (in some cases, crosstalk can be completely eliminated) even with filters having nominal values of Δf and A_s. This will be elaborated more qualitatively in the later sections. As an illustration, consider design #4 in Table 6.1. For filters having the same specifications (and same length), the crosstalk error (defined in Section 6.3) using the traditional design approach is 1.932 E-03 (54.3 dB) whereas with the crosstalk cancellation (CC) approach, it is 3.338 E-08 (149.5 dB), which is an improvement of 95.2 dB. In concept the CC approach may be compared to the QMF solution to the subband coding problem, which focuses on Aliasing Cancellation rather than on suppressing it.

In [Vet87], a necessary and sufficient condition for Crosstalk-free transmultiplexers was presented. The condition was obtained in terms of the analysis and synthesis filters of the transmultiplexer. In this chapter we present the derivation of an equivalent necessary and sufficient condition, based on the polyphase component matrices of the analysis and synthesis filters. This approach will throw additional light on the understanding of the problem. It also provides a direct method of designing crosstalk-free transmultiplexer filters by starting from an arbitrary, alias-free QMF bank. We will also show that *approximately* crosstalk-free transmultiplexer filters can be obtained

from a QMF bank in which the alias cancellation condition is only approximately satisfied.

The main focus of this approach to the transmultiplexer problem is

1. Crosstalk Cancellation (CC).

2. Elimination of amplitude and phase distortions, i.e., exact recovery of the signals in

TDM $\rightarrow$ FDM $\rightarrow$ TDM conversion.

Terminology : If both the above conditions are satisfied, it will be called Perfect Reconstruction Transmultiplexer (PR-TMUX). If only the first condition is satisfied, then it will be called Crosstalk-free Transmultiplexer (CF-TMUX). In both of the above cases, crosstalk is canceled *completely.* This should however be contrasted with the traditional approaches to transmultiplexer design, which aim to suppress crosstalk and hence, there is always *residual crosstalk.* We will often refer to the following QMF abbreviations viz., PR-QMF for Perfect Reconstruction QMF and AF-QMF for Alias-free QMF. Since both the transmultiplexer circuit and the QMF circuit involve their respective *analysis* and *synthesis* filters, the filters and matrices associated with the QMF circuit always have a *prime* notation associated with them (as in $H'(z)$), while the filters and matrices associated with the transmultiplexer do not. Further, $\{H_i(z), F_i(z)\}$ is an abbreviation for "transmultiplexer with M analysis filters $H_i(z)$ and M synthesis filters $F_i(z)$, $0 \leq i \leq M-1$." Similarly, $\{H_i'(z), F_i'(z)\}$ refer to the analysis and synthesis filters of the QMF circuit of Fig. 1.1.

Outline of the Chapter

In Section 6.1, an analysis of the transmultiplexer circuit, based on the polyphase component matrices of the analysis (FDM $\rightarrow$ TDM) and synthesis (TDM $\rightarrow$ FDM) filters, is presented. This formulation and subsequent simplifications help to bring out the fact that the above transmultiplexer circuit, if considered as a MIMO system,

is Linear Time Invariant (LTI), even though there are time-varying components such as decimators and interpolators in the circuit. Based on this framework, Lemma 6.1, which gives a necessary and sufficient condition for CC, is presented in Section 6.1.2. In the next subsection, it is shown in Lemma 6.2 that we can always obtain a CF-TMUX from a 1-skewed AF-QMF bank. This gives a design procedure for CF-TMUX filters based on the design of AF-QMF banks, thereby utilizing the extensive results available in the areas of AF-QMF and PR-QMF designs. Then, the main result of this section is presented in Lemma 6.3, which establishes the relation between CF-TMUX filters and 1-skewed AF-QMF banks, and hence is a stronger result than Lemma 6.2.

Section 6.1.4 contains a brief derivation of the necessary and sufficient condition for CC obtained in [Vet87]. Then, in Section 6.1.5, Fact 6.3 is used to show the equivalence between this result and the necessary and sufficient condition given in Lemma 6.3. Further, in [Vet86] it was observed that filters (designed by using the pseudo-QMF theory) that satisfy the AC condition approximately, can be used in the design of a TMUX that is approximately crosstalk-free. A formal justification for the exact condition under which this result holds is presented in Section 6.2. It is also shown that we can obtain approximately CF-TMUX filters from any approximately AF-QMF bank. In Section 6.3, a detailed comparison of the performance of transmultiplexers (designed by both methods – the CC approach and the traditional method) is given.

6.1 Transmultiplexer Analysis

6.1.1 Simplified Equivalent of the Transmultiplexer

A schematic of the digital transmultiplexer is given in Fig. 6.1. Using the polyphase decompositions of Types 1 and 2 [Vai90], we can express the analysis and synthesis

filter of the transmultiplexer circuit as

$$H_k(z) = \sum_{\ell=0}^{M-1} z^{-\ell} E_{k,\ell}(z^M), \qquad 0 \le k, \ell \le M-1, \tag{6.1}$$

$$F_k(z) = \sum_{\ell=0}^{M-1} z^{-(M-1-\ell)} R_{\ell,k}(z^M), \qquad 0 \le k, \ell \le M-1. \tag{6.2}$$

Let $\mathbf{E}(z)$ and $\mathbf{R}(z)$ be the polyphase component matrices of the analysis and synthesis filter banks respectively. The elements of the $M \times M$ matrices $\mathbf{E}(z)$ and $\mathbf{R}(z)$ are given by $[\mathbf{E}(z)]_{k,\ell} = E_{k,\ell}(z)$ and $[\mathbf{R}(z)]_{k,\ell} = R_{k,\ell}(z)$, where $0 \le k, \ell \le M-1$. Representing the analysis and synthesis filter banks in terms of their respective polyphase component matrices, we get Fig. 6.3. Then, applying the standard identities of multirate signal processing [Vai87c], the interpolators and decimators can be moved appropriately to yield Fig. 6.4. This structure can be further simplified in view of the readily verifiable fact given below.

Fact 6.1 : If an input signal $u(n)$ is passed through an interpolator, a delay of k units and a decimator as shown in Fig. 6.5, then in the *Z-transform* domain the output can be expressed in terms of the input as

$$V(z) = \begin{cases} 0, & \text{if } k \neq \text{multiple of } M, \\ z^{-k/M} U(z), & \text{if } k \text{ is a multiple of } M. \end{cases} \tag{6.3}$$

Applying this result in Fig. 6.4, we obtain Fig. 6.6 which is a simplified equivalent representation of the transmultiplexer system. It is important to note that this is a Linear Time Invariant (but multi-input, multi-output) system, even though time-varying components such as decimators and interpolators are present in the original representation (Fig. 6.1). This equivalent circuit will be used throughout this chapter. It adds insight to note that the FDM signal $y(n)$ can be considered as a 'time-multiplexed version' of the signals $y_i(n)$ in Fig. 6.4, since the interpolators and the delay chain on the synthesis side implement a time domain multiplexer. On the other hand, the delay chain and decimators on the analysis side implement a time domain demultiplexer.

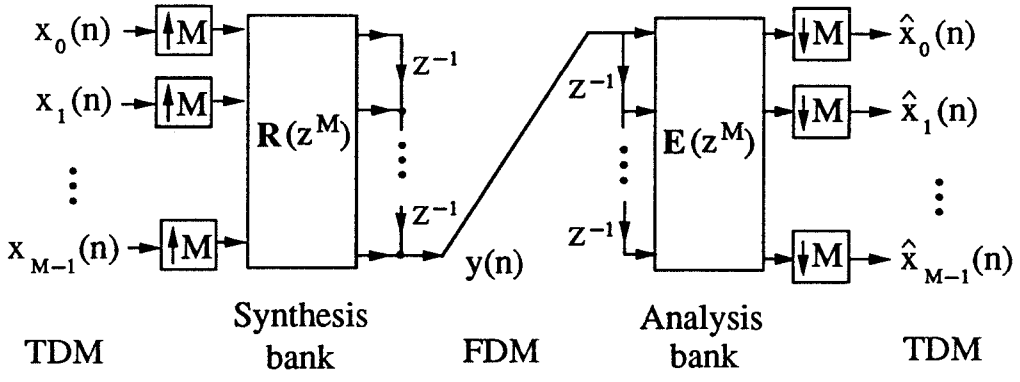

Fig. 6.3. The polyphase representation of the transmultiplexer system in Fig. 6.1.

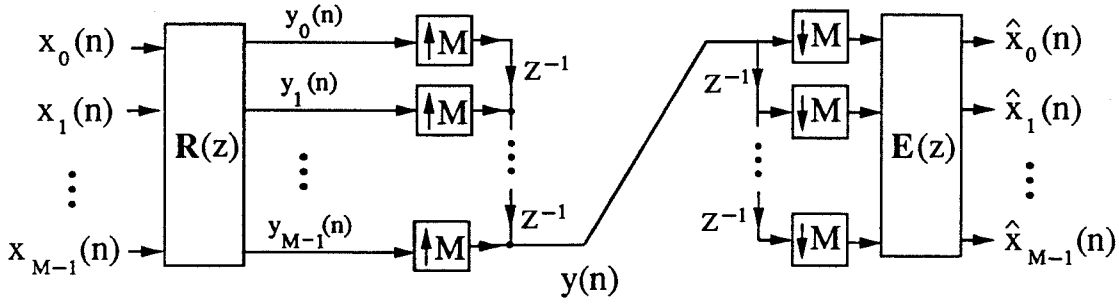

Fig. 6.4. Equivalent structure for the transmultiplexer system in Fig. 6.3.

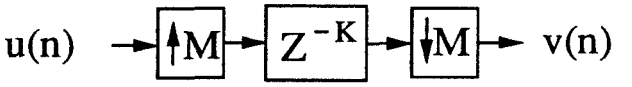

Fig. 6.5. A circuit with an interpolator, a delay and a decimator.

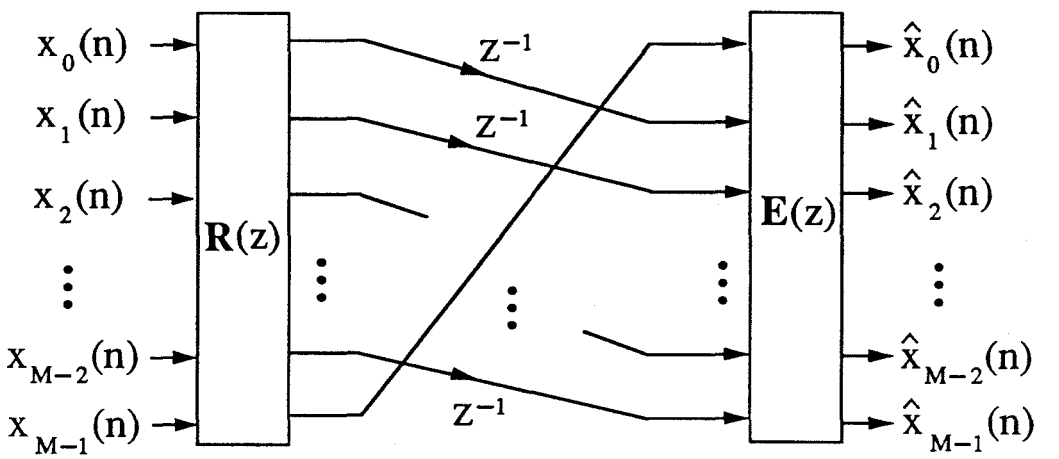

Fig. 6. 6. The simplified equivalent representation of the transmultiplexer system in Fig. 6.1.

6.1.2 Necessary and Sufficient Condition for CC

From Fig. 6.6, we can write

$$\begin{bmatrix} \widehat{X}_0(z) \\ \widehat{X}_1(z) \\ \vdots \\ \widehat{X}_{M-1}(z) \end{bmatrix} = \mathbf{E}(z) \begin{bmatrix} \mathbf{0} & 1 \\ z^{-1}\mathbf{I}_{M-1} & \mathbf{0} \end{bmatrix} \mathbf{R}(z) \begin{bmatrix} X_0(z) \\ X_1(z) \\ \vdots \\ X_{M-1}(z) \end{bmatrix}. \tag{6.4}$$

To cancel crosstalk, it is evidently *necessary and sufficient* that

$$\mathbf{E}(z) \begin{bmatrix} \mathbf{0} & 1 \\ z^{-1}\mathbf{I}_{M-1} & \mathbf{0} \end{bmatrix} \mathbf{R}(z) = \mathbf{C}\mathbf{T}(z), \tag{6.5}$$

where $\mathbf{T}(z) = \text{diag}\,[T_0(z), T_1(z), \cdots T_{M-1}(z)]$ (with $T_i(z)$, $0 \leq i \leq M-1$, being stable transfer functions) and $\mathbf{C}$ is an arbitrary permutation matrix. If (6.5) is satisfied, we get a CF-TMUX. To simplify the notation, we shall restrict our attention

to the case when $\mathbf{C} = \mathbf{I}_M$, the identity matrix.

A special case of CF-TMUX (which has all $T_i(z)$ equal) is obtained when $\mathbf{T}(z) = S(z)\mathbf{I}_M$. In this case (6.5) becomes

$$\mathbf{E}(z)\begin{bmatrix} \mathbf{0} & 1 \\ z^{-1}\mathbf{I}_{M-1} & \mathbf{0} \end{bmatrix}\mathbf{R}(z) = S(z)\mathbf{I}_M. \tag{6.6}$$

The condition on $\mathbf{R}(z)$ in terms of $\mathbf{E}(z)$ in order to achieve CC is

$$\mathbf{R}(z) = S(z)\begin{bmatrix} \mathbf{0} & z\mathbf{I}_{M-1} \\ 1 & \mathbf{0} \end{bmatrix}\mathbf{E}^{-1}(z), \tag{6.7}$$

provided that $\mathbf{E}^{-1}(z)$ is stable. From (6.7) we see that the elements of $\mathbf{R}(z)$ may not be FIR even if the elements of $\mathbf{E}(z)$ are FIR, unless the determinant of $\mathbf{E}(z)$ is a delay.‡ Multiplying both sides of (6.7) by $\mathbf{E}(z)$, we get a *necessary and sufficient condition* for a CF-TMUX (which has all $T_i(z)$ equal)

$$\mathbf{P}(z) \triangleq \mathbf{R}(z)\mathbf{E}(z) = S(z)\begin{bmatrix} \mathbf{0} & z\mathbf{I}_{M-1} \\ 1 & \mathbf{0} \end{bmatrix} = zS(z)\begin{bmatrix} \mathbf{0} & \mathbf{I}_{M-1} \\ z^{-1} & \mathbf{0} \end{bmatrix}. \tag{6.8}$$

If $S(z)$ is a pure delay, then the CF-TMUX achieves perfect reconstruction (PR). So from (6.8) we can write the *necessary and sufficient condition* for a PR-TMUX as

$$\mathbf{P}(z) = z^{-k}\begin{bmatrix} \mathbf{0} & z\mathbf{I}_{M-1} \\ 1 & \mathbf{0} \end{bmatrix} = z^{-(k-1)}\begin{bmatrix} \mathbf{0} & \mathbf{I}_{M-1} \\ z^{-1} & \mathbf{0} \end{bmatrix}. \tag{6.9}$$

where k is a non-negative integer. We can summarize these results in the following lemma.

Lemma 6.1 : Let $\mathbf{E}(z)$ and $\mathbf{R}(z)$ represent the polyphase component matrices of the transmultiplexer filters $\{H_i(z), F_i(z)\}$ (obtained by using (6.1), (6.2)). The necessary and sufficient condition for $\{H_i(z), F_i(z)\}$ to yield a CF-TMUX, with all $T_i(z)$ equal,

‡A special case of this type of polynomial matrix (which has been extensively studied in the QMF context [Vai87a,Vai89]) is when $\mathbf{E}(z)$ satisfies the property $\widetilde{\mathbf{E}}(z)\mathbf{E}(z) = c\mathbf{I}_M$, where $c > 0$. Then, $\mathbf{E}(z)$ is called *lossless* and we can express (6.7) as

$$\mathbf{R}(z) = \frac{1}{c}S(z)\begin{bmatrix} \mathbf{0} & z\mathbf{I}_{M-1} \\ 1 & \mathbf{0} \end{bmatrix}\widetilde{\mathbf{E}}(z).$$

is that the matrix $\mathbf{P}(z)$ [$= \mathbf{R}(z)\mathbf{E}(z)$] should satisfy (6.8) for some stable, scalar system $S(z)$. The same filters yield a PR-TMUX if $S(z)$ in (6.8) is a pure delay.

$\Diamond$

6.1.3 Relation between CF-TMUX filters and AF-QMF banks

Let $\mathbf{E}'(z)$ and $\mathbf{R}'(z)$ be the polyphase component matrices of the analysis and synthesis filter banks of an M-channel, maximally decimated QMF circuit $\{H_i'(z), F_i'(z)\}$, shown in Fig. 1.1. From the results in [Vai88b,Vai90], we know that the QMF circuit is alias free (AF) if and only if the matrix $\mathbf{P}'(z)$, defined as $\mathbf{P}'(z) \triangleq \mathbf{R}'(z)\mathbf{E}'(z)$, is a *pseudo-circulant* matrix. A special case of a pseudo-circulant matrix is obtained if $\mathbf{P}'(z)$ has the following form

$$\mathbf{P}'(z) = S'(z) \begin{bmatrix} \mathbf{0} & \mathbf{I}_{M-n} \\ z^{-1}\mathbf{I}_n & \mathbf{0} \end{bmatrix}, \qquad 0 \leq n < M, \tag{6.10}$$

where $S'(z)$ is a stable, scalar system. The overall transfer function $T(z)$ (also called the distortion function) of the AF-QMF bank $\{H_i'(z), F_i'(z)\}$ is given by

$$T(z) = z^{-(M-1)} z^{-n} S'(z^M). \tag{6.11}$$

If $S'(z)$ in (6.11) is a pure delay, then the AF-QMF bank satisfies perfect reconstruction (PR). In that case it is called a PR-QMF bank. This result is also contained in Lemma 3.2 [Vai87a], which states that the necessary and sufficient condition for a PR-QMF bank is that the matrix $\mathbf{P}'(z)$ should have the form

$$\mathbf{P}'(z) = z^{-k_1} \begin{bmatrix} \mathbf{0} & \mathbf{I}_{M-n} \\ z^{-1}\mathbf{I}_n & \mathbf{0} \end{bmatrix}, \tag{6.12}$$

where k_1 is a non-negative integer and $0 \leq n \leq M-1$.

If a QMF bank satisfies (6.10) with $n = 0$, it will be called a *standard* AF-QMF bank, whereas if it satisfies (6.10) with $n \neq 0$, it will be called an *n-skewed* AF-QMF bank. From (6.11), the distortion function of a standard AF-QMF bank is given

by $T(z) = z^{-(M-1)}S'(z^M)$. The following fact relates standard AF-QMF banks and n-skewed AF-QMF banks.

Fact 6.2 : An n-skewed AF-QMF bank $\{H_i''(z), F_i''(z)\}$ is always obtainable from a standard AF-QMF bank $\{H_i'(z), F_i'(z)\}$ by choosing the filters as $H_i''(z) = H_i'(z)$ and $F_i''(z) = z^{-n}F_i'(z), \quad 0 \leq i \leq M-1.$ $\Diamond$

Proof : Since $\{H_i'(z), F_i'(z)\}$ is a standard AF-QMF bank, we know that $\mathbf{P}'(z) = \mathbf{R}'(z)\mathbf{E}'(z) = S'(z)\mathbf{I}_M$. We want to obtain $\{H_i''(z), F_i''(z)\}$ such that

$$\mathbf{P}''(z) = \mathbf{R}''(z)\mathbf{E}''(z) = S'(z)\begin{bmatrix} \mathbf{0} & \mathbf{I}_{M-n} \\ z^{-1}\mathbf{I}_n & \mathbf{0} \end{bmatrix}. \tag{6.13}$$

Since $H_i''(z) = H_i'(z), \ \forall\, i$, we have $\mathbf{E}''(z) = \mathbf{E}'(z)$. Comparing the expressions for $\mathbf{R}'(z)$ and $\mathbf{R}''(z)$, we get

$$\mathbf{R}''(z) = \begin{bmatrix} \mathbf{0} & \mathbf{I}_{M-n} \\ z^{-1}\mathbf{I}_n & \mathbf{0} \end{bmatrix}\mathbf{R}'(z). \tag{6.14}$$

The synthesis filter bank $\mathbf{f}'(z)$ corresponding to $\mathbf{R}'(z)$ is

$$\mathbf{f}'(z) \triangleq \begin{bmatrix} F_0'(z) & F_1'(z) & \cdots & F_{M-1}' \end{bmatrix}^T = \mathbf{R}'^T(z^M)\mathbf{e}(z), \tag{6.15}$$

where $\mathbf{e}(z) = \begin{bmatrix} z^{-(M-1)} & z^{-(M-2)} & \cdots & 1 \end{bmatrix}^T$. Similarly we can write

$$\mathbf{f}''(z) = \mathbf{R}''^T(z^M)\mathbf{e}(z), \tag{6.16}$$

$$= \mathbf{R}'^T(z^M)\begin{bmatrix} \mathbf{0} & z^{-M}\mathbf{I}_n \\ \mathbf{I}_{M-n} & \mathbf{0} \end{bmatrix}\mathbf{e}(z) = z^{-n}\mathbf{R}'^T(z^M)\mathbf{e}(z) = z^{-n}\mathbf{f}'(z), \tag{6.17}$$

proving that $F_i''(z) = z^{-n}F_i'(z)$.

$\nabla\nabla\nabla$

Note : To obtain the above result, we used the choice $H_i''(z) = H_i'(z), \ F_i''(z) = z^{-n}F_i'(z)$. It can be readily verified that the choice $H_i''(z) = z^{-n}H_i'(z), \ F_i''(z) = F_i'(z)$ will also enable us to obtain an n-skewed AF-QMF bank from a standard AF-QMF bank.

Comparing (6.8) and (6.10), we see that the CF-TMUX filters and the filters of a 1-skewed AF-QMF bank satisfy the same condition. This enables us to establish the relation between them, as summarized in the following lemma.

Lemma 6.2 : Let $\{H_i'(z), F_i'(z)\}$ represent a 1-skewed AF-QMF bank. Choose the filters $H_i(z)$ and $F_i(z)$ as $H_i(z) = H_i'(z), \quad F_i(z) = F_i'(z), \quad \forall\, i$. Then $\{H_i(z), F_i(z)\}$ represents a CF-TMUX. $\Diamond$

Proof: By definition, the matrix $\mathbf{P}'(z)$ of the 1-skewed AF-QMF bank $\{H_i'(z), F_i'(z)\}$ satisfies,

$$\mathbf{P}'(z) = \mathbf{R}'(z)\mathbf{E}'(z) = S'(z) \begin{bmatrix} \mathbf{0} & \mathbf{I}_{M-1} \\ z^{-1} & \mathbf{0} \end{bmatrix}, \tag{6.18}$$

So, for the TMUX filters, the matrix $\mathbf{P}(z)$ satisfies $\mathbf{P}(z) = \mathbf{R}(z)\mathbf{E}(z) = \mathbf{P}'(z)$. Hence, from (6.18), we can write

$$\mathbf{R}(z) = S'(z) \begin{bmatrix} \mathbf{0} & \mathbf{I}_{M-1} \\ z^{-1} & \mathbf{0} \end{bmatrix} \mathbf{E}^{-1}(z). \tag{6.19}$$

Using (6.19) in (6.4), we get $\widehat{X}_i(z) = z^{-1}S'(z)X_i(z), \ \forall\, i$. Thus, $\{H_i(z), F_i(z)\}$ represents a CF-TMUX in which all the $T_i(z)$ are equal and are given by $T_i(z) = z^{-1}S'(z), \ \forall\, i$.

$\nabla\nabla\nabla$

Design procedure for CF-TMUX filters : The above result highlights the close relation between CF-TMUX filters and the filters of 1-skewed AF-QMF banks. Hence, it yields a design procedure for CF-TMUX filters, starting with an arbitrary AF-QMF bank. This is an advantage because the design of AF-QMF banks is well known. The design steps are

1. Design an AF-QMF bank $\{H_i'(z), \ F_i'(z)\}$.
2. Using Fact 6.2, obtain a 1-skewed AF-QMF bank (by inserting appropriate delays).
3. Choose the CF-TMUX filters to be the same as the 1-skewed AF-QMF bank (as given in Lemma 6.2).

Since PR-QMF banks are a subset of the class of AF-QMF banks, the above results are valid for PR-QMF banks also. In particular, if we start the design with a PR-

QMF bank, then we obtain a PR-TMUX. Extensive work has been done in the area of designing PR-QMF banks [Vai87a,Ngu88b,Vai89] and these results can be fully used in the design of PR-TMUX filters.

Comment on IIR Designs : From Lemma 6.2 we see that if we start from a 1-skewed AF-QMF bank with distortion function $T(z) = z^{-M}S'(z^M)$, then we can obtain the filters for a CF-TMUX such that the distortion function in each channel is $T_i(z) = z^{-1}S'(z), \quad \forall\, i$. In particular, this means that if the QMF bank is free from amplitude distortion, then so is the transmultiplexer. For example, the techniques described in [Swa86] and [Vai87b] show two methods of obtaining IIR QMF banks that are free from aliasing and amplitude distortions. (In both cases, $T(z)$ is an allpass function.) By Lemma 6.2, we can obtain IIR analysis and synthesis filters for a CF-TMUX with no amplitude distortion. This emphasizes the fact that the CC results derived earlier are valid both in the FIR case and in the IIR case.

Lemma 6.2 shows that if we have a 1-skewed AF-QMF bank, then we can always obtain a CF-TMUX. However, this result is further strengthened by the next lemma, which establishes the relation between CF-TMUX filters and the filters of an AF-QMF bank.

Lemma 6.3 : Let $\{H_i'(z),\ F_i'(z)\}$ represent an AF-QMF bank. If the TMUX filters, $\{H_i(z), F_i(z)\}$, are chosen such that $H_i(z) = H_i'(z)$ and $F_i(z) = F_i'(z)$, then the TMUX is Crosstalk-free with all $T_i(z)$ equal if and only if $\{H_i'(z),\ F_i'(z)\}$ is a 1-skewed AF-QMF bank. $\Diamond$

Proof : Let $\mathbf{E}(z)$ and $\mathbf{R}(z)$ be the polyphase component matrices of the TMUX and $\mathbf{E}'(z)$ and $\mathbf{R}'(z)$ be the polyphase components of the AF-QMF bank. By choice of TMUX filters,

$$\mathbf{E}(z) = \mathbf{E}'(z) \quad \text{and} \quad \mathbf{R}(z) = \mathbf{R}'(z). \tag{6.20}$$

From (6.8) we have

"TMUX is crosstalk free and all $T_i(z)$ are equal"

$$\Leftrightarrow \mathbf{P}(z) = \mathbf{R}(z)\mathbf{E}(z) = S'(z)\begin{bmatrix} \mathbf{0} & \mathbf{I}_{M-1} \\ z^{-1} & \mathbf{0} \end{bmatrix}, \tag{6.21}$$

$$\Leftrightarrow \mathbf{P}'(z) = \mathbf{R}'(z)\mathbf{E}'(z) = S'(z)\begin{bmatrix} \mathbf{0} & \mathbf{I}_{M-1} \\ z^{-1} & \mathbf{0} \end{bmatrix}, \quad \text{(by using (6.20))} \tag{6.22}$$

$$\Leftrightarrow \{H_i'(z),\ F_i'(z)\}\text{is a 1-skewed AF-QMF bank, (from (6.10), by defn.)} \tag{6.23}$$

$\nabla\nabla\nabla$

6.1.4 Alternate Derivation of the CC Condition (Vetterli)

The main result on transmultiplexers in [Vet86,Vet87] is the necessary and sufficient condition under which a given set of filters can be used to obtain an AF-QMF bank as well as a CF-TMUX (i.e., the filters will simultaneously satisfy AC and CC). This result is derived in terms of the analysis and synthesis filters. In this subsection, we re-derive the same result for two reasons – firstly, to prove (in Fact 6.3) the equivalence between this result and the result of Lemma 6.3 and secondly, to develop the framework based on the analysis/synthesis filters, which will be used to extend the CC results to the case of approximate CC, which is presented in Section 6.2.

Let $\{H_i(z), F_i(z)\}$ be a set of TMUX filters. In Fig. 6.1, the FDM signal $y(n)$ can be expressed as

$$Y(z) = \sum_{i=0}^{M-1} F_i(z)X_i(z^M). \tag{6.24}$$

After the FDM $\rightarrow$ TDM conversion, we have,

$$\widehat{X}_i(z) = \frac{1}{M}\sum_{\ell=0}^{M-1} H_i(z^{\frac{1}{M}}W^\ell)Y(z^{\frac{1}{M}}W^\ell), \qquad 0 \le i \le M-1, \tag{6.25}$$

where $W = e^{-j\frac{2\pi}{M}}$. Rewriting (6.25) in matrix form we get,

$$\begin{bmatrix} \widehat{X}_0(z) \\ \widehat{X}_1(z) \\ \vdots \\ \widehat{X}_{M-1}(z) \end{bmatrix} = \frac{1}{M}\begin{bmatrix} H_0(z^{\frac{1}{M}}) & H_0(z^{\frac{1}{M}}W) & \cdots & H_0(z^{\frac{1}{M}}W^{M-1}) \\ H_1(z^{\frac{1}{M}}) & H_1(z^{\frac{1}{M}}W) & \cdots & H_1(z^{\frac{1}{M}}W^{M-1}) \\ \vdots & \vdots & \ddots & \vdots \\ H_{M-1}(z^{\frac{1}{M}}) & H_{M-1}(z^{\frac{1}{M}}W) & \cdots & H_{M-1}(z^{\frac{1}{M}}W^{M-1}) \end{bmatrix}\begin{bmatrix} Y(z^{\frac{1}{M}}) \\ Y(z^{\frac{1}{M}}W) \\ \vdots \\ Y(z^{\frac{1}{M}}W^{M-1}) \end{bmatrix} \tag{6.26}$$

Expressing the FDM signal $u(n)$ in terms of the inputs,

$$\begin{bmatrix} \widehat{X}_0(z) \\ \widehat{X}_1(z) \\ \vdots \\ \widehat{X}_{M-1}(z) \end{bmatrix} = \frac{1}{M}\mathbf{H}^T(z^{\frac{1}{M}})\mathbf{F}^T(z^{\frac{1}{M}}) \begin{bmatrix} X_0(z) \\ X_1(z) \\ \vdots \\ X_{M-1}(z) \end{bmatrix}, \tag{6.27}$$

where

$$\mathbf{H}^T(z^{\frac{1}{M}}) = \begin{bmatrix} H_0(z^{\frac{1}{M}}) & H_0(z^{\frac{1}{M}}W) & \cdots & H_0(z^{\frac{1}{M}}W^{M-1}) \\ H_1(z^{\frac{1}{M}}) & H_1(z^{\frac{1}{M}}W) & \cdots & H_1(z^{\frac{1}{M}}W^{M-1}) \\ \vdots & \vdots & \ddots & \vdots \\ H_{M-1}(z^{\frac{1}{M}}) & H_{M-1}(z^{\frac{1}{M}}W) & \cdots & H_{M-1}(z^{\frac{1}{M}}W^{M-1}) \end{bmatrix}$$

and

$$\mathbf{F}^T(z^{\frac{1}{M}}) = \begin{bmatrix} F_0(z^{\frac{1}{M}}) & F_1(z^{\frac{1}{M}}) & \cdots & F_{M-1}(z^{\frac{1}{M}}W) \\ F_0(z^{\frac{1}{M}}W) & F_1(z^{\frac{1}{M}}W) & \cdots & F_{M-1}(z^{\frac{1}{M}}W) \\ \vdots & \vdots & \ddots & \vdots \\ F_0(z^{\frac{1}{M}}W^{M-1}) & F_1(z^{\frac{1}{M}}W^{M-1}) & \cdots & F_{M-1}(z^{\frac{1}{M}}W^{M-1}) \end{bmatrix}.$$

In (6.27), for CC we need,

$$\mathbf{H}^T(z^{\frac{1}{M}})\mathbf{F}^T(z^{\frac{1}{M}}) = \text{diag } [T_0(z) \;\; T_1(z) \;\; \cdots \;\; T_{M-1}(z)], \tag{6.28}$$

where $T_i(z), \;\; 0 \leq i \leq M-1$, are stable transfer functions. Eqn. (6.28) can be re-written as

$$\mathbf{F}(z)\mathbf{H}(z) = \text{diag } [T_0(z^M) \;\; T_1(z^M) \;\; \cdots \;\; T_{M-1}(z^M)]. \tag{6.29}$$

This is the necessary and sufficient condition for CC [Vet86,Vet87] in terms of the analysis and synthesis filters. From QMF theory [Vet87,Vai87a] we know that the Aliasing Cancellation (AC) equations (for the choice $H_i'(z) = H_i(z)$ and $F_i'(z) = F_i(z), \;\; \forall \; i$) can be written as

$$\mathbf{H}(z)\mathbf{F}(z) = \mathbf{H}'(z)\mathbf{F}'(z) = \text{diag } [T(z) \;\; T(zW) \;\; \ldots \;\; T(zW^{M-1})]. \tag{6.30}$$

So, from (6.29) and (6.30) AC and CC are simultaneously satisfied if and only if

$$\mathbf{F}^{-1}(z) \begin{bmatrix} T_0(z^M) & & & \\ & T_1(z^M) & & \\ & & \ddots & \\ & & & T_{M-1}(z^M) \end{bmatrix} = \begin{bmatrix} T(z) & & & \\ & T(zW) & & \\ & & \ddots & \\ & & & T(zW^{M-1}) \end{bmatrix} \mathbf{F}^{-1}(z), \tag{6.31}$$

i.e., if and only if

$$\begin{bmatrix} T_0(z^M) & & & \\ & T_1(z^M) & & \\ & & \ddots & \\ & & & T_{M-1}(z^M) \end{bmatrix} \mathbf{F}(z) = \mathbf{F}(z) \begin{bmatrix} T(z) & & & \\ & T(zW) & & \\ & & \ddots & \\ & & & T(zW^{M-1}) \end{bmatrix}. \tag{6.32}$$

Comparing the j^{th} column of LHS and RHS of (6.32), we get the equivalent condition

$$T_i(z^M) = T(z), \quad 0 \le i \le M-1, \quad \text{unless} \quad F_{i,j}(z) \equiv 0, \quad \forall\, j. \tag{6.33}$$

where $F_{i,j}(z)$ are the elements of $\mathbf{F}(z)$. In summary, "CC and AC simultaneously satisfied iff $T_i(z^M) = T(z)$, $\forall\, i$." This is the main result on transmultiplexers that is presented in [Vet86,Vet87]. The equivalence between the above result and the result of Lemma 6.3 is shown next.

6.1.5 Relation between Vetterli's result and Lemma 6.3

Fact 6.3 : Let $\{H_i'(z), F_i'(z)\}$ be an AF-QMF bank. Then the overall transfer function $T(z)$ of the AF-QMF system is a (rational) function of z^M if and only if $\{H_i'(z), F_i'(z)\}$ form a *1-skewed* AF-QMF bank. $\Diamond$

Proof : Since $\{H_i'(z), F_i'(z)\}$ is an AF-QMF bank, the corresponding $\mathbf{P}'(z)$ is necessarily a pseudo-circulant matrix. From the results in [Vai88b,Vai90], we know that the transfer function of the AF-QMF system (in terms of $P_{i,j}'(z)$, the elements of $\mathbf{P}'(z)$) is given by

$$T(z) = \frac{\widehat{X}(z)}{X(z)} = z^{-(M-1)} \sum_{j=0}^{M-1} z^{-j} P_{0,j}'(z^M). \tag{6.34}$$

From (6.34), see that

"$T(z)$ is a function of z^M iff $P_{0,j}'(z) = 0$, for all $j \neq 1$," and hence,

$$\mathbf{P}'(z) = P_{0,1}'(z) \begin{bmatrix} \mathbf{0} & \mathbf{I}_{M-1} \\ z^{-1} & \mathbf{0} \end{bmatrix}, \tag{6.35}$$

which is of the form in equation (6.10) with $n = 1$, thereby proving that $\{H_i'(z), F_i'(z)\}$ is a 1-skewed AF-QMF bank. $\nabla\nabla\nabla$

Hence, it can be readily seen that the necessary and sufficient condition in Lemma 6.3 is equivalent to the one presented in [Vet86,Vet87].

6.2 Approximate Crosstalk Cancellation

A number of papers [Roth83,Nus81,Mas85,Nus84,Cox86,Chu85] deal with the problem of approximate aliasing cancellation (AC) in the subband coding problem. In Section 6.1.3, we presented the relation between AF-QMF banks and CF-TMUX filters. We will now show that there is a similar relation between filters that satisfy *approximate* aliasing cancellation and TMUX filters that achieve *approximate* CC. First, we consider pseudo-QMF banks and then generalize the result to cover all approximately AF-QMF banks.

For the pseudo-QMF bank $\{H'_k(z), F'_k(z)\}$, the approximate AC condition can be expressed as

$$\begin{bmatrix} H'_0(z) & H'_1(z) & \cdots & H'_{M-1}(z) \\ H'_0(zW) & H'_1(zW) & \cdots & H'_{M-1}(zW) \\ \vdots & \vdots & \ddots & \vdots \\ H'_0(zW^{M-1}) & H'_1(zW^{M-1}) & \cdots & H'_{M-1}(zW^{M-1}) \end{bmatrix} \begin{bmatrix} F'_0(z) \\ F'_1(z) \\ \vdots \\ F'_{M-1}(z) \end{bmatrix} = \begin{bmatrix} T(z) \\ \simeq 0 \\ \vdots \\ \simeq 0 \end{bmatrix}. \tag{6.36}$$

The aliasing terms are small ($\simeq 0$) but not exactly zero. (6.36) can also be expressed as

$$\mathbf{H}'(z)\mathbf{F}'(z) \simeq \text{ diag}\left[T(z)\ T(zW)\ \cdots\ T(zW^{M-1})\right], \tag{6.37}$$

where the non-diagonal entries in (6.37) are small but not necessarily zero and the matrices $\mathbf{H}'(z)$, $\mathbf{F}'(z)$ are as defined in (6.27).

The main results from pseudo-QMF theory are given in Chapter 2. The pseudo-QMF bank is derived from a lowpass prototype $H'(z)$ (length=N) as given in (2.34) and (2.35). $T(z)$, the overall transfer function of the approximately alias-free system is

given by (as in (2.40))

$$T(z) = \frac{1}{M}\sum_{k=0}^{M-1} H_k'(z)F_k'(z) = \frac{z^{-(N-1)}}{M}\sum_{k=0}^{M-1} H_k'(z)H_k'(z^{-1}). \tag{6.38}$$

It is shown in Appendix B that $\left\{z^{(N-1)}T(z)\right\}$ is approximately a function of z^{2M}. Let the constants p_0, p_1 be defined as $p_0 \triangleq (N-1)_{modulo\ M}$ and $p_1 \triangleq M - p_0$. If we choose $H_k'' = H_k'$ and $F_k'' = z^{-p_1}F_k'$, then the overall transfer function $T_1(z) = \frac{1}{M}\sum_{k=0}^{M-1} H_k''(z)F_k''(z) \simeq$ a function of z^M. So the *approximate* AC condition (6.37) can be written as

$$\mathbf{H}''(z)\mathbf{F}''(z) \simeq T_1(z)\mathbf{I}_M, \tag{6.39}$$

since $T_1(z)$ is approximately a function of z^M. Using Fact 6.3, we can conclude that $\{H_i''(z), F_i''(z)\}$ yield an 'approximately' *1-skewed* AF-QMF bank. The immediate question that arises is : "Can we obtain an approximately crosstalk-free transmultiplexer by choosing $H_i(z) = H_i''(z)$ and $F_i(z) = F_i''(z)$?"

The answer is in the affirmative as shown next. The term *approximately* crosstalk-free is also made more quantitative.

Fact 6.4 : If $\mathbf{H}''(z)\mathbf{F}''(z) \simeq T_1(z)\mathbf{I}_M$, then $\mathbf{F}''(z)\mathbf{H}''(z) \simeq T_1(z)\mathbf{I}_M$.

Proof : We will prove this by a continuity argument for the inverse of complex matrices. Let

$$\mathbf{H}''(z)\mathbf{F}''(z) = T_1(z)\mathbf{I}_M + \mathbf{\Delta}(z), \tag{6.40}$$

$$\mathbf{F}''(z)\mathbf{H}''(z) = T_1(z)\mathbf{I}_M + \mathbf{\Gamma}(z). \tag{6.41}$$

Given any $\epsilon > 0$, however small, we will show how to find a $\delta > 0$ such that

$$\text{if} \quad |\Delta_{i,j}| \leq \delta, \quad \forall\ i,j, \qquad \text{then,} \quad |\Gamma_{i,j}| \leq \epsilon, \quad \forall\ i,j. \tag{6.42}$$

From (6.40), we get

$$\mathbf{F}''(z) = T_1(z)\left[\mathbf{H}''(z)\right]^{-1} + \left[\mathbf{H}''(z)\right]^{-1}\mathbf{\Delta}(z). \tag{6.43}$$

Let $\mathbf{J}(z) = [\mathbf{H}''(\mathbf{z})]^{-1}$. So we can write,

$$\mathbf{F}''(z)\mathbf{H}''(z) = T_1(z)\mathbf{I}_M + \underbrace{\mathbf{J}(z)\mathbf{\Delta}(z)\mathbf{H}''(z)}_{\mathbf{\Gamma}(z)}. \tag{6.44}$$

From (6.44),

$$\Gamma_{i,j}(z) = \sum_{k,\ell} J_{i,k}(z)\Delta_{k,\ell}(z)H''_{l,j}(z), \tag{6.45}$$

$$|\Gamma_{i,j}(z)| \leq \delta \sum_{k,\ell} |J_{i,k}(z)| \ |H''_{\ell,j}(z)|. \tag{6.46}$$

So, given ϵ, choose

$$\delta \leq \frac{\epsilon}{\sum_{k,\ell} |J_{i,k}(z)| \ |H''_{\ell,j}(z)|}. \tag{6.47}$$

Then, $|\Gamma_{i,j}(z)| \leq \epsilon, \quad \forall \ i,j,$ thereby proving the stated fact.

$\nabla\nabla\nabla$

In summary, the above fact shows that since the QMF bank $\{H''_k(z), F''_k(z)\}$ (obtained from the pseudo-QMF bank $\{H'_k(z), F'_k(z)\}$) satisfies (6.39), then the transmultiplexer filters chosen as $H_k(z) = H''_k(z), \quad F_k(z) = F''_k(z), \quad \forall \ k,$ satisfy the condition

$$\mathbf{F}(z)\mathbf{H}(z) = \mathbf{F}''(z)\mathbf{H}''(z) \simeq T(z)\mathbf{I}_M. \tag{6.48}$$

We conclude that $\{H_i(z), F_i(z)\}$ yield a transmultiplexer in which the crosstalk terms are negligibly small. Therefore we say that the TMUX is approximately crosstalk-free.

The above result pertains to approximately AF-QMF banks designed according to pseudo-QMF theory. This can be generalized to cover all filter banks that satisfy the approximate AC condition as follows: Let $\{H'_i(z), F'_i(z)\}$ be any approximately AF-QMF bank in standard form, i.e., $\mathbf{P}'(z) = \mathbf{R}'(z)\mathbf{E}'(z) \simeq S'(z)\mathbf{I}_M$. Then we can get approximately CF-TMUX filters by choosing them according to design procedure in Section 6.1.3.

6.3 Design Comparison

In this section, we compare the performance of 24-channel transmutilplexers designed by the new crosstalk cancellation (CC) method and the traditional approach. Let $\{H'_k(z),\ F'_k(z)\}$ be a 24-channel pseudo-QMF bank derived from a prototype of length N. From the definitions in Section 6.2, $p_1 = M - (N-1)_{modulo\ M}$. And the choice of transmultiplexer filters $\{F_k(z),\ H_k(z)\}$ given by

$$H_k(z) = H'_k(z) \quad \text{and} \quad F_k(z) = z^{-p_1} F'_k(z), \quad 0 \le k \le 23, \tag{6.49}$$

yields an approximate CF-TMUX. On the other hand, in traditional TMUX designs (where crosstalk is not canceled using multirate techniques), the analysis and synthesis filters are chosen to have similar specifications. For example, in the choice

$$H_k(z) = H'_k(z) \quad \text{and} \quad F_k(z) = F'_k(z) = z^{-(N-1)} \widetilde{H}_k(z), \quad 0 \le k \le 23, \tag{6.50}$$

the analysis and synthesis filters of the TMUX have identical magnitude responses. Here, the crosstalk depends only on the sharpness of the filters (the transition bandwidth) and their stopband attenuation A_s.

In order to do the comparison, we define a quantitative measure of the performance of the transmultiplexer. Equation (6.27) relates the inputs and outputs of the transmultiplexer. We define the transfer function matrix $\mathbf{C}(z^M) \triangleq \mathbf{H}^T(z)\mathbf{F}^T(z)$ where

$$\left[\mathbf{C}(z^M)\right]_{k,\ell} = C_{k,\ell}(z^M) = \frac{\widehat{X}_k(z^M)}{X_\ell(z^M)}, \quad 0 \le k, \ell \le M-1. \tag{6.51}$$

For $\ell \neq k$, $C_{k,\ell}(z^M)$ gives the crosstalk transfer functions. The total crosstalk error for the k^{th} channel is defined as

$$e_k \triangleq \int_0^{\frac{\pi}{M}} \sum_{\substack{\ell=0 \\ \ell \neq k}}^{M-1} |C_{k,\ell}(e^{jM\omega})|^2 \, d\omega. \tag{6.52}$$

The integration is done in the interval $[0, \frac{\pi}{M}]$ since the transfer functions are functions

of z^M. The maximum crosstalk error is

$$e_{max} \triangleq \max_{0 \le k \le M-1} e_k. \tag{6.53}$$

Next, we design a 24-channel pseudo-QMF bank with prototype length $N = 96$. Hence, $p_1 = 24 - (95)_{modulo\ 24} = 1$ and the approximate CF-TMUX is obtained by choosing the TMUX filters as in (6.49) (with $p_1 = 1$). For the traditional TMUX approach, the filters are chosen as in (6.50). For both designs, the maximum crosstalk error (6.53) is computed. The above steps are repeated with 24-channel TMUX designs with filter lengths $N = 48, 144$ and 192. The maximum crosstalk error for each design (along with the stopband attenuation (A_s) and the stopband edge (ω_s) of the respective prototypes) is shown in Table 6.1. In these four design examples, it can be seen that as the filter length increases, the A_s of the filters increases while the transition bandwidth (Δf) remains approximately constant. In the traditional method, e_{max} stays relatively the same (since it depends on Δf) while with the CC method, e_{max} decreases (since it depends mainly on A_s).

Next, we have another comparison of TMUX designs with filters of the same length ($N = 192$) but whose prototypes had different A_s and Δf. These results are shown in Table 6.2. In these design examples, as A_s increases, Δf also increases. In the traditional method, as Δf increases, e_{max} also increases (even though A_s is higher) while on the other hand, for the CC method, e_{max} decreases. From these two tables, it can be seen that the transmultiplexers designed by the CC approach perform consistently better than those designed by the traditional method.

Note : The traditional TMUX designs [Sch81,Bon78] differ from the approaches discussed in this chapter. To elaborate this point, consider the TMUX design in [Bon78]. For the 60-channel TMUX, the voice channels are each restricted to be in the 0.3–3.6 KHz band (by bandpass filtering) and then multiplexed into frequency slots which are 4 KHz wide as shown in Fig. 6.7 (and the spectral gaps are then

utilized for transmitting the signaling information). This, however, differs from the multiplexing scheme considered in Fig. 6.2(b). On account of this difference, a direct comparison between the method in this chapter and the traditional designs is not applicable.

6.4 Summary

In this chapter, we have presented new results in the theory of Crosstalk-Free Transmultiplexers (CF-TMUX). A necessary and sufficient condition for *complete* Crosstalk Cancellation is derived. It is shown that the filters for a CF-TMUX are the same as those for a 1-skewed AF-QMF bank. In addition, if the QMF bank satisfies the perfect reconstruction (PR) property, the TMUX also satisfies PR. The relation between AF-QMF banks and CF-TMUX filters yields a design procedure for CF-TMUX filters.It is also shown that pseudo-QMF banks and other approximately AF-QMF banks can be used to obtain approximately CF-TMUX filters. Lastly, examples to demonstrate the improved performance of transmultiplexers designed by the CC method, over the traditional TMUX designs, are included.

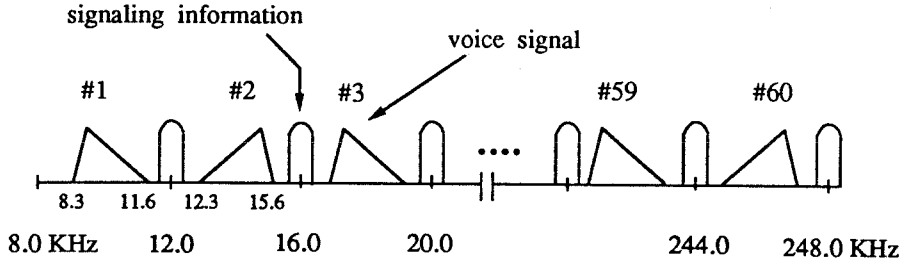

Fig. 6.7. Conventional 60-channel FDM signal with voice and signaling information . (Refer to Bonnerot et al. [Bon78].)

Table 6.1. Comparison of performance of transmultiplexers designed by the CC method and the traditional method (each design with different N, A_s).

24-Channel TMUX				
Prototype			e_{max}	
Length N	A_s (dB)	ω_s (rads)	New CC method	Traditional method
48	19.64	0.0448π	6.582 E-06	3.895 E-03
96	27.69	0.0430π	1.329 E-06	2.846 E-03
144	38.87	0.0406π	1.115 E-07	2.114 E-03
192	47.00	0.0400π	3.338 E-08	1.932 E-03

Table 6.2. Comparison of performance of transmultiplexers designed by the CC method and the traditional method (each design with different A_s, $\triangle f$).

24-Channel TMUX				
Prototype			e_{max}	
Length N	A_s (dB)	ω_s (rads)	New CC method	Traditional method
192	40.38	0.0374π	6.173 E-08	1.808 E-03
192	47.00	0.0400π	3.338 E-08	1.932 E-03
192	50.32	0.0414π	1.947 E-08	2.002 E-03

Appendix A

Spectral Factorization using the Inverse LPC Technique

A.1 Introduction

In this appendix, we present a new algorithm for spectral factorization. This efficient, non-iterative algorithm is based on the Inverse Linear Predictive Coding (LPC) technique and can be used to compute the minimum phase spectral factor of any moving average (MA) autocorrelation sequence. The moving average (MA) process is one of the basic models of time-series analysis and stochastic modeling of linear systems. In a variety of situations, we are interested in finding a spectral factor of an MA power spectrum. The spectral factorization problem can be stated as follows : Given a real, MA autocorrelation sequence $r(k)$, satisfying $r(k) = 0$, $|k| > N$ and $r(-k) = r(k)$. $S(z)$, the Z-transform of $r(k)$ is given by $S(z) = \sum_{k=-N}^{N} r(k)z^{-k}$ and $S(e^{j\omega})$ is the power spectrum of $r(k)$. Spectral factorization involves the computation of a polynomial $C(z) = \sum_{n=0}^{N} c(n)z^{-n}$, such that it satisfies $S(z) = C(z)C(z^{-1})$. In order to obtain a unique solution for $C(z)$, we impose the constraint that $C(z)$ should be minimum phase (i.e., none of the zeros are outside the unit circle in the Z-plane).

An overview of the different methods :

In [Fri83] and [Mul87], we find two approaches to solve the above-mentioned problem along with a comparison of the relative merits of some of the other methods. We can classify the different approaches broadly into two categories – the iterative meth-

ods and the non-iterative ones. In [Wil69], an iterative Newton-Raphson approach is used to compute the spectral factor and [Mul87] contains an efficient algorithm for the same. The main advantage of this method and other iterative algorithms is that successive approximations can be made till the error becomes smaller than a specified value. In [Fri83], an iterative, lattice-based approach is presented which computes the spectral factor via Cholesky decomposition of a banded Toeplitz matrix. The convergence of these methods [Fri83,Mul87,Wil69] is dependent on the data, i.e., on how close the zeros of $S(z)$ are to the unit circle.

A robust, non-iterative algorithm for spectral factorization is given in [Mia82]. This method is based on Cepstral techniques. It works successfully in most cases (even when the zeros are on the unit circle) - with a suitable choice of the scaling parameter ρ. The only drawback is the need for obtaining the unwrapped phase (this computation may fail in some cases).

In parametric modeling [Kay88], given the autocorrelation sequence, the parameters of the AR model can be determined by solving the Yule-Walker equations (which are linear). On the other hand, computing the MA model parameters involves non-linear equations and so, an indirect approach is to use AR modeling to do the desired computation. Two such methods are given in [Dur59] and [Cle72] respectively. These approaches can also be used in spectral factorization, which itself can be viewed as the computation of an MA model of specific order.

The method in [Dur59] involves obtaining two AR models, the first one of order $L >> N$, to fit the given autocorrelation sequence, and the second one of order N to fit the autocorrelation of the parameters of the denominator part of the first model. This is referred to as the 'double inversion' method and as pointed out in [Mul87], the spectral factor obtained is, at best, an approximation.

We will now present a 'one-pass' algorithm (non-iterative) based on the method

in [Cle72], where the MA parameters are obtained by evaluating the AR model parameters corresponding to the *inverse autocorrelations.* This is known as the 'Inverse LPC method' [Schm83]. The underlying theory is simple and well understood. This method works very well for most cases (it fails only if the zeros of $S(z)$ are on the unit circle) and compares favorably with the other iterative and non-iterative algorithms in speed (computation time) and in the accuracy of the spectral factor. This will be substantiated by the examples.

A.2 Linear Predictive Coding (LPC)

Let $x(n)$ be a wide sense stationary (WSS) random process. We can express $\widehat{x}(n)$, the predicted value of the current sample (based on an AR model of order N), as a linear combination of the past N samples

$$\widehat{x}(n) = -[a_1 x(n-1) + a_2 x(n-2) + \cdots + a_N x(n-N)]. \tag{A.1}$$

The prediction error $e(n)$ is given by

$$e(n) = x(n) - \widehat{x}(n) = x(n) + a_1 x(n-1) + a_2 x(n-2) + \cdots + a_N x(n-N). \tag{A.2}$$

The error sequence $e(n)$ is also WSS and can be considered to be the output of a linear system $A_N(z) = 1 + \sum_{k=1}^{N} a_k z^{-k}$, with $x(n)$ as its input. Let $S_{xx}(e^{j\omega})$ and $S_{ee}(e^{j\omega})$ be the power spectra of the input $x(n)$ and the output $e(n)$ respectively. They are related as

$$S_{ee}(e^{j\omega}) = |A_N(e^{j\omega})|^2 S_{xx}(e^{j\omega}). \tag{A.3}$$

If $x(n)$ is an AR process and if $A(z)$ is obtained by minimizing the expected value $E[e^2(n)]$ (with the order of $A(z)$ being appropriately chosen), then $e(n)$ is 'white noise,' so that

$$S_{xx}(e^{j\omega}) = \frac{G^2}{|A_N(e^{j\omega})|^2}, \tag{A.4}$$

where G is a real constant. The coefficients of $A_N(z)$ are estimated from the autocorrelation sequence of $x(n)$ by solving the Yule-Walker equations (using the Levinson-Durbin recursion). It must be noted that $A_N(z)$ is guaranteed to satisfy the minimum phase property.

A.3 The Spectral Factorization Algorithm

This method of computing the minimum phase spectral factor (using the Inverse LPC technique) involves the following steps :

1. Compute the samples of the power spectrum $S(e^{j\omega})$ by evaluating the DFT (using FFT) of the MA autocorrelation sequence $r(n)$.

$$R(k) \triangleq S(e^{j\omega})\Big|_{\omega=\frac{2\pi}{M}k} = \sum_{n=-N}^{N} r(n)W_M^{nk}, \quad 0 \leq k \leq M-1, \tag{A.5}$$

   where $W_M = e^{-j\frac{2\pi}{M}}$. M, the number of DFT points, is typically chosen to be much larger than $(2N+1)$, the length of the autocorrelation sequence (as justified in step 3).

2. Obtain the DFT samples of the inverse power spectrum,

$$S_{inv}(e^{j\omega})\Big|_{\omega=\frac{2\pi}{M}k} = R_{inv}(k) \triangleq \frac{1}{R(k)}, \quad 0 \leq k \leq M-1, \tag{A.6}$$

   where the inverse power spectrum $S_{inv}(e^{j\omega})$ is defined as the reciprocal of the original power spectrum $S(e^{j\omega})$, assuming that $S(e^{j\omega})$ does not have any zeros on the unit circle.

3. Obtain the inverse autocorrelation sequence (i.e., the autocorrelation sequence associated with the inverse power spectrum) $r_{inv}(n) = \text{IDFT}\ [R_{inv}(k)]$. Typically, $r_{inv}(n)$ is a doubly infinite sequence. In order to avoid time-domain aliasing (which is an artifact of DFT), we choose $M >> (2N+1)$.

4. Using $r_{inv}(n)$, the coefficients of the AR model are obtained by using the Levinson-Durbin recursion. This satisfies the equation (from (A.4))

$$S_{inv}(e^{j\omega}) = \frac{1}{S(e^{j\omega})} = \frac{G^2}{|A_N(e^{j\omega})|^2}. \tag{A.7}$$

The quantity $S(z)$ is therefore given by $S(z) = C(z)C(z^{-1})$, with $C(z) = \frac{A(z)}{G}$, where $A(z)$ is guaranteed to be minimum phase. Once $A(z)$ is computed, the scale factor G can easily be evaluated and thus $C(z)$, the desired minimum phase spectral factor of the MA spectrum $S(z)$, is obtained.

A.3.1 Computational Complexity

Using the inverse LPC method, the total computation involved is two M-point FFTs, the reciprocation of the DFT samples $S(k)$ and a Levinson-Durbin recursion of order N. In the first step, while evaluating $S(k)$, we have a real sequence $r(n)$ of length $(2N+1) << M$. In the third step, in evaluating $r_{inv}(n)$, we need only the values in the range $0 \leq n \leq N$. So additional savings in computation are possible in both these steps. It must be noted that as the value of M is increased, the accuracy of the spectral factor also increases.

A.4 Comparison

The inverse LPC method for computing the spectral factor has been tested with a large number of examples that have different degrees of difficulty (depending on the length of the autocorrelation sequence and on how close the zeros of $S(z)$ are to the unit circle). Here we will consider three specific examples, and in each case the proposed method is compared with the iterative method (lattice based) in [Fri83] and the non-iterative method (using Cepstral techniques) in [Mia82]. In order to obtain a basis for comparison, we define a 'computation error.' If $S'(z) = \sum_{n=-N}^{N} r'(n)z^{-n} = C(z)C(z^{-1})$, where $C(z)$ is the computed spectral factor, the computation error e is

defined as

$$e = \sum_{n=0}^{N} [r(n) - r'(n)]^2, \tag{A.8}$$

which gives a measure of the accuracy of the spectral factor. The error and the total computation time (on a VAX 11/750) measured in seconds are tabulated for the three methods for each of the three examples. The column titled 'FFT' represents 'M' which is the number of points in the FFT.

Example A.1 : Consider an autocorrelation sequence $r(n)$ of length 17 and whose 'ideal' minimum phase spectral factor $C(z)$ (order = 8) has complex conjugate zeros at radii $0.995, 0.99, 0.975$ and real zeros at radii $0.97, 0.96$. This is the same example that is considered in [Fri83] and [Wil69]. The performance of the three methods are compared below :

Lattice Method			Cepstral Method			Inverse LPC		
Iter	error	Time	FFT	error	Time	FFT	error	Time
50	2.165e-02	0.6	64	1.773e-02	0.5	64	2.337e-02	0.4
100	3.797e-05	0.8	128	6.053e-05	0.7	128	9.192e-03	0.5
300	9.869e-07	1.5	256	1.665e-08	0.9	256	1.478e-04	0.6
500	4.414e-09	2.2	512	6.413e-13	1.4	512	1.828e-05	0.8
1000	1.904e-13	4.2	1024	8.284e-13	2.5	1024	5.663e-08	1.2
						2048	1.558e-12	1.9

Example A.2 : Consider a linear phase FIR filter $F(z) = \sum_{n=0}^{2N} f(n) z^{-n}$ (designed using the McClellan-Parks Program [Mcc73]) with length 21 and $\omega_s = 0.5\pi$. The resulting response has a stopband attenuation $A_s = 34.5$ dB (i.e., the stopband deviation $\delta_2 = 0.0188$). A new filter $F'(z) = \sum_{n=0}^{2N} f'(n) z^{-n}$ is defined such that

$$\begin{aligned} f'(N) &= f(N) + \delta_2 + \epsilon, \quad \epsilon \geq 0, \\ f'(n) &= f(n), \quad n \neq N. \end{aligned}$$

The zero-phase response of $F'(e^{j\omega})$ is non-negative (it is strictly positive if $\epsilon > 0$). In this case, $\epsilon = 0.001$ was used. So $F'(e^{j\omega})$ can be regarded as a power spectrum with $f'(n)$ as the autocorrelation sequence associated with it. The minimum phase spectral

factor $C(z)$, satisfying $F'(z) = C(z)C(z^{-1})$, was computed by the three methods and the results are tabulated below :

Lattice Method			Cepstral Method			Inverse LPC		
Iter	error	Time	FFT	error	Time	FFT	error	Time
25	1.239e-05	0.5	64	2.238e-07	0.5	64	9.461e-04	0.4
50	4.025e-07	0.7	128	5.843e-09	0.7	128	4.548e-05	0.5
100	3.230e-09	0.9	256	1.479e-11	0.9	256	3.024e-07	0.6
250	6.480e-14	1.6	512	2.859e-16	1.4	512	1.890e-11	0.8
500	4.324e-22	2.7	1024	7.608e-17	2.5	1024	4.958e-20	1.2
						2048	7.582e-31	1.9

Note : One of the applications of spectral factorization is in the design of two-channel perfect reconstruction QMF (PR-QMF) banks [Smi84,Vai86b]. In this application, $F(z)$ is designed as a linear phase, half-band filter of order $2N$, where N is odd. $F'(z)$ is obtained as in the above example by using an appropriate value of ϵ. Using spectral factorization, $C(z)$ is obtained. With $C(z)$ chosen as one of the analysis filters of the two-channel PR-QMF circuit, the remaining filters can be derived from $C(z)$ [Smi84].

Example 3 : Proceeding exactly as in the previous example, we design $F(z)$, a linear-phase filter of length 101, $\omega_s = 0.5\pi$ and $A_s = 94.59$ dB (the corresponding $\delta_2 = 0.0000186$). $F'(z)$ is obtained by using $\epsilon = 0.00001$. As demonstrated in the table below, the Inverse LPC method works well in this case, where $F'(z)$ has a large number of zeros very close to the unit circle. Fig. A.1 shows the magnitude responses of (a) $F'(e^{j\omega})$ and (b) $C(e^{j\omega})$ using 2048 FFT points respectively.

Lattice Method			Cepstral Method			Inverse LPC		
Iter	error	Time	FFT	error	Time	FFT	error	Time
100	5.102e-07	2.7	128	4.582e-09	1.3	128	8.552e-04	1.3
250	1.973e-09	5.9	256	5.194e-10	1.5	256	2.604e-05	1.4
500	3.781e-12	11.3	512	2.814e-12	2.0	512	8.293e-07	1.6
			1024	2.540e-15	3.1	1024	4.595e-09	2.0
			2048	phase est. failed		2048	2.047e-14	2.8

A.5 Applications of Spectral Factorization

In examples A.2 and A.3, it was demonstrated that the inverse LPC approach to spectral factorization works well even for cases when the zeros of $S(z)$ are very close to the unit circle (but not on it). So this method can be used in most applications, including applications in QMF design and multistage design [Smi84,Ngu88a,Vai89].

If the zeros of $S(z)$ are on the unit circle, the spectrum can be raised by using $\epsilon << 1$, as explained in example A.2. The minimum phase spectral factor computed by the inverse LPC approach does not have zeros on the unit circle, but they are very close to it. This fact is demonstrated in Fig. A.2, where the solid curve is the spectral factor obtained in example 3 (with $\epsilon = 0.00001$), while the dotted line is the response of $|F'(e^{j\omega})|^{\frac{1}{2}}$ (which would be the response of a spectral factor of $F'(z)$ with $\epsilon = 0$).

In [Ngu88a], we find a procedure for obtaining a spectral factor $\hat{G}(z)$ of an M^{th}-band filter $G(z)$, satisfying $G(z) = \hat{G}(z)\hat{G}(z^{-1})$. $G(z)$ itself is designed as the cascade, $G(z) = G_0(z)G_1^2(z)$, where $G_1(z)$ has all zeros on the unit circle and $G_0(z)$ has no zeros on the unit circle. The spectral factor $\hat{G}(z)$ is obtained as $\hat{G}(z) = \hat{G}_0(z)G_1(z)$. This involves the computation of $\hat{G}_0(z)$, a spectral factor of $G_0(z)$. Since $G_0(z)$ does not have any zeros on the unit circle, the inverse LPC method can be directly used for this application.

A.6 Summary

In this appendix, a non-iterative method of spectral factorization based on the Inverse LPC technique is presented. The computations in this method involve two FFTs and a Levinson-Durbin recursion of appropriate order. It works well for most cases, even when the order of the spectral factor is high and the zeros of the spectrum are close to the unit circle. The method fails only if some zeros of the spectrum are on the unit circle. This method compares well with the other well known methods.

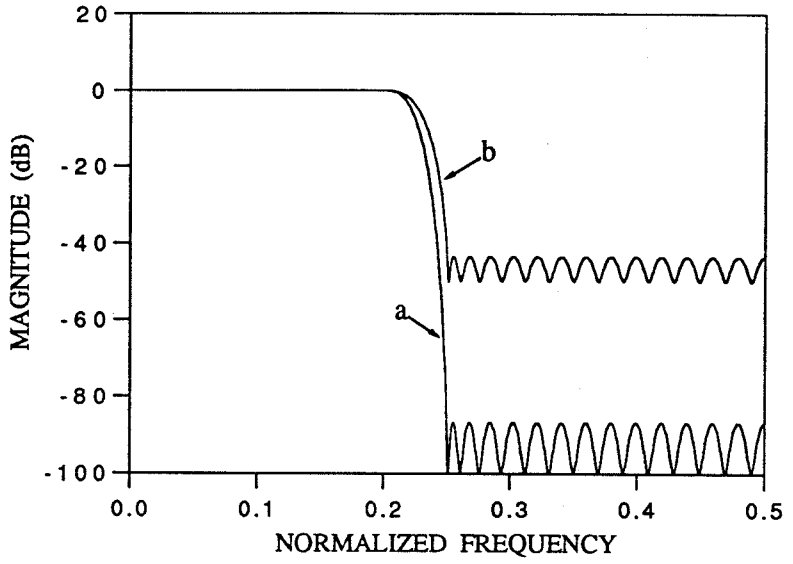

Fig. A.1. Design example A.3
Magnitude responses of (a) F'(z) and (b) C(z)

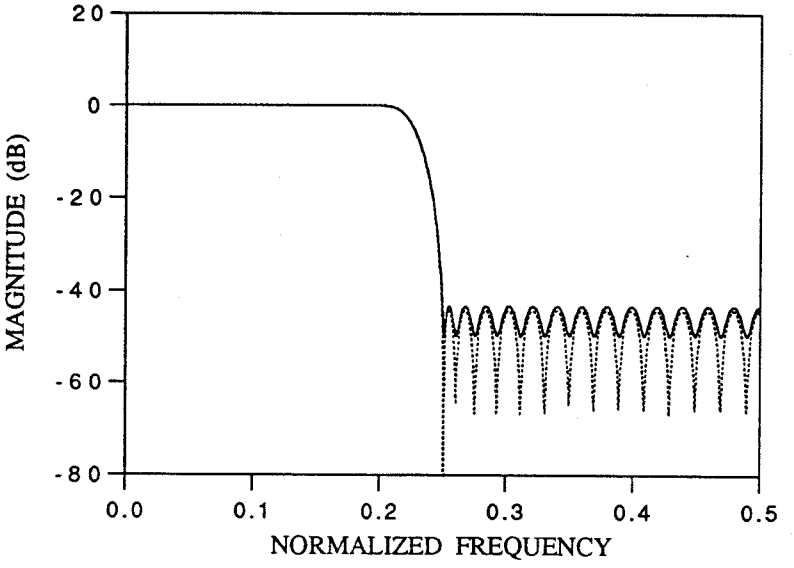

Fig. A.2. Design example A.3
Magnitude responses of C(z) (solid line) and
the spectral factor with epsilon=0 (dotted line)

Appendix B

A Pseudo-QMF Design Example

The main results from pseudo-QMF theory have been summarized in Section 2.4. In this appendix, we present an example of a conventional pseudo-QMF design [Roth83, Cox86]. Pseudo-QMF designs have been widely used [Cro83,Cox86]. The analysis filters $H_k(z)$ and the synthesis filters $F_k(z)$ are obtained by cosine modulation of the prototype filter $H(z)$ as given in (2.34) and (2.35). The conditions on θ_k are given in (2.37) - (2.39). $T(z)$, the overall transfer function of the analysis/synthesis system can be expressed as (from (2.40))

$$T(z) = \frac{1}{M}\sum_{k=0}^{M-1} H_k(z)F_k(z) = \frac{z^{-(N-1)}}{M}\sum_{k=0}^{M-1} H_k(z)H_k(z^{-1}). \qquad \text{(B.1)}$$

We will first prove the following result :

Fact B.1 : Consider a pseudo-QMF design in which the analysis and synthesis filters are obtained from a prototype filter $H(z)$ of length N (with θ_k chosen as in (2.39), and $T(z)$ is the overall transfer function. Then $z^{N-1}T(z)$ is approximately a (rational) function of z^{2M}. $\Diamond$

Proof : Substituting in (B.1) for $H_k(z)$ and $F_k(z)$ from (2.32) and (2.33) respectively and retaining only the significant terms, we get

$$z^{(N-1)}T(z) \simeq \frac{z^{(N-1)}}{M}\sum_{k=0}^{M-1}\left[c_k^2 H^2\left(ze^{-j(2k+1)\frac{\pi}{2M}}\right) + c^{*2}H^2\left(ze^{j(2k+1)\frac{\pi}{2M}}\right)\right], \qquad \text{(B.2)}$$

where $c_k = e^{j(2k+1)\frac{\pi}{2M}(\frac{N-1}{2})}$. Substituting $W_{2M} = e^{-j\frac{2\pi}{2M}}$ in (B.2),

$$z^{(N-1)}T(z) \simeq \frac{1}{M}\sum_{k=0}^{M-1}\left[\left(zW_{2M}^{(k+\frac{1}{2})}\right)^{N-1} H^2\left(zW_{2M}^{(k+\frac{1}{2})}\right) + \left(zW_{2M}^{-(k+\frac{1}{2})}\right)^{N-1} H^2\left(zW_{2M}^{-(k+\frac{1}{2})}\right)\right], \tag{B.3}$$

$$\simeq \frac{1}{M}\sum_{k=0}^{2M-1}\left(zW_{2M}^{(k+\frac{1}{2})}\right)^{N-1} H'^2\left(zW_{2M}^{(k+\frac{1}{2})}\right), \tag{B.4}$$

since $W_{2M}^{-(k+\frac{1}{2})} = W_{2M}^{2M-(k+\frac{1}{2})} = W_{2M}^{(2M-1-k)+\frac{1}{2}}$. Define $A(z)$ as shown below :

$$A(z) \triangleq \left(zW_{2M}^{\frac{1}{2}}\right)^{N-1} H'^2\left(zW_{2M}^{\frac{1}{2}}\right). \tag{B.5}$$

Expressing (B.4) in terms of $A(z)$ and using the property of W_{2M}, we get

$$z^{(N-1)}T(z) \simeq \frac{1}{M}\sum_{k=0}^{2M-1} A\left(zW_{2M}^{k}\right) = \text{a function of } z^{2M}. \tag{B.6}$$

$\nabla\nabla\nabla$

B.1 Design Considerations

The two important design criteria in pseudo-QMF banks are :

1. **Aliasing Cancellation** : The analysis and synthesis filters must be designed with narrow transition bands and high stopband attenuation. This will force the aliasing due to the overlap of non-adjacent bands to be negligible. The significant aliasing terms are canceled by the phase quadrature (introduced by the constants θ_ks) between filters in adjacent bands. The condition on the choice of θ_k is given in (2.37)–(2.39).

2. **Flatness Constraint** : We want the overall transfer function $T(z)$ (given in (2.40)) to have 'flat' (uniform) response at all frequencies. This ensures that there are no spectral gaps or nulls and that the reconstructed signal $\hat{x}(n)$ resembles the original signal $x(n)$.

The prototype filter, $H(z) = \sum_{n=0}^{N-1} h(n)z^{-n}$, is a linear phase filter. The above two conditions translate into design requirements on the prototype filter as given below :

$$\left|H(e^{j\omega})\right| \simeq 0, \qquad |\omega| > \frac{\pi}{2M} + \epsilon, \tag{B.7}$$

where $\epsilon < \frac{\pi}{2M}$ and

$$\left|H(e^{j\omega})\right|^2 + \left|H(e^{j(\omega-\frac{\pi}{M})})\right|^2 \simeq 1. \qquad 0 \leq |\omega| \leq \frac{\pi}{M}. \tag{B.8}$$

The typical magnitude response of the prototype filter of an M-channel pseudo-QMF bank is shown in Fig. B.1(a). The condition in (B.7) will ensures that the analysis and synthesis filters are 'good' filters, while the condition in (B.8) ensures that the magnitude squared responses of the prototype (Fig. B.1(a)) and its shifted version (Fig. B.1(b)) , shifted by $\frac{\pi}{M}$, (which is the separation between the center frequencies of filters in two adjacent bands), add to unity. This condition is known as the *flatness constraint* and is shown pictorially in Fig. B.1(c).

Optimization : The lowpass prototype $H(z)$ is an FIR linear phase filter (symmetric impulse response). The design of $H(z)$ is done by using the optimization routine *e04jaf* [NAG]. The objective function for the optimization is formulated as follows :

$$E = \alpha E_f + (1-\alpha)E_s, \tag{B.9}$$

where E_f is the error in satisfying the flatness constraint and is given by

$$E_f = \left[1 - \left|H(e^{j\omega})\right|^2 - \left|H(e^{j(\omega-\frac{\pi}{M})})\right|^2\right]^2, \tag{B.10}$$

and E_s is the stopband energy given by

$$E_s = \int_{\frac{\pi}{M}}^{\pi} \left|H(e^{j\omega})\right|^2 d\omega, \tag{B.11}$$

and α is a positive, real constant in $[0,1]$ and is used as a relative weighting factor between E_f and E_s.

Note : Evaluating (B.11) can be done by computing the DFT of $h(n)$, followed by numerical integration. This method yields only an approximate value and also it

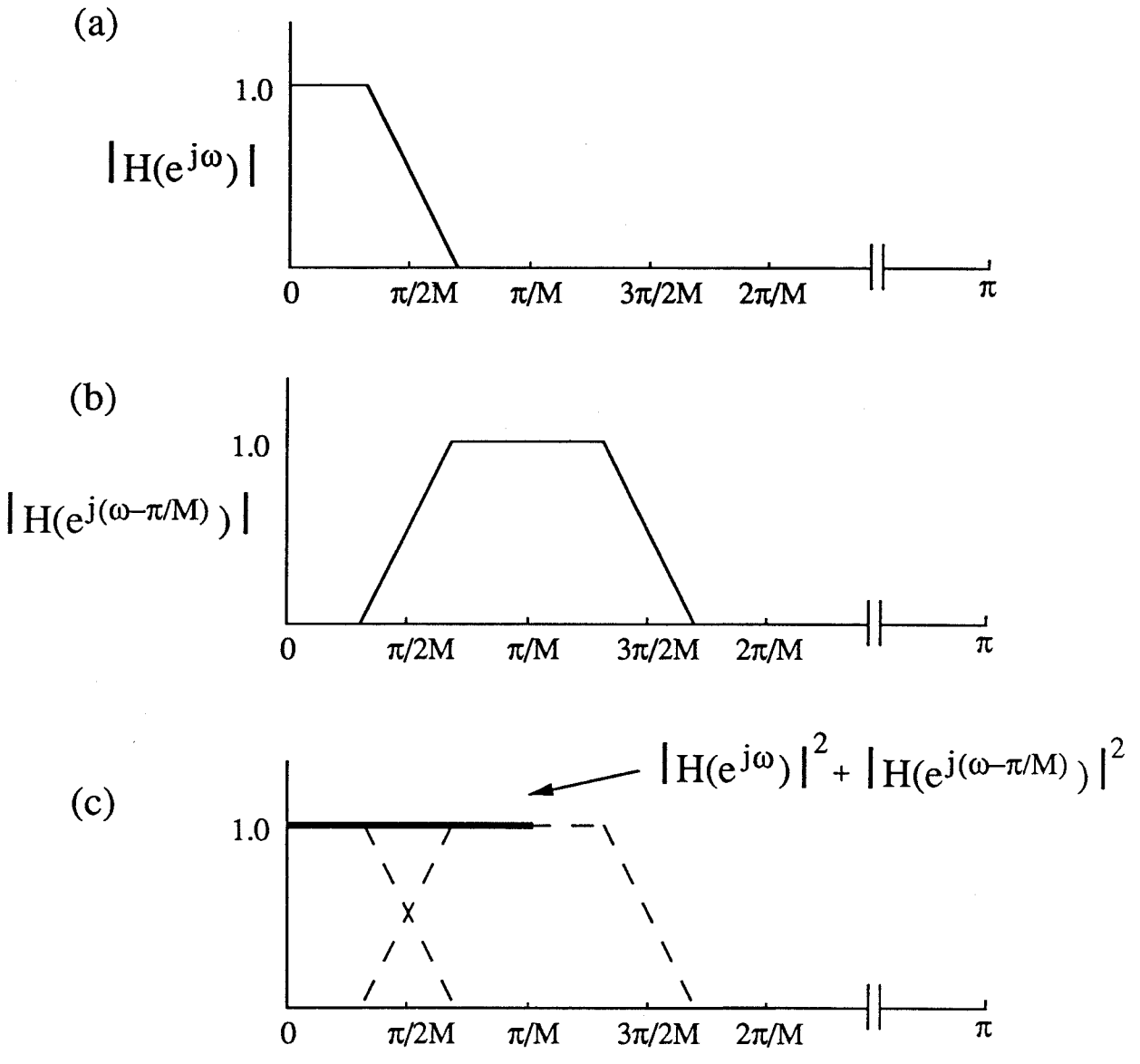

Fig. B.1. Pseudo-QMF design
(a). The desired response of the prototype H(z),
(b). The response of the prototype shifted by π/M,
(c). The "flatness constraint."

involves a lot of computation. The following is a better approach to evaluate E_s. We observe that

$$\left|H(e^{j\omega})\right|^2 = H(z)H(z^{-1})\Big|_{z=e^{j\omega}} \tag{B.12}$$

and $H(z)H(z^{-1})$ is the *Z-transform* of the autocorrelation sequence of $h(n)$, denoted by $R_{hh}(n)$. Since all autocorrelation sequences are even order and symmetric, we can write

$$E_s = H(z)H(z^{-1}) = \sum_{\ell=0}^{N-1} r_\ell \cos(\ell\omega), \tag{B.13}$$

where $r_0 = R_{hh}(0)$ and $r_\ell = 2R_{hh}(\ell)$, $1 \leq \ell \leq N-1$. Then, E_s can be expressed as (in closed form)

$$E_s = \int_{\frac{\pi}{M}}^{\pi} \left|H(e^{j\omega})\right|^2 d\omega = \int_{\frac{\pi}{M}}^{\pi} \sum_{\ell=0}^{N-1} r_\ell \cos(\ell\omega) d\omega, \tag{B.14}$$

$$E_s = r_0\left(\pi - \frac{\pi}{M}\right) - \sum_{\ell=1}^{N-1} \frac{r_\ell \sin(\ell\frac{\pi}{M})}{\ell}, \tag{B.15}$$

which can be easily evaluated.

Design example B.1 : This example involves the design of a linear phase prototype filter $H(z)$, for an 8-channel pseudo-QMF bank. The length of $H(z)$ is $N = 40$. Hence, the number of variables to be optimized is 20 ($=\frac{N}{2}$). These variables are initialized by using a lowpass filter based on a Hamming window (length = 40). After initialization, the optimization is done to minimize the objective function in (B.9). The value of $\alpha = 0.5$. Fig. B.2(a) shows the magnitude response of the optimized prototype filter. The impulse response coefficients of the prototype are given in Table B.1.

In order to obtain the analysis and synthesis filters, we will use two sets of choices for θ_k (while using the same prototype filter).

Case 1 : The θ_k are chosen as in (2.39)

$$\theta_k = \begin{cases} \frac{\pi}{4}, & k = 0,2,4,6. \\ -\frac{\pi}{4}, & k = 1,3,5,7. \end{cases} \tag{B.16}$$

The magnitude responses of all the analysis/synthesis filters are shown in Fig. B.2(b). With this choice of θ_k, the overall transfer function $T(z)$ has a 'flat' frequency response

as shown in Fig. B.3(a). The total aliasing error is plotted in Fig. B.3(c). The values of the peak-to-peak reconstruction error E_{p-p} and the aliasing error E_a as defined in Chapter 5 are E_{p-p} = 1.081 E-02 and E_a = 2.259 E-03. Hence, it can be verified that all the significant aliasing terms are indeed canceled. It is shown in Fact B.1 that $z^{N-1}T(z) \simeq$ a function of z^{2M}. Let $T'(z) \triangleq z^{N-1}T(z)$. (Note that $T'(z)$ is non-causal.) For this example, the non-zero impulse response coefficients of $T'(z)$ are shown in Table B.2. Hence, it can be verified that in this 8-channel design, $T'(z)$ is approximately a function of z^{16}.

Case 2 : The θ_k are chosen as

$$\theta_k = \begin{cases} \frac{\pi}{2}, & k = 0,2,4,6. \\ 0, & k = 1,3,5,7. \end{cases} \tag{B.17}$$

This choice of θ_k satisfies (2.37) but not (2.38) and the overall transfer function $T(z)$ has singularities at $\omega = 0$ and $\omega = \pi$, as shown in Fig. B.3(b).

Singularities : Since we have incorporated a flatness constraint in the design of the prototype, the transfer function will not have singularities in the frequency region $\frac{\pi}{M} < \omega < \frac{M-1}{M}\pi$. The singularities, if any, will occur around $\omega = 0$ and $\omega = \pi$. This depends on the choice of θ_0 and θ_{M-1}. In order to avoid singularities in $T(z)$, they must be chosen as in (2.38).

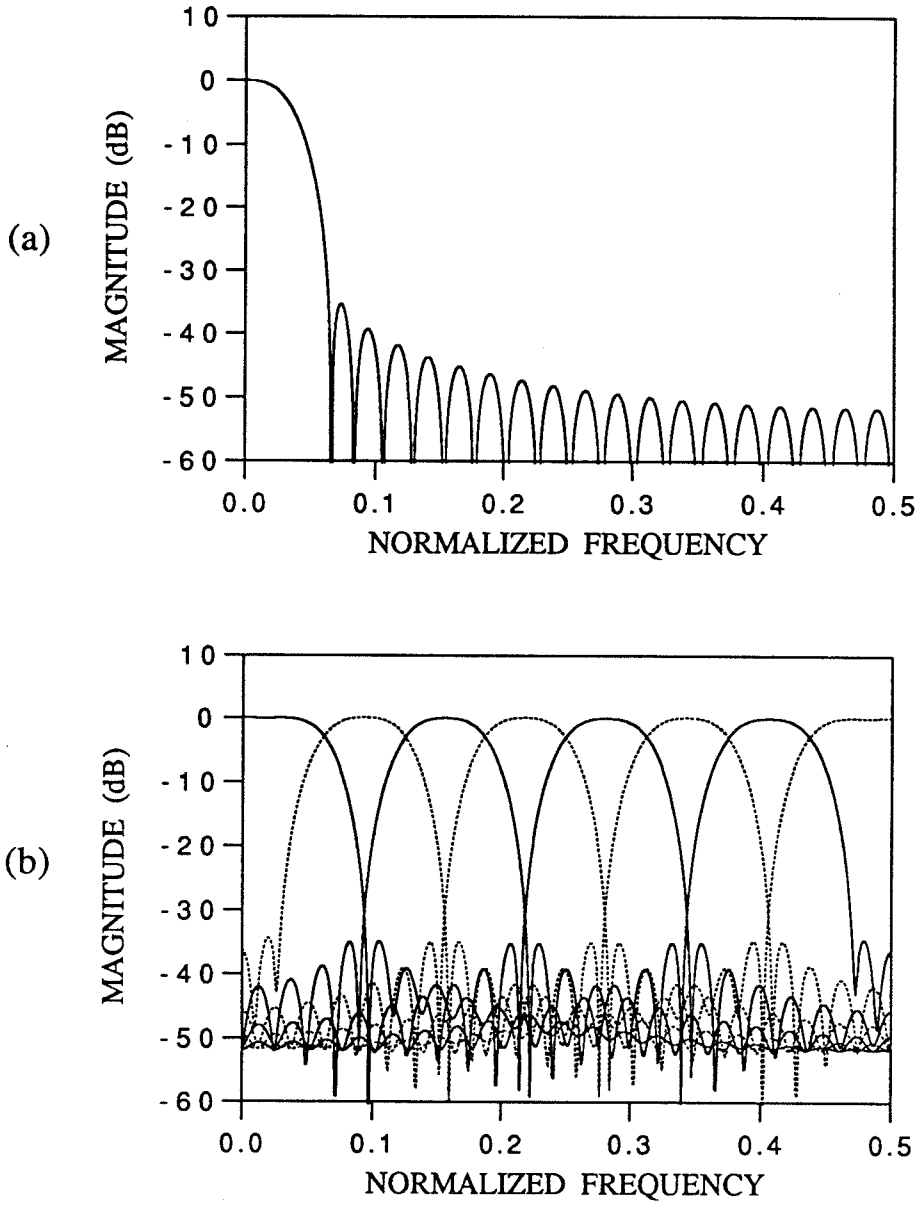

Fig. B.2. Design example B.1. 8-channel pseudo-QMF bank
(a). The magnitude response of the prototype (length = 40),
(b). The responses of the analysis/synthesis filters.

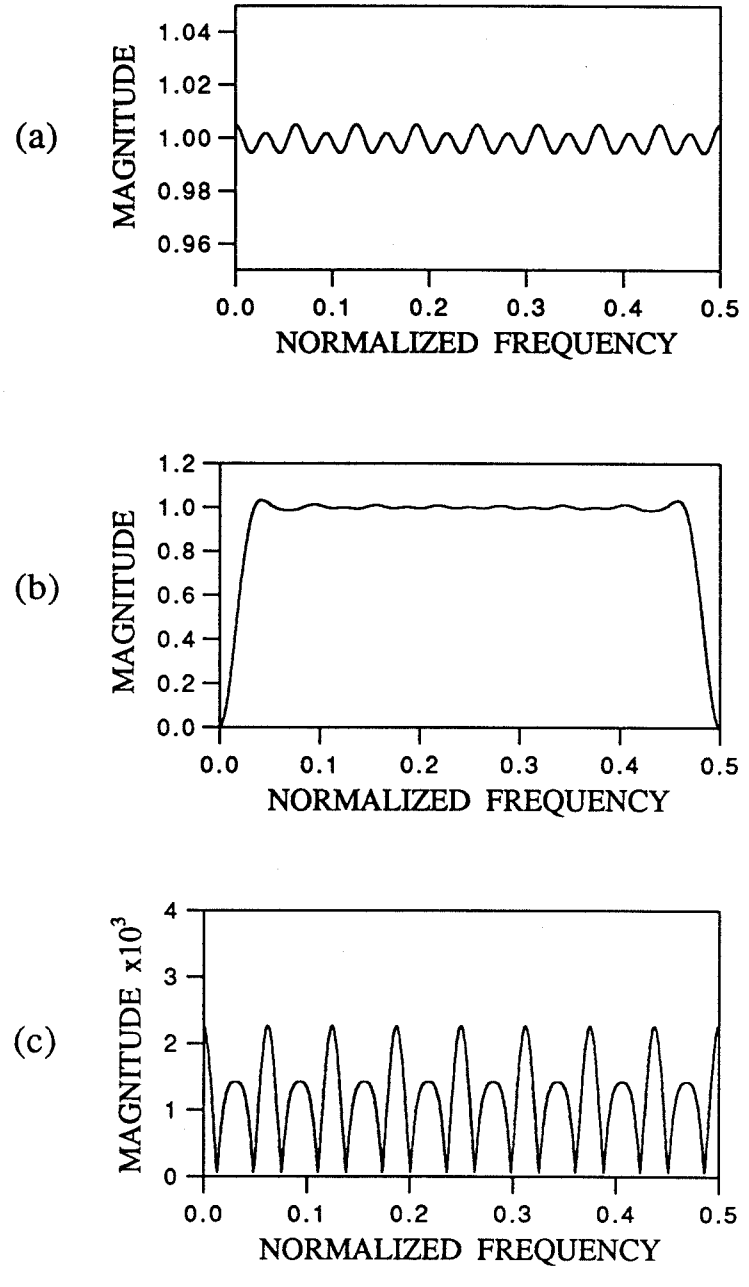

Fig. B.3. Design example B.1
(a). Magnitude response of T(z) - case 1,
(b). Magnitude response of T(z) - case 2,
(c). Plot of the total aliasing error.

Table B.1 : Design example B.1. Impulse response coefficients of the linear phase prototype $H(z)$ (length=40). Hence $h(n) = h(39 - n)$.

n	$h(n)$
0	-2.9592102709470403 E-03
1	-4.0188526633265142 E-03
2	-4.9104756341462651 E-03
3	-5.4331752687432552 E-03
4	-5.3730961268726261 E-03
5	-4.5222384816740284 E-03
6	-2.6990817812652507 E-03
7	2.3096828893352886 E-04
8	4.3373152645501453 E-03
9	9.6099829886898726 E-03
10	1.5951440304172473 E-02
11	2.3175399970121024 E-02
12	3.1013019308541570 E-02
13	3.9127130100292250 E-02
14	4.7132593992753699 E-02
15	5.4622061070010781 E-02
16	6.1194772166336148 E-02
17	6.6485873218751379 E-02
18	7.0193888324294740 E-02
19	7.2103806603295031 E-02

Table B.2 : Design example B.1. Impulse response coefficients of $T'(z)$ (only the non-zero coefficients are shown)

n	$t'(n)$
-32	0.0022752
-16	0.0008191
0	0.9988325
16	0.0008191
32	0.0022752

Bibliography

[Bel76] M. G. Bellanger, G. Bonnerot and M. Coudreuse, "Digital filtering by polyphase network : application to sample rate alteration and filter banks," *IEEE Trans. on Acoutics, Speech and Signal Processing*, vol. ASSP-24, pp. 109-114, April 1976.

[Bel82] M. G. Bellanger, "On computational complexity in digital transmultiplexer filters,"*IEEE Trans. on Communications*, vol. COM-30, No.7, pp. 1461-1465, July 1982.

[Bon78] G. Bonnerot, M. Coudreuse and M. G. Bellanger, "Digital processing techniques in 60 channel transmultiplexer," *IEEE Trans. on Communications*, vol. COM-26, No. 5, May 1978, pp. 698-706.

[Chu85] P. L. Chu, "Quadrature Mirror filter design for an arbitrary number of equal bandwidth channels," *IEEE Trans. on Acoustics, Speech and Signal Processing*, vol. ASSP-33, No.1, pp. 203-218, February 1985.

[Cle72] W. S. Cleveland, "The inverse autocorrelations of a time series and their applications," *Technometrics*, vol. 14, No.2, pp. 277-293, May 1972.

[Com78] Special issue on TDM-FDM conversion, *IEEE Trans. on Communications*, vol. COM-26, No.5, May 1978.

[Com82] Special issue on Transmultiplexers, *IEEE Trans. on Communications*, vol. COM-30, No. 7, July 1982.

[Cox86] R. V. Cox, "The design of uniformly and non-uniformly spaced pseudo-quadrature mirror filters," *IEEE Trans. on Acoustics, Speech and Signal Processing*, vol. ASSP-34, No. 5, pp. 1090-1096, October 1986.

[Cro83] R. E. Crochiere and L. R. Rabiner, "Multirate Digital Signal Processing," *Prentice-Hall*, Englewood Cliffs, NJ, 1983.

[Croi76] A. Croisier, D. Esteban and C. Galand, "Perfect channel splitting by use of interpolation/ decimation/ tree decomposition techniques, " *International Conference on Information Science and Systems*, Patras, Greece, 1976, pp. 443-446.

[Doga88] Z. Doganata, P. P. Vaidyanathan and T. Q. Nguyen, "General synthesis procedures for FIR lossless transfer matrices for perfect reconstruction multirate filter bank applications," *IEEE Trans. on Acoustics, Speech and Signal Processing* pp. 1561-1574, October 1988.

[Dur59] J. Durbin, "Efficient estimation of parameters in moving average models," *Biometrika*, vol. 46, pp. 306-316, 1959.

[Fet78] A. Fettweis, "Multiplier-free modulation schemes for PCM/FDM and audio/FDM conversion," *Archiv Elecktr. Übertragungstechnik,* vol. AEÜ-32, pp. 477-485, December 1978.

[Fre80] S. L. Freeny, "TDM/FDM translation as an application of digital signal processing," *IEEE Communications Magazine*, pp 5-15, January 1980.

[Fri83] B. Friedlander, "A lattice algorithm for factoring the spectrum of a moving average process," *IEEE Trans. on Automatic Control*, vol. AC-28, No.11, pp. 1051-1055, November 1983.

[Gil72] P. E. Gill and W. Murray, "Quasi-Newton methods for uncontrained optimization," *Journal of the Institue of Math. Applications*, vol. 9, pp. 91-108,

1972.

[Gil81] P. E. Gill, W. Murray and M. H. Wright, "Practical Optimization," *Academic Press*, London, 1981.

[IMSL] Fortran subroutines for mathematical applications - Math/Library, version 1.0, *IMSL*, Houston, Texas, April 1987.

[Jon80] J. D. Johnston, "A filter family designed for use in Quadrature Mirror Filter banks," Proc. of IEEE Int. Conf. on Acoustics, Speech and Signal Processing (ICASSP), April 1980, pp. 291-294.

[Kay88] S. M. Kay, "Modern Spectral Estimation : Theory and Applications," *Prentice Hall*, Englewood Cliffs, NJ, 1988.

[Koi89] R. D. Koilpillai, T. Q. Nguyen and P. P. Vaidyanathan, "New results in the theory of crosstalk-free transmultiplexers," *California Institute of Technology Report*, September 1989.

[Koi90] R. D. Koilpillai and P. P. Vaidyanathan, "A new approach to the design of FIR perfect reconstruction QMF banks," *Proc. IEEE Int. Symposium on Circuits and Systems (ISCAS)*, New Orleans, May 1990, pp. 125-128.

[Mal90a] H. S. Malvar, "Lapped transforms for efficient transform/subband coding," *IEEE Trans. on Acoustics, Speech and Signal Processing*, vol. ASSP-38, pp. 969-978, June 1990.

[Mal90b] H. S. Malvar, "Modulated QMF filter banks with perfect reconstruction," *Electronics Letters*, Vol. 26, June 1990, pp 906-907.

[Mas85] J. Masson and Z. Picel, "Flexible design of computationally efficient nearly perfect QMF filter banks, " *Proc. IEEE Int. Conf. on Acoustics, Speech and Signal Processing (ICASSP)*, Tampa, FL, March 1985, pp. 14.7.1-14.7.4.

[Mcc73] J. H. McClellan and T. W. Parks, "A unified approach to the design of optimum FIR linear-phase digital filters," *IEEE Trans. on Circuit Theory*, vol. 20, pp. 697-701, November 1973.

[Mia82] G. A. Mian and A. P. Nainer, "A fast procedure to design equiripple minimum phase FIR filters," *IEEE Trans. on Circuits and Systems*, pp. 327-331, May 1982.

[Min82] F. Mintzer, "On half-band, third-band, and Nth-band FIR filters and their design," *IEEE Trans. Acoustics, Speech and Signal Processing*, Vol. 30, pp. 734-738, October 1982.

[Mul87] C. T. Mullis and C. J. Demeure, "The Jury matrix and a Newton-Raphson procedure for moving average spectral factorization," *Proc. of Asilomar Conf. on Signals, Systems and Computers*, 1987, pp. 635-639.

[Mur62] F. D. Murnaghan, "The Unitary and Rotation Groups," *Spartan Books*, Washington D.C., 1962.

[NAG] NAG Fortran Library - Mark 13, *The Numerical Algorithms Group*, Downers Grove, IL, July 1988.

[Nay90] K. Nayebi, T. P. Barnwell and M. J. T. Smith, "A general time domain analysis and design framework for exactly reconstructing FIR analysis/ synthesis filter banks," *Proc. IEEE Int. Symposium on Circuits and Systems (ISCAS)*, New Orleans, May 1990, pp. 2022-2025.

[Ngu88a] T. Q. Nguyen, T. Saramaki and P. P. Vaidyanathan, "Eigenfilters for the design of special transfer functions with applications in multirate signal processing," *Proc. IEEE Int. Conf. on Acoustics, Speech and Signal Processing (ICASSP)*, New York, April 1988, pp. 1467-1470.

[Ngu88b] T. Q. Nguyen and P. P. Vaidyanathan, "Maximally decimated perfect reconstruction FIR filter banks with pairwise mirror-image analysis (and synthesis) frequency responses," *IEEE Trans. on Acoustics, Speech and Signal Processing*, vol. ASSP-36, pp. 693-706, May 1988.

[Nus81] H. Nussbaumer, "Pseudo QMF filter bank," *IBM Technical Disclosure Bulletin*, vol. 24, No. 6, pp. 3081-3087, November 1981.

[Nus84] H. J. Nussbaumer and M. Vetterli, "Computationally efficient QMF filter banks," *Proc. IEEE Int. Conf. on Acoustics, Speech and Signal Processing (ICASSP)*, San Diego, CA, March 1984, pp. 11.3.1-11.3.4.

[Opp75] A. V. Oppenheim and R. W. Schafer, "Digital Signal Processing," *Prentice-Hall Inc.*, Englewood Cliffs, NJ 1975.

[Prin86] J. P. Princen and A. B. Bradley,"Analysis/ synthesis filter bank design based on time domain aliasing cancellation," *IEEE Trans. on Acoustics, Speech and Signal Processing*, vol. ASSP-34, pp. 1153-1161, October 1986.

[Rab75] L. R. Rabiner and B. Gold, "Theory and applications of digital signal processing," *Prentice-Hall Inc.*, Englewood Cliffs, NJ 1975.

[Rab78] L. R. Rabiner and R. W. Schafer, "Digital Processing of Speech Signals," *Prentice-Hall Inc.*, Englewood Cliffs, NJ 1978.

[Roth83] J. H. Rothweiler, "Polyphase quadrature filters - a new subband coding technique," *IEEE Int. Conference on Acoustics, Speech and Signal Processing (ICASSP)*, Boston 1983, pp. 1280-1283.

[Sca85] L. E. Scales, "Introduction to non-linear optimization," *Springer-Verlag*, New York 1985.

[Sch81] H. Scheuermann and H. Göckler, "A comprehensive survey of digital transmultiplexing methods," *Proc. of the IEEE*, vol. 69, No.11, pp. 1419-1450,

November 1981.

[Schm83] C. E. Schmid, "Design of IIR/ FIR filters using a frequency domain bootstrapping technique and LPC methods," *IEEE Trans. on Acoustics, Speech and Signal Processing*," vol. ASSP-31, No.4, pp. 999-1006, August 1983.

[Smi84] M. J. T. Smith and T. P. Barnwell, "A procedure for designing exact reconstruction filter banks for tree-structured subband coders," *Proc. IEEE Int. Conf. on Acoustics, Speech and Signal Processing (ICASSP)*, San Diego, March 1984, pp. 27.1.1 - 27.1.4.

[Swa86] K. Swaminathan and P. P. Vaidyanathan, "Theory and design of uniform DFT, parallel, quadrature mirror filter banks," *IEEE Trans. on Circuits and Systems*, vol. CAS-33, pp. 1170-1191, December 1986.

[Tsu78] T. Tsuda, S. Morita and Y. Fujii, "Digital TDM-FDM translator with multistage structure," *IEEE Trans. on Communications*, vol. COM-26, No. 5, pp. 734-741, May 1978.

[Vai85] P. P. Vaidyanathan, "On power-complementary FIR filters," *IEEE Trans. on Circuits and Systems*, pp. 1308-1310, December 1985.

[Vai86a] P. P. Vaidyanathan, S. K. Mitra, Y. Neuvo, " A new approach to the realization of low sensitivity IIR digital filters," *IEEE Trans. on Acoustics, Speech and Signal Processing*, vol. ASSP-34, No. 2, pp. 350-361, April 1986.

[Vai86b] P. P. Vaidyanathan, "Passive cascaded-lattice structures for low sensitivity FIR filter design, with application to filter banks," *IEEE Trans. on Circuits and Systems*, Vol. CAS-33, No.11, pp. 1045-1064, November 1986.

[Vai87a] P. P. Vaidyanathan, "Theory and design of M-channel maximally decimated Quadrature Mirror Filters with arbitrary M, having the perfect

reconstruction property," *IEEE Trans. on Acoustics, Speech and Signal Processing*, vol. ASSP-35, No. 4, pp. 476-492, April 1987.

[Vai87b] P. P. Vaidyanathan, P. A. Regalia and S. K. Mitra, "Design of doubly-complementary IIR digital filters using a single complex allpass filter, with multirate applications," *IEEE Trans. on Circuits and Systems*, vol. CAS-34, pp. 378-389, April 1987.

[Vai87c] P. P. Vaidyanathan, "Quadrature Mirror Filter Banks, M-band extensions and perfect reconstruction techniques," *IEEE ASSP Magazine*, vol. 4, pp. 4-20, July 1987.

[Vai87d] P. P. Vaidyanathan and K. Swaminathan, "Alias-free, real-coefficient M-band QMF banks for arbitrary M," *IEEE Trans. on Circuits and Systems*, vol. CAS-34, No.12, pp. 1485-1496, December 1987.

[Vai88a] P. P. Vaidyanathan and P. Q. Hoang, "Lattice structures for optimal design and robust implementation of two-channel perfect reconstruction QMF banks, " *IEEE Trans. on Acoustics, Speech and Signal Processing*, vol. ASSP-36, pp. 81-94, January 1988.

[Vai88b] P. P. Vaidyanathan and S. K. Mitra, "Polyphase networks, block digital filtering, LPTV systems and alias-free QMF banks : a unified approach based on pseudocirculants," *IEEE Trans. on Acoustics, Speech and Signal Processing*, vol. ASSP-36, No. 3, pp. 381-391, March 1988.

[Vai89] P. P. Vaidyanathan, T. Q. Nguyen, Z. Doganata and T. Saramaki, "Improved technique for design of perfect reconstruction FIR QMF banks with lossless polyphase matrices," *IEEE Trans. on Acoustics, Speech and Signal Processing*, vol. ASSP-37, pp. 1042-1056, July 1989.

[Vai90] P. P. Vaidyanathan, "Multirate digital filters, filter banks, polyphase networks and applications : A tutorial," *Proc. of the IEEE*, vol. 78, No. 1, pp. 56-93, January 1990.

[Vet86] M. Vetterli, "Perfect transmultiplexers," *IEEE Int. Conference on Acoustics, Speech and Signal Processing (ICASSP)*, Tokyo, April 1986, pp. 2567-2570.

[Vet87] M. Vetterli, "A theory of multirate filter banks," *IEEE Trans. on Acoustics, Speech and Signal Processing*, vol. ASSP-35, No. 3, pp. 356-372, March 1987.

[Vet89] M. Vetterli and D. Le Gall, "Perfect reconstruction FIR filter banks : some properties and factorizations," *IEEE Trans. on Acoustics, Speech and Signal Processing*, vol. ASSP-37, pp. 1057-1061, July 1989.

[Wil69] G. Wilson, "Factorization of the covariance generating function of a pure moving average process," *SIAM Journal of Numerical Analysis*, vol. 6, No.1, pp. 1-7, March 1969.

[Yip87] P. Yip and K. R. Rao, "Fast Discrete Transforms," *Chapter 6, Handbook of Digital Signal Processing*, ed. D. F. Elliot, Academic Press, 1987.